AD-A115 151 LEHIGH UNIV BETHLEHEM PA DEPT OF MECHANICAL ENGINEE--ETC F/G 20/4
AN OPTIMIZATION TECHNIQUE FOR THE DEVELOPMENT OF TWO-DIMENSIONA--ETC(U)
MAR 82 L J YUMAS, J D WALKER F49620-78-C-0071
UNCLASSIFIED TR-FM-82-1 AFOSR-TR-82-0417 NL

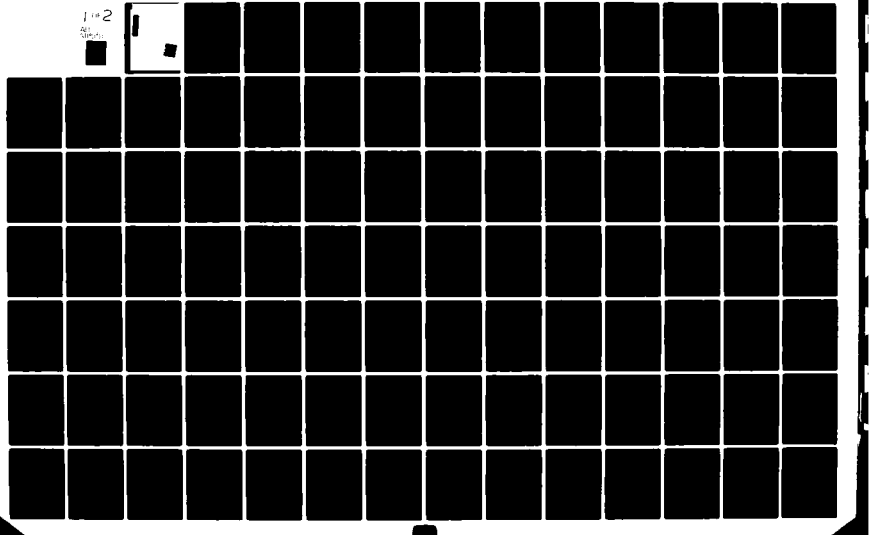

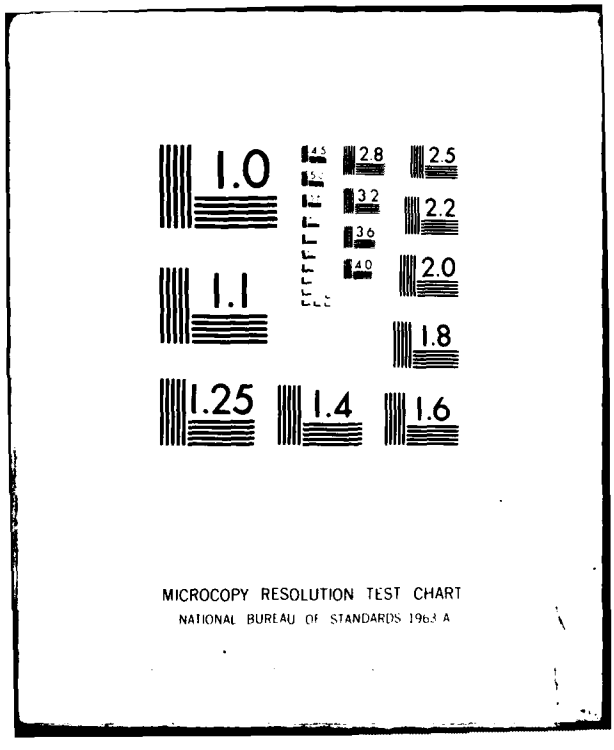
1.0
1.1
1.25
1.4
1.6
1.8
2.0
2.2
2.5
2.8
3.2
3.6
4.0
MICROCOPY RESOLUTION TEST CHART
NATIONAL BUREAU OF STANDARDS 1963 A

AN OPTIMIZATION TECHNIQUE FOR THE DEVELOPMENT OF TWO-DIMENSIONAL STEADY TURBULENT BOUNDARY LAYER MODELS

by

L.J. Yuhas and J.D.A. Walker

Department of Mechanical Engineering and Mechanics

Lehigh University, Bethlehem, PA.

Technical Report FM-82-1

Approved for public release; distribution unlimited.

Qualified requestors may obtain additional copies from the Defense Technical Information Service.

UNCLASSIFIED

SECURITY CLASSIFICATION OF THIS PAGE *(When Data Entered)*

REPORT DOCUMENTATION PAGE		READ INSTRUCTIONS BEFORE COMPLETING FORM
1. REPORT NUMBER AFOSR-TR- 82-0417	2. GOVT ACCESSION NO. AD-A115151	3. RECIPIENT'S CATALOG NUMBER
4. TITLE *(and Subtitle)* AN OPTIMIZATION TECHNIQUE FOR THE DEVELOPMENT OF TWO-DIMENSIONAL STEADY TURBULENT BOUNDARY LAYER MODELS		5. TYPE OF REPORT & PERIOD COVERED INTERIM 6. PERFORMING ORG. REPORT NUMBER
7. AUTHOR(s) L J YUHAS J D A WALKER		8. CONTRACT OR GRANT NUMBER(s) F49620-78-C-0071
9. PERFORMING ORGANIZATION NAME AND ADDRESS LEHIGH UNIVERSITY DEPT OF MECHANICAL ENGINEERING & MECHANICS BETHLEHEM, PA 18015		10. PROGRAM ELEMENT, PROJECT, TASK AREA & WORK UNIT NUMBERS 61102F 2307/A2
11. CONTROLLING OFFICE NAME AND ADDRESS AIR FORCE OFFICE OF SCIENTIFIC RESEARCH/NA BOLLING AIR FORCE BASE, DC 20332		12. REPORT DATE MARCH 82 13. NUMBER OF PAGES 148
14. MONITORING AGENCY NAME & ADDRESS*(if different from Controlling Office)*		15. SECURITY CLASS. *(of this report)* UNCLASSIFIED 15a. DECLASSIFICATION/DOWNGRADING SCHEDULE

16. DISTRIBUTION STATEMENT *(of this Report)*

Approved for public release; distribution unlimited.

17. DISTRIBUTION STATEMENT *(of the abstract entered in Block 20, if different from Report)*

18. SUPPLEMENTARY NOTES

19. KEY WORDS *(Continue on reverse side if necessary and identify by block number)*

TURBULENCE	REYNOLDS AVERAGED EQUATIONS
TURBULENCE MODELING	EDDY VISCOSITY
BOUNDARY LAYERS	MAINSTREAM TURBULENCE
FLUID MECHANICS	PRESSURE GRADIENTS

20. ABSTRACT *(Continue on reverse side if necessary and identify by block number)*

A procedure for the development of a simple boundary layer turbulence model to account for different physical effects is described; the method is applied here to produce models for both pressure gradient and mainstream turbulence effects. Asymptotic theory is used to isolate the leading terms in an expansion for the mean velocity profile for high Reynolds numbers for both the inner and outer regions of a nominally steady two-dimensional boundary layer. The velocity profile in the outer layer satisfies a partial differential equation containing

DD FORM 1 JAN 73 1473 EDITION OF 1 NOV 65 IS OBSOLETE

UNCLASSIFIED

SECURITY CLASSIFICATION OF THIS PAGE *(When Data Entered)*

a Reynolds stress term and this term is modeled by a simple eddy viscosity function which contains two parameters. The velocity profile in the inner wall layer is modeled using an analytical expression which has been previously derived by consideration of the observed characteristics of the time-dependent flow in the wall layer and which contains a single independent parameter. For a self-similar flow, the outer layer equation becomes an ordinary differential equation; this equation is solved numerically and in conjunction with the analytical inner layer profile, a composite profile spanning the entire boundary layer is defined. This composite profile contains three parameters which may be adjusted systematically to obtain a best fit to a given set of experimental data. A computer optimization code is described in which any or all of the three profile parameters may be varied. This optimization code may be used simply to obtain a close analytical representation of a given set of data. The primary use described here, however, is to develop correlations for various physcial effects from the results of the optimizations. In particular, correlations for the effects of mainstream pressure gradients and mainstream turbulence for the profile parameters are given. In principle, these correlations may then be used in a prediction method.

ACKNOWLEDGEMENTS

The authors wish to acknowledge the Air Force Office of Scientific Research for providing financial support for this study under Contract No. F49620-78-C-0071. The present investigation is a part of a larger overall program "Theoretical and Experimental Investigation of Coherent Structure in the Turbulent Boundary Layer". This program is directed at developing an improved understanding of the behavior of turbulent boundary layers and consequently better predictive models. The authors are grateful for the support and encouragement of Captain Mike Francis and Lt. Col. Lowell Ormand.

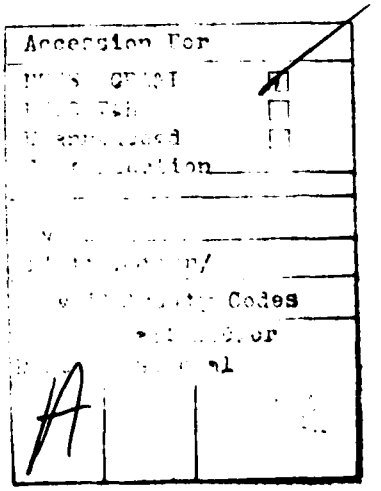

ABSTRACT

A procedure for the development of a simple boundary layer turbulence model to account for different physical effects is described; the method is applied here to produce models for both pressure gradient and mainstream turbulence effects. Asymptotic theory is used to isolate the leading terms in an expansion for the mean velocity profile for high Reynolds numbers for both the inner and outer regions of a nominally steady two-dimensional boundary layer. The velocity profile in the outer layer satisfies a partial differential equation containing a Reynolds stress term and this term is modeled by a simple eddy viscosity function which contains two parameters. The velocity profile in the inner wall layer is modeled using an analytical expression which has been previously derived by consideration of the observed characteristics of the time-dependent flow in the wall layer and which contains a single independent parameter. For a self-similar flow, the outer layer equation becomes an ordinary differential equation; this equation is solved numerically and in conjunction with the analytical inner layer profile, a composite profile spanning the entire boundary layer is defined. This composite profile contains three parameters which may be adjusted systematically to obtain a best fit to a given set of experimental data.

A computer optimization code is described in which any or all of the three profile parameters may be varied. This optimization code may be used simply to obtain a close analytical representation of a given set of data. The primary use described here, however, is to develop correlations for various physical effects from the results of the optimizations. In particular, correlations for the effects of mainstream pressure gradients and mainstream turbulence for the profile parameters are given. In principle, these correlations may then be used in a prediction method.

TABLE OF CONTENTS

LIST OF TABLES

List of Tables (cont.)

LIST OF FIGURES

List of Figures (cont.)

1. INTRODUCTION

Turbulent boundary layers occur in a wide variety of engineering applications including, for example, flows over turbine blades, airfoils, and in subsonic diffusers. In these and many other situations it is important to be able to develop the capability to accurately predict characteristics such as skin friction, lift, drag, and the onset of boundary layer separation. At present, the complex nature of turbulence seems to preclude any predictive analysis based on first principles. For a turbulent boundary layer which is steady in the time-mean sense, the classical approach to prediction has been to attempt to deal with the Reynolds time-averaged equations for the mean velocity components. These equations contain unknown functions referred to as Reynolds stresses; physically these terms are related to long time averages of products of fluctuations of the velocity components about their mean values. As a first step, the development of any prediction method requires a model to represent the behavior of the Reynolds stress terms. The objective of this study is to develop an approach which can be used to investigate the influence of various physical effects on the turbulent boundary layer and to incorporate these effects in a simple turbulence model. To this end, a general optimization code is developed in

which the parameters in the turbulence model may be varied systematically to obtain the best representation of measured mean profile data. As one example of how this code may be used, the method is applied to determine the influence of pressure gradients on the mean profile and a correlation for pressure gradient effects is developed. As a second example, the method is applied to some recent constant pressure profile data with mainstream turbulence and a correlation is obtained to reflect the effects of mainstream turbulence.

An immediate problem which arises in the modeling process is that the dynamics of turbulent boundary layers are not well understood. Previous investigators have attempted to resolve this problem by postulating the functional form for the Reynolds stress terms. These functional forms normally contain a number of unknown constants which are selected in a procedure often known as "computer optimization." The details of this procedure vary with the originator of the particular model and invariably are not well documented. However, the general approach is that particular data sets usually consisting of measured velocity profiles at numerous streamwise locations are "predicted" using various combinations of values of the "constants" associated with a given model. Some type of subjective judgement is then made as to which set of values of the constants best

"predict" as many data sets as possible. The approach adopted in this study is rather different and will now be discussed in detail.

An ideal approach to the modeling problem would be to isolate the primary features in the time-dependent turbulent flow and to pattern the turbulence model after motions which reflect the true physics of the turbulent boundary layer. Such a model would adequately replace the information lost in the time averaging and would presumeably not contain or require a large number of adjustable constants. This approach is partially adopted in this study in the model used for the inner region of the turbulent boundary layer.

Since the objective is to isolate which effects are important and which are not for large Reynolds number, singular perturbation theory and the method of matched asymptotic expansions are used throughout the present study. It is worthwhile at this stage to summarize some of the main results concerning the asymptotic structure of the time mean boundary layer equations in the limit of large Reynolds numbers; these results have formally been demonstrated by Fendell (1972) and Mellor (1972). The turbulent boundary layer is a composite double layer consisting of a relatively thick outer layer having a thickness $O(u^*)$, (where $u^* = u_\tau/U_e(x)$ is the ratio of friction

to mainstream velocity) and a thin inner layer having a thickness $O(1/(Re\ u^*))$, where Re is the Reynolds number. In the joining region between the two layers, the velocity profile must be logarithmic for a self consistent asymptotic description. The complete mathematical results for the streamwise momentum equations are summarized in §2. One particularly important result concerns the inner layer and is that, to leading order, the convective terms are negligible in the time mean equations; consequently, if the mean profile is known in the inner layer, the Reynolds stress may be calculated and vice versa. In the present study, rather than a model for Reynolds stresses, a model for the inner region velocity profile is used; this model is based upon the observed coherent structure of the wall layer flow and will now be briefly described.

Over the past decade, it has been well documented (see, for example, Kline & Runstadler, 1959; Kline et al., 1967; Corino & Brodkey, 1969; Willmarth, 1975) that there is a considerable degree of ordered structure in the time dependent flow in the wall layer of a turbulent boundary layer. In particular, it is well known that there are two important phases associated with an observed cyclic behavior of the wall layer flow. In the first phase, if attention is focused on a fixed small area of the plate, the wall layer will be observed to

be in the quiescent state (Kline et al., 1967) for a majority of the total observation time. During this quiescent period, the wall layer streaks are observed with what appear to be longitudinal counter-rotating vortices between the streaks, the wall layer flow is relatively well ordered and no important interactions occur between the wall layer and the flow in the outer portion of the boundary layer; in this state, the wall layer may be regarded as passive. Eventually the second phase occurs which is generally known as the bursting phenomenon and which is characterized by a rapid and violent ejection from the wall layer into the outer layer. The ejection is of relatively short duration and is followed by an inrush of fluid from the outer layer; the streak structure appears again very rapidly and another quiescent period begins. Although many questions exist as to the causes and effects of these and other subsidiary events, the gross features of the cyclic behavior described above are now well established.

To incorporate such information in a prediction method for the time-mean flow, it is necessary in principle to analyze a typical event in the turbulence and then assess the contribution of this event to the time-mean quantities. To this end, Walker and Abbott (1977) argue, by consideration of the observed length and time scales in the wall layer, that during the quiescent period the equations for all three velocity components

must be linear and of the heat conduction type in the limit of large Reynolds number; in other words, the convective terms in the Navier-Stokes equations are negligible to leading order whenever the wall layer flow is in the quiescent state. Walker and Scharnhorst (1977) then go on to consider all possible similarity solutions of these equations which are compatible with theory and experiment; the similarity solutions correspond to the organized motion between streaks during the quiescent period and are radically different from the oscillatory Stokes type solutions which form the basis of the Van Driest (1956) model. Walker and Scharnhorst (1977) compute a time-average of the similarity solutions over a quiescent period and assess which solutions produce an important contribution to the time-mean profile and which do not. The final result is an analytical model which will be given in §2 for the inner region profile and which contains a single parameter S that is related to the mean period between bursts. The contribution to the mean profile during the bursting process and breakdown of the wall layer flow is neglected on the grounds that the breakdown is of short duration relative to the quiescent period; note that there are various theoretical reasons as well as a body of experimental evidence that verify that the period of breakdown must be small with respect to the quiescent period. On the

other hand, the vertical velocity (Walker & Abbott, 1977 and Walker & Scharnhorst, 1977) is so small during the quiescent period that there can be no contribution to the Reynolds stress to leading order during this period of time and the major contribution to the Reynolds stress must be made during the bursting process. Consequently, in this theoretical description of the wall layer flow, the dominant contribution to the mean profile occurs during the quiescent period, while the major contribution to the Reynolds stress occurs during the breakdown phase; both mean quantities are directly related to each through the leading order time-mean equations in the wall layer (since the convective terms are negligible to leading order).

In principle, it is desirable to develop a model for the outer layer which is also based on the observed dynamics of the time dependent flow in the outer region. However, the outer region problem is more complex ; it appears necessary to model the Reynolds stress terms directly and unfortunately the dynamics of the outer layer are not well understood. In the outer region, large scale motions are observed which appear to be recirculating agglomerations of numerous smaller scale structures; these smaller scale structures have dimensions on the general magnitude of 100 wall layer units (y^+) and appear at times to be intensely vorticular in nature. At any stage, these small

vorticular structures are in various stages of coalescence and decay and when they pass close to the wall layer, are observed to induce eruptions of fluid. A number of authors have suggessted that it is the vortex motion in the outer layer which induces the wall layer bursting (Nychas et al., 1973; Doligalski & Walker, 1978; Walker, 1978) and leads to the creation of new vortex structures in the outer layer; a regenerative mechanism for the production of new turbulence has recently been proposed by Doligalski, Smith & Walker (1981) and Doligalski (1981) on the basis of the observed unsteady effect of vortices on wall boundary layers. These studies demonstrate that for the vortex motions considered (two-dimensional vortices convected in a uniform flow and in a shear flow and ring vortices above a plane wall) that an eruption of the boundary layer flow near the wall will occur. However, these studies are as yet in an exploratory stage and, while a physical mechanism for the bursting is indicated, it is not yet possible to develop a constitutive model for the outer layer on this basis.

The bursting phenomena is a complex time-dependent viscous-inviscid interaction between the inner and outer layers which leads to the introduction of new vorticity into the outer layer and which occurs intermittently. However, during these brief periods of localized breakdown of the two layer structure, the

majority of the contribution to the outer layer (and inner layer) Reynolds stress occurs. For this reason, the simplifications which were possible in obtaining the wall layer model are not possible and it appears necessary to consider a typical burst and time average the results in order to model the $\overline{u'v'}$ term. As discussed by Doligalski & Walker (1978) and Doligalski, Smith & Walker (1981) the inviscid-viscous interaction is a formidable theoretical problem at present; moreover, many other aspects of the outer layer are still not well understood and, at present, development of an outer layer model based on the characteristics of time dependent flow in the outer layer is not feasible.

For these reasons, a conventional type of eddy viscosity model is used in the present study for closure in the outer layer; this type of model is used here because of its simplicity and the good degree of success it has had in other prediction methods. The eddy viscosity hypothesis is commonly termed a first-order closure scheme; it assumes that there is a functional relation between the Reynolds stress and the mean profile and further that the Reynolds stress may be written as an eddy viscosity function times the mean velocity gradient. Here a model for the eddy viscosity which is similar to the Cebeci-Smith (1974) and Mellor & Herring models (1968) will

be adopted; this model is a monotonically increasing function of the outer variable behaving linearly with slope κ (the von Karman "constant") near the logarithmic zone and approaching a value K at the boundary layer edge. Note that the wall layer profile model contains κ in addition to the cycle time parameter S. Consequently the present turbulence model contains the three parameters (s,κ,K).

It is common practice in many turbulence models to assume constant universal values for the parameters appearing in the model. Scharnhorst (1978), for example, has attempted a prediction method with ($s = 10.495$, $\kappa = 0.41$, $K = .0168$)(the latter two values are also used by Cebeci & Smith, 1974); however, it was determined (after the prediction method was compared to a number of data sets,) that the velocity profiles were not well predicted, particularly in flows with pressure gradient. The objective of this study is to investigate a systematic way of determining any trends in these parameters for various effects such as pressure gradients or mainstream turbulence, with the ultimate goal of obtaining correlations of these parameters for use in a prediction method.

This will be carried out here in a somewhat different way from previous investigations. It has become common practice in recent times to determine values of "universal constants"

in turbulence models through a process known as computer optimization; this procedure is often associated with turbulence models that have a sizeable number of adjustable constants (see, for example, Murthy, 1977) and is usually carried out as follows. One data set or a number of data sets are chosen, each of which consists of a number of measured profiles at various downstream locations from some initial point; a prediction method with a preassigned set of constants in the turbulence model is started at the initial data station and the downstream data is "predicted." On the basis of comparison with either the integral parameters and/or the skin friction coefficient, a decision is made as to whether adjust the "constants" in the turbulence model to achieve better "predictions"; the prediction method is then used to obtain another "prediction" of the downstream data. This iterative method continues until some optimal set of constants is obtained.

One undesireable feature of this scheme is that the basis for adjusting the constants is usually not clearly defined and in any case is based upon comparisons with the gross properties such as the integral quantities or quantities obtained indirectly from experiment such as the skin friction. The details of how the iterative process is carried

out and what criteria are used to decide on the optimal set of constants are normally not supplied in the literature, particularly when the number of data sets involved are large; presumeably the choice is based ultimately on some type of integrated subjective average.

In the present study, the trends in the turbulence model parameters and eventually the correlations are also determined by comparison to experimental data but the procedure is different and precisely defined. First, only equilibrium data sets are considered; an equilibrium turbulent boundary layer, by definition, is a boundary layer in which the mainstream velocity varies algebraically with streamwise distance. Such a boundary is expected (Clauser, 1956; Mellor, 1972; Fendell, 1972; Scharnhorst et al., 1978) to successively approach a self-similar flow at large distances from wherever the boundary layer flow is initiated. For this reason, equilibrium boundary layers have historically been of considerable interest.

It is worthwhile to remark, however, that, in order for self-similar velocity profiles to exist, equilibrium is a necessary but by no means a sufficient condition. To expand on this point, consider the case of laminar boundary layers where similar solutions satisfy the well known Falkner-Skan equation. The existence of such solutions in laminar flows

has been discussed by Brown & Stewartson (1965) who argue that similar solutions may be expected in two physical situations. The first of these is at an x station where the velocity profile is an initiator of the boundary-layer flow downstream; such a situation occurs physically at the front stagnation point of a bluff body or the leading edge of a flat plate, for example. In these cases, the Falkner-Skan profile gives the proper laminar boundary-layer solution at a point of attachment of the mainstream and provides the initial condition to initiate a boundary-layer calculation downstream. For turbulent boundary layers, there appears to be no analogue of this physical situation. In the absence of mainstream turbulence, the flow at a point of attachment of the mainstream is observed to be laminar and when the downstream boundary-layer flow is turbulent, there is a transition zone in between the laminar and the turbulent flow. Moreover, a wide variety of upstream experimental conditions can lead to transition and an eventual fully-developed turbulent boundary layer downstream for the same mainstream velocity distribution. Consequently, there would appear to be no reason to expect that the flow in the outer region of an equilibrium boundary layer will be self-similar at the initial stations of a fully developed turbulent flow.

For laminar boundary layers, the other case discussed by Brown and Stewartson (1965) is that where a similarity solution becomes what may be described as a terminator of a more general boundary-layer flow and two cases of this behavior are considered by Brown and Stewartson (1965). A physical case where this can occur is at a point of detachment of the inviscid flow; examples of such behavior are known in magneto-hydrodynamic flow (Leibovich, 1967a,b) and in rotating flows (Walker & Stewartson, 1972) at the rear stagnation point of symmetrical and two-dimensional bluff bodies. Another case is flat plate flow and here if the initial velocity profile at any arbitrary location on the plate is not given by the Blasius solution, then the Blasius profile can only become the relevant solution at an infinite distance downstream. For turbulent boundary-layer flows, an analogous type of situation is expected; that is, similarity solutions are only anticipated as terminators and usually at large distances downstream from wherever the boundary layer is initiated.

In practice, one would expect to be able to measure turbulent boundary-layer profiles, at large distances downstream of the transition zone, which become arbitrarily close to being self-similar; however, near the transition zone, there is no reason to expect a self-similar behavior. In zero and favorable pressure gradients, measured profiles in an equilibrium flow should increasingly approach self-similarity

at subsequent data stations downstream. In adverse pressure gradient flows, there is an additional difficulty in that reversed flow and boundary layer separation may occur before similarity is achieved.

The self-similar flow is particularly attractive insofar as turbulence model development is concerned because the parabolic partial differential equation governing the turbulent boundary layer flow becomes an ordinary differential equation of the boundary value type. In the present study, the ordinary differential equation associated with the outer layer is solved numerically for a given set of the turbulence model parameters (κ,K) to determine an outer layer velocity profile; this outer layer profile is matched with an inner layer profile containing the inner profile parameters (s,κ) and a composite velocity profile for the entire boundary layer is defined. The composite profile is then compared directly to measured experimental velocity profile data and a root-mean-square error is defined as a criterion of how well the profile represents the data. The optimization procedure then adjusts one or more of the three profile parameters (s,κ,K) until a "best fit" to each profile is obtained. Once this procedure has been carried out for several data stations, the results are plotted to determine any trends in the profile parameters; the

objective here is to obtain correlations for the turbulence model parameters for use in a prediction method. In the present study, this procedure is carried out for two situations and correlations are obtained for κ and K for the effects of pressure gradients and mainstream turbulence. Note that this type of procedure is only applicable to measured profiles for which the mainstream velocity is of the equilibrium type and where the data is at locations far downstream of wherever the turbulent boundary layer was initiated. The final correlations for the effects of pressure gradients and mainstream turbulence lead to excellent representations of the velocity profile data. In principle, the models developed here may be used in a prediction method for non-equilibrium flows.

The plan of this report is as follows. In §2, the basic equations and principle results of the asymptotic theory are summarized. In §3 the optimization procedure is described and in §4 and §5 the results of the method for pressure gradients and mainstream turbulence effects respectively are given. A description and test cases for the optimization code are given in Appendices C and D. Finally, the conclusions of the study are discussed in §6.

2. THE TURBULENT BOUNDARY LAYER TIME MEAN EQUATIONS

2.1 Basic Equations

The turbulent boundary layer equations governing two-dimensional, incompressible time-mean flow are the mass continuity equation and the Reynolds equation for streamwise momentum:

$$\frac{\partial \bar{u}}{\partial x} + \frac{\partial \bar{v}}{\partial y} = 0 \ , \tag{2.1}$$

$$\bar{u} \frac{\partial \bar{u}}{\partial x} + \bar{v} \frac{\partial \bar{u}}{\partial y} = U_\infty \frac{dU_\infty}{dx} + \frac{1}{Re} \frac{\partial^2 \bar{u}}{\partial y^2} + \frac{\partial \sigma}{\partial y} \ . \tag{2.2}$$

In these equations, (x,y) represent Cartesian coordinates with corresponding mean velocities ($\bar{u}$,$\bar{v}$). All lengths and velocity components have been made dimensionless with respect to L and U_0, a reference length and velocity respectively. The Reynolds number is defined as $\frac{U_0 L}{\nu}$ and is assumed to be large; here ν is the kinematic viscosity. The momentum equation (2.2) contains an additive stress term σ for turbulent flow which is related to the usual turbulent shear stress by

$$\sigma = \frac{\overline{-u'v'}}{U_0^2} \ . \tag{2.3}$$

In equation (2.3) the primed quantities are instantaneous velocity fluctuations about the corresponding mean values and the over bar signifies a long time average. The boundary conditions

associated with the equations (2.1) and (2.2) are

$$u(x,0) = v(x,0) = 0 \ ,$$
$$u(x,y) \to U_\infty(x) \text{ as } y \to \infty \ . \tag{2.4}$$

In addition to the above boundary conditions, the turbulent shear stress term must be chosen to satisfy

$$\sigma(x,0) = 0, \ \sigma(x,y) \to 0 \text{ as } y \to \infty \ . \tag{2.5}$$

To completely specify the problem, an initial velocity profile

$$u(0,y) = f(y) \text{ for } 0 \leq y < \infty \ , \tag{2.6}$$

must be given at some x-station in the fully turbulent region of the flow which is denoted here by x=0. Note that the problem is indeterminate until a model for the Reynolds shear stress term is specified; however, it is possible through asymptotic analysis of this problem to provide useful information about the velocity components and shear stress without the introduction of any specific functional form for the Reynolds stress term. Before this is carried out, it is desirable to define an important physical parameter, u^*, that will play an important role in the asymptotic analysis. The dimensional wall shear stress is given by

$$\tau_w = \frac{\mu_w U_o}{L} \frac{\partial \bar{u}}{\partial y}\bigg|_{y=0} , \qquad (2.7)$$

and is used to define the dimensional skin friction velocity

$$u_\tau = \sqrt{\tau_w/\rho_w} , \qquad (2.8)$$

where μ_w and ρ_w represent the dynamic viscosity and density at the wall respectively. A dimensionless skin friction velocity can be defined as

$$u^* = \frac{u_\tau}{U_o U_\infty(x)} . \qquad (2.9)$$

Note that equation (2.7) can be rewritten in an equivalent form as

$$u^{*2} U_\infty{}^2 = \frac{1}{Re} \frac{\partial u}{\partial y}\bigg|_{y=0} . \qquad (2.10)$$

The asymptotic structure of equation (2.2) in the limit of large Reynolds number will now be considered.

2.2 Asymptotic Structure of the Time-Mean Equations

It is well known that the turbulent boundary layer is a composite double layer consisting of a thin inner layer adjacent to the wall and a relatively thick outer layer. A number of authors, including Fendell (1972) and Mellor (1972), have

considered the asymptotic structure of the time-mean momentum equations for a constant property incompressible flow; in these studies, asymptotic methods are used to isolate the leading terms in an expansion for large Reynolds number for the flow quantities in both the inner and outer region of the turbulent boundary layer. These expansions are then matched in a manner which is consistent mathematically and which is also consistent with experimental measurements of the time-mean flow quantities for both regions. Fendell (1972) also examines the conditions necessary for self-similar flow in the outer region. The asymptotic results that follow summarize the work of Fendell (1972) and are also discussed by Scharnhorst et al (1978).

In the outer region of the turbulent boundary layer, the velocity profile may be written as a small perturbation about the mainstream value as $Re \to \infty$, according to,

$$\bar{u} = U_\infty(x)\{1+u^*(x;Re)\frac{\partial F_1}{\partial \eta}(x,\eta) + \ldots\}, \qquad (2.11)$$

Here u^* is the dimensionless skin friction velocity defined by equation (2.9) and $u^* \to 0$ as $Re \to \infty$. In the outer region, the turbulence term σ may be written to leading order as

$$\sigma = U_\infty^2(x)\{u^{*2}(x;Re)\Sigma_1(\eta,x)+ \ldots\} \quad . \qquad (2.12)$$

Here η is the scaled normal coordinate for the outer region

defined by,

$$\eta = y/\Delta_0 \quad . \tag{2.13}$$

The dimensionless outer region length scale Δ_0 is proportional to the boundary layer thickness and is $O(u^*)$; a convenient choice for Δ_0 is made in section 2.4. It is of interest to note that the shear stress term given in (2.12) is equivalent to the result that $\overline{u'v'}$ is $O(u^2{}_\tau)$ which, in general, is confirmed by experimental measurement. When the velocity profile expansion (2.11) and the turbulence term expansion (2.12) is substituted into (2.2) and terms quadratic in the perturbation u^* are neglected, an equation for the velocity defect function $u_1 = \partial F_1/\partial\eta$ is obtained according to

$$\frac{\partial \Sigma_1}{\partial \eta} = \frac{\Delta_0}{u^{*2}U^2_\infty}\,(u^*U_\infty{}^2)'\,\frac{\partial F_1}{\partial \eta} - \frac{1}{u^*U_\infty}\,(U_\infty\Delta_0)'\eta\,\frac{\partial^2 F_1}{\partial \eta^2} + \frac{\Delta_0}{u^*}\,\frac{\partial^2 F_1}{\partial \eta \partial x}\,. \tag{2.14}$$

Here a prime denotes differentiation with respect to x.

This equation is subject to the boundary conditions

$$F_1(x,\eta) \to 0 \text{ as } \eta \to 0\,, \tag{2.15}$$

and

$$\frac{\partial F_1}{\partial \eta}\,(x,\eta) \to 0 \text{ as } \eta \to \infty \quad . \tag{2.16}$$

In the inner layer, sometimes referred to as the wall layer, the velocity profile and turbulence stress term expansions may be written to leading order according to

$$\bar{u} = u^* U_\infty(x) \frac{\partial f_1}{\partial y^+}(x,y^+) + \ldots , \tag{2.17}$$

and

$$\sigma = U_\infty^2(x) u^* \sigma_1(x,y^+) + \ldots , \tag{2.18}$$

where

$$y^+ = \frac{u_\tau L}{\nu} y = Re\, u^* U_\infty(x) y , \tag{2.19}$$

is the inner region variable. The matching of the leading order terms in the asymptotic expansions (2.11) and (2.17) and (2.12) and (2.18) occur in the limits $\eta \to 0$ and $y^+ \to \infty$ for the inner and outer layers respectively. A self consistent mathematical structure which is compatible with experimental measurement may be obtained if both velocity profiles merge smoothly with a logarithmic profile behavior according to

$$u_1 \sim \frac{1}{\kappa(x)} \log \eta + C_o(x), \text{ as } \eta \to 0 , \tag{2.20}$$

and

$$u^+ \sim \frac{1}{\kappa(x)} \log y^+ + C_i(x), \text{ as } y^+ \to \infty. \tag{2.21}$$

Here κ, C_o and C_i are in general functions of x. Although κ

is analogous to the von Karman "constant" which is normally assumed to have a value of about 0.41, in general κ could depend on local flow conditions. It is worthwhile to note that the conditions for the turbulence terms also follow from the analysis (Fendell, 1972) and are

$$\Sigma_1 \to 1 \quad \text{as} \quad \eta \to 0 \ , \tag{2.22}$$

and

$$\sigma_1 \to 1 \quad \text{as} \quad y^+ \to \infty \ . \tag{2.23}$$

First order matching of the inner and outer asymptotic expansions leads to the velocity match condition given by,

$$\frac{1}{u^*} = \frac{1}{\kappa(x)} \log\{\Delta_0 \ \mathrm{Re} \ u^* U_\infty(x)\} + C_i - C_o \ . \tag{2.24}$$

This skin friction relation connects u^* and the outer region length scale Δ_0. The match condition to leading order as $\mathrm{Re} \to \infty$ implies that

$$u^* \sim \frac{\kappa(x)}{\log \mathrm{Re}} \ . \tag{2.25}$$

and since Δ_0 is $O(u^*)$ the turbulent boundary layer thickness approaches zero as the inverse of a logarithm in the high Reynolds number limit.

A composite velocity profile valid to leading order across the entire boundary layer can be formulated. Van Dyke (1975)

defines a composite expansion according to

$$[\text{composite expansion}] = [\text{inner expansion}] + [\text{outer expansion}] - [\text{common terms}]. \qquad (2.26)$$

The common terms represent the behavior of the inner and outer expansions in the matching region. A composite streamwise velocity profile is defined here according to,

$$\bar{u} = u^* U_\infty \left[U^+ + U_1 - \{ \frac{1}{\kappa(x)} \log \eta + C_0 \} \right]. \qquad (2.27)$$

Alternatively, an equivalent expression could be composed by using equation (2.24) for the common terms in terms of the inner region variable y^+.

The question of determining good model profile approximations for the inner profile U^+ and the outer profile U_1 will now be considered.

2.3 Similarity in the Outer Region

The model profile that will be used for the outer region flow is a self-similar profile and for this reason it is of interest to examine the conditions necessary for self-similar flow in the outer region. The terms self-similar and equilibrium are often used interchangeably in the literature but it is important to make a distinction here. The term equilibrium is understood to apply

to a turbulent boundary layer for which the mainstream velocity behaves as $U_\infty(x) \sim x^\alpha$ or $U_\infty(x) \sim e^{\beta x}$ where α and β are constants; on the other hand, self similarity of the outer layer velocity profile can only occur when the boundary layer is exposed to the equilibrium outer velocity contributions for large streamwise distances. Consequently, equilibrium is a necessary but not sufficient condition for the existence of self-similar profiles.

The necessary conditions for similarity follow from equation (2.17) for U_1 and are that,

$$\frac{\Delta_o}{u^{*2}U_\infty^2}\,(u^*U_\infty^2)' = -2\beta = \text{constant} \tag{2.28}$$

and

$$\frac{1}{u^*U_\infty}\,(\Delta_o\, U_\infty)' = \alpha = \text{constant}. \tag{2.29}$$

To assess the magnitude of the ratio $u^{*\prime}/u^*$ which appears in equation (2.28), the match condition, given by equation (2.24), is differentiated with respect to x to obtain,

$$-\frac{u^{*\prime}}{u^{*2}} = \frac{-\kappa'}{\kappa^2}\log\{\Delta_o Re\; u^*U_\infty(x)\} + \frac{1}{\kappa}\left\{\frac{\Delta_o'}{\Delta_o} + \frac{u^{*\prime}}{u^*} + \frac{U_\infty'}{U_\infty}\right\} + C_i' - C_o'. \tag{2.30}$$

This equation can be simplified by using the match condition (2.24) to eliminate the first term on the right hand side and this procedure yields

$$\frac{u^{*\prime}}{u^*} = \frac{\kappa'}{\kappa} - \frac{u^*}{\kappa}\left\{\frac{\Delta_o'}{\Delta_o} + \frac{u^{*\prime}}{u^*} + \frac{U_\infty'}{U_\infty} + \kappa'(C_i - C_o) + \kappa(C_i - C_o)'\right\}. \tag{2.31}$$

Since κ must approach a constant for a self-similar flow, the order of magnitude of the ratio $u^{*\prime}/u^*$ follows from equation (2.31) and

$$\frac{u^{*\prime}}{u^*} \approx O(u^*). \tag{2.32}$$

Terms containing this ratio may be neglected to leading order in (2.28) and (2.29) which become

$$q\,\frac{U_\infty'}{U_\infty} = -\beta \tag{2.33}$$

and

$$q' + \frac{U_\infty'}{U_\infty}\,q = \alpha \tag{2.34}$$

respectively where $q = \Delta_o/u^*$. These two equations are combined to give

$$q' = \alpha + \beta \quad . \tag{2.35}$$

As a result, there are only two types of mainstream velocity distributions which can lead to self-similar solutions in the outer layer and these are:

$$U_\infty(x) = D_1(x - x_o)^{\alpha_1} \quad \text{for } \alpha + \beta \neq 0 \tag{2.36}$$

where

$$\alpha_1 = \frac{-\beta}{\alpha+\beta} \ , \ q = \frac{\Delta_o}{u^*} = (\alpha+\beta)(x-x_o) \qquad (2.37)$$

and

$$U_\infty(x) = D_2 e^{-\alpha_2 x} \text{ for } \alpha + \beta = 0 \qquad (2.38)$$

where

$$a_2 = \frac{\beta}{x_o} \ , \ q = \frac{\Delta_o}{u^*} = x_o \ . \qquad (2.39)$$

Here D_1, D_2, and x_o are all arbitrary constants.

Equilibrium flows have been examined experimentally for a number of years and an equilibrium boundary layer has been defined experimentally as a flow in which the dimensionless velocity defect $(U_e - \bar{u}^*)/u_\tau$ expressed as a function of y/δ becomes close to being invariant with downstream distance. After careful experimentation, Clauser (1954,1956) concluded that the criterion for equilibrium was a constant value of the parameter β_c which is defined as

$$\beta_c = - \frac{\delta^*}{u^2_\tau} U_e \frac{dU_e}{dx} \ . \qquad (2.40)$$

Here δ^* represents the dimensionless displacement thickness defines as

$$\delta^* = \int_o^\infty (1 - \frac{\bar{u}}{U_\infty(x)})dy \ . \qquad (2.41)$$

From the definition of δ^* and equations (2.11) and (2.13) it

follows that,

$$\delta^* = -\Delta_0 u^* F_1(x,\infty) + \ldots \quad . \tag{2.42}$$

As self-similarity conditions are approached, the x dependence must vanish and $F_1(x,\infty)$ must approach a constant value, say $F_1(\infty)$. Thus (2.40) becomes

$$\beta_c = \frac{\Delta_0 F_1(\infty)}{u^* U_\infty} \frac{dU_\infty}{dx} = -\beta F_1(\infty) \quad . \tag{2.43}$$

Note that a constant value of β implies a constant value of β_c and therefore Clauser's (1954,1956) experimental results are consistent with theory.

2.4 The Eddy Viscosity Model for the Outer Region

In order to obtain a solution of the outer layer equations, a constitutive relation for $\overline{u'v'}$ in the outer layer must be specified and for the reasons discussed in section 1, a simple eddy viscosity model will be used here. It is worthwhile to note that although it is customarily assumed that some functional relationship exists between $\overline{u'v'}$ and the mean velocity profile, no such relationship has been demonstrated either experimentally or theoretically; consequently, the eddy viscosity hypothesis should be regarded at present as a convenient approximation which is expected to be supplanted in the future by constitutive

models based on the observed coherent structure of the turbulent boundary layer.

For the outer region, the Reynolds stress is defined as

$$-\overline{u'v'} = \varepsilon_o \frac{U_o}{L} \frac{\partial \bar{u}}{\partial y} = U_o^2 \sigma \quad , \tag{2.44}$$

and from equations (2.12) and (2.13), the stress function Σ_1 becomes

$$\Sigma_1 = \frac{\varepsilon_o}{\Delta_o U_o U_\infty(x) L u^*} \frac{\partial U_1}{\partial \eta} \quad , \tag{2.45}$$

where ε_o depends upon both x and η. The functional form for ε_o is the same type as that used in the Cebeci-Smith (1969) and Mellor and Herring (1969) prediction methods. In this model, ε_o is selected to approach a constant value for fixed x near the outer edge of the outer layer. Thus,

$$\varepsilon_o \rightarrow K\, U_e(x) \delta^* L \tag{2.46}$$

where δ^* is the dimensionless displacement thickness and K is an empirically determined constant. The value of K differs slightly according to the model; Cebeci and Smith (1969) take K = 0.0168 while Mellor and Herring (1968) use K = 0.016. In the present study, a universal value for K is not assumed; rather one objective is to determine if this parameter depends in any way on the pressure gradient.

Near the inner edge of the outer layer, the eddy viscosity must behave linearly to satisfy the matching condition for Σ_1 given in equation (2.22); it is convenient to define a dimensionless eddy viscosity function $\epsilon(\eta)$ according to

$$\epsilon(\eta) = \frac{\varepsilon_o}{\delta^* U_o U_\infty(x) L} , \tag{2.47}$$

whereupon equation (2.45) becomes

$$\varepsilon_1 = \frac{\delta^*}{u^* \Delta_o} \epsilon(\eta) \frac{\partial U_1}{\partial \eta} . \tag{2.48}$$

The function $\epsilon(\eta)$ must assume the following limiting values:

$$\epsilon \to \kappa \eta \left(\frac{u^* \Delta_o}{\delta^*}\right) \quad \text{as} \quad \eta \to 0 , \tag{2.49}$$

and

$$\epsilon \to K \quad \text{as} \quad \eta \to \infty . \tag{2.50}$$

A particularly convenient choice for the outer region length scale Δ_o is

$$\Delta_o = \frac{\delta^*}{u^*} , \tag{2.51}$$

and it follows that $F_1(x,\infty)=-1$ from equation (2.42). Detailed reasons behind this choice for Δ_o are discussed by Scharnhorst et al. (1978) and Scharnhorst (1978) and Weigand (1978). Equations (2.45) and (2.49) may now be rewritten as

$$\varepsilon_1 = \varepsilon(\eta) \frac{\partial U_1}{\partial \eta} \tag{2.52}$$

and

$$\varepsilon \to \kappa\eta \quad \text{as} \quad \eta \to \infty \, . \tag{2.53}$$

In general, the functional form of $\varepsilon(\eta)$ must be specified. The model of Mellor and Gibson (1966) and Mellor and Herring (1969) use a simple form of two straight lines defined by

$$\varepsilon(\eta) = \varepsilon_m(\eta) = \begin{cases} K & \text{for} \quad \eta \geq \eta_1 \, , \\ \kappa\eta & \text{for} \quad \eta < \eta_1 \, , \end{cases} \tag{2.54}$$

where $\eta_1 = K/\kappa$. An awkward feature of this model lies in the discontinuous derivative at $\eta = \eta_1$ which may be expected to give rise to difficulties in a numerical solution of the outer layer equation; this problem is handled by Cebeci and Smith (1974) by using an artificial smoothing of the model in equation (2.54). An alternative functional form for $\varepsilon(\eta)$ must reflect the linear behavior near η=0 in equation (2.53) and the limiting constant value in equation (2.50) for large η; moreover, such a function should be monotonically increasing with η. A rather complex function meeting these requirements was assumed by Scharnhorst et al. (1977) who, in addition, determined that it appeared to be desireable for $\varepsilon(\eta)$ to approach the linear behavior $\kappa\eta$ exponentially quickly for small values of η. It also appeared

important for $\varepsilon(\eta)$ to approach the upper bound K relatively quickly for large η.

A particularly simple form of a function that satisfies all the desired features of $\varepsilon(\eta)$ is

$$\varepsilon(\eta) = \kappa\eta\{1-e^{-C/\eta^N}\}^{1/N} \tag{2.55}$$

which is plotted in Figure 2.1 for integral values of N = 1, 2, and 4. Here, the term C is given by

$$C = \left(\frac{K}{\kappa}\right)^N \quad . \tag{2.56}$$

This monotonically increasing function (2.55) meets the requirements as $\eta \to 0$,

$$\varepsilon(\eta) \to \kappa\eta \, , \tag{2.57}$$

and as $\eta \to \infty$,

$$\varepsilon(\eta) \to K\{1 + O(\frac{1}{\eta^N})\} \quad . \tag{2.58}$$

Note that this function for N=4 is virtually identical to the form used by Scharnhorst et al. (1977) but is a much simpler form.

The outer region eddy viscosity function given by equation (2.55) was used throughout this study with N=4.

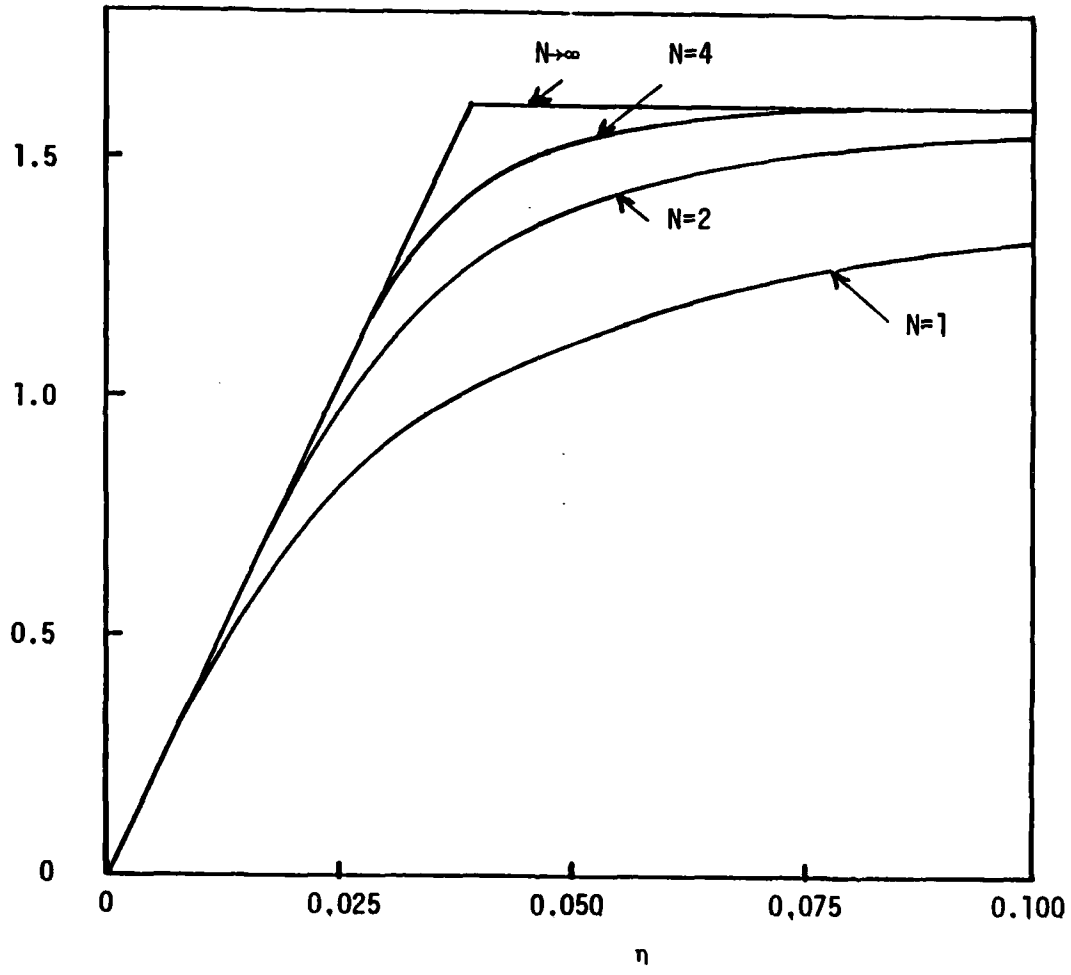

FIGURE 2.1 The Eddy Viscosity Function

2.5 Outer Layer Similarity Model

With the outer layer stress function defined by equation (2.52), it may be shown that the outer layer equation (2.14) becomes

$$\frac{\partial}{\partial\eta}\{\varepsilon(\eta)\frac{\partial U_1}{\partial\eta}\} + \frac{(U_\infty\Delta_o)'}{u^*U_\infty}\,\eta\,\frac{\partial U_1}{\partial\eta} - \frac{\Delta_o(u^*U_\infty{}^2)'}{u^{*2}U_\infty{}^2}\,U_1 = \frac{\Delta_o}{u^*}\frac{\partial U_1}{\partial x}\,, \tag{2.59}$$

where $U_1 = \partial F_1/\partial\eta$. For a self-similar flow, equation (2.59) reduces to the ordinary differential equation

$$\frac{d}{d\eta}\{\varepsilon\,\frac{dU_1}{d\eta}\} + \{\frac{\delta^{*\prime}}{u^{*2}} - \beta_c\}\,\eta\,\frac{dU_1}{d\eta} + 2\beta_c\,U_1 = 0\,, \tag{2.60}$$

where β_c is the Clauser pressure gradient parameter obtained from equation (2.40) as $\beta_c = -\delta^*U_\infty'/(u^{*2}U_\infty)$. Integration of equation (2.60) across the boundary layer yields the relation

$$\frac{\delta^{*\prime}}{u^{*2}} = 1 + 3\beta_c\,, \tag{2.61}$$

which can be substituted back into (2.60) to obtain

$$\frac{d}{d\eta}\{\varepsilon(\eta)\,\frac{dU_1}{d\eta}\} + (1+2\beta_c)\eta\,\frac{dU_1}{d\eta} + 2\beta_c\,U_1 = 0. \tag{2.62}$$

To find the velocity profile in the outer region, equation (2.62) must be solved subject to the boundary conditions,

$$U_1 \sim \frac{1}{\kappa} \log \eta + C_0 \quad \text{as} \quad \eta \to 0 \,, \tag{2.63}$$

$$U_1 \to 0 \quad \text{as} \quad \eta \to \infty \,. \tag{2.64}$$

Note that the constant C_0 is unknown. This problem was solved by a combination of a series solution near $\eta=0$ and a fully numerical solution for $\eta>0$; the procedure is described in Appendix A.

Note that there are two parameters associated with equation (2.62) and the boundary condition (2.63); these are the eddy viscosity parameters K and the von Karman constant κ which appears in the eddy viscosity and in the boundary condition. In addition to the physical boundary layer quantities, the skin friction u_τ and the displacement thickness are contained in the parameter β_c which is defined in equation (2.40) and which appears in equation (2.62).

2.6 Wall Layer Model

The wall layer model used in this study incorporates what are believed to be the important features of the time dependent flow in the wall layer. A complete discussion of the ideas that develop the unsteady wall layer model is given in Walker, Abbott and Scharnhorst (1976), Walker and Abbott (1977), and Walker and Scharnhorst (1977). This "unsteady wall layer model" has

been extensively compared to experimental data by Scharnhorst et al. (1977) who demonstrate that the model closely represents measured velocity profile data in the wall layer even in flows with pressure gradient; moreover, the representation is considerably better than that obtained by a conventional Van Driest (1956) type of model and, finally, the model is simpler to use. For these reasons, this "unsteady wall layer model" was used exclusively in the present study.

The profile given by Walker and Scharnhorst (1977) is

$$U^+ = [1 + \frac{t_o^+}{S^2}][R(S^2,t_o^+)Q(H) + Z(H) + P(S^2,t_o^+)W(H)] - \frac{t_o^+}{S^2}[R(0,t_o^+)Q(H_o) + Z(H_o) + P(0,t_o^+)W(H_o)], \quad (2.65)$$

where

$$H = \frac{y^+}{2\sqrt{S^2+t_o^+}} \quad , \quad H_o = \frac{y^+}{2\sqrt{t_o^+}} \quad , \quad (2.66)$$

and

$$R(S^2,t_o^+) \equiv C_i - \frac{1}{\kappa}\{\frac{\gamma_o}{2} - \log 2\} + \frac{1}{2}p^+(S^2+2t_o^+) + \frac{1}{2\kappa}\log(S^2+t_o^+) \quad , \quad (2.67)$$

$$Q(H) \equiv (2H^2+1)\,\mathrm{erf}\,H + \frac{2}{\sqrt{\pi}}H\,e^{-H^2} \quad , \quad (2.68)$$

$$Z(H) \equiv \frac{4}{\kappa\sqrt{\pi}}[(2H^2+1)\Xi(H) + H\Xi'(H) - \frac{\sqrt{\pi}}{8}(6H^2+1)\mathrm{erf}\,H - \frac{3}{4}H\,e^{-H^2}], \quad (2.69)$$

$$P(S^2,t_o^+) \equiv -\frac{2}{3}\, p^+(S^2+t_o^+) \ , \tag{2.70}$$

$$W(H) = [H^4+3H^2+\frac{3}{4}]\mathrm{erf}\ H - \frac{H}{\sqrt{\pi}}\,[H^2+\frac{5}{2}]e^{-H^2} - 3H^2 \ . \tag{2.71}$$

In the equations above, the Ξ function is defined as

$$\Xi(\eta) = \int_0^h e^{-x^2} \int_0^x e^{y^2} \int_0^y e^{-t^2}\, dt\, dy\, dx \ . \tag{2.72}$$

A detailed description of the Ξ function and its properties is given in Appendix B. For large y^+ in the inner region, the asymptotic form of the profile (2.65) is

$$U^+ \sim \frac{1}{\kappa} \log y^+ + C_i \ . \tag{2.73}$$

Note that the model contains κ and C_i as parameters in addition to t_o^+ and S; these last two parameters are associated with the physics of the wall layer time dependent flow and are discussed in detail by Walker and Scharnhorst (1977) and Scharnhorst (1978). The mean velocity profile of (2.65) must satisfy

$$\left.\frac{\partial U^+}{\partial y^+}\right|_{y^+=0} = 1 \ , \tag{2.74}$$

and the wall compatibility condition

$$\left.\frac{\partial^3 U^+}{\partial y^{+3}}\right|_{y^+=0} = 0 \ , \tag{2.75}$$

which leads to the auxiliary relations

$$(S^2+t_o^+)^{\frac{1}{2}}[R(S^2,t_o^+)-\frac{1}{\kappa}+P(S^2,t_o^+)]$$
$$-(t_o^+)^{\frac{1}{2}}[R(0,t_o^+)-\frac{1}{\kappa}+P(0,t_o^+)]=\frac{\sqrt{\pi}}{2}S^2\,, \qquad (2.76)$$

and

$$(S^2+t_o^+)^{-\frac{1}{2}}[R(S^2,t_o^+)+3P(S^2,t_o^+)]$$
$$-(t_o^+)^{-\frac{1}{2}}[R(0,t_o^+)+3P(0,t_o^+)]=0\,, \qquad (2.77)$$

respectively. Note that equations (2.76) and (2.77) are two relations for the four parameters κ, C_i, S, and t_o^+ and consequently only two of these parameters are independent. In the data comparisons that are carried out here, κ and S were generally assumed to be variables that were adjusted to obtain the best fit to the data; thus, at any stage in the optimization procedure for specified values of κ and S, equations (2.76) and (2.77) were solved for t_o^+ and C_i.

2.7 Summary

A composite similarity velocity profile valid to leading order for the entire boundary layer has been developed in this section according to

$$\bar{u}=u^*U_\infty\left[U^+ + U_1 - \{\frac{1}{\kappa(x)}\log\eta + C_o\}\right]. \qquad (2.78)$$

Here U^+ is the unsteady wall layer model given in section 2.6; this model is an analytic expression given by equation (2.65) which contains the independent parameters κ and S. The outer region profile $U_1(\eta)$ must be obtained as a numerical solution of differential equation (2.62) developed in section 2.5; this numerical solution will implicitly contain the parameters κ and K which appear in the eddy viscosity model. Thus, the composite profile contains the three independent model parameters S, κ and K that may be adjusted in a computer optimization routine to obtain a best fit with experimental velocity profile data.

3. THE OPTIMIZATION TECHNIQUE

3.1 Background

The present turbulence velocity profile model contains three adjustable model parameters S, κ, and K that affect the basic shape of the analytical profile. This section addresses the development of a systematic method to determine the optimum values of the model parameters that minimize the difference between the analytical model profile and experimental data. The method described here can, in principle, be applied to any test data to attempt to determine any trends in the data with different physical effects; in particular, the procedure is applied here to data for several pressure gradient flows and mainstream turbulence levels.

Before examining the optimization method, a basis for determining a best fit must be defined. For this study a root-mean-square error ε was selected according to

$$\varepsilon^2 = \frac{1}{N} \sum_{n=1}^{N} \left\{ \frac{\bar{u}_{DATA}(y_n) - \bar{u}_{ANALYTICAL}}{U_e} \right\}^2 \qquad (3.1)$$

where

N = number of data points

$\bar{u}_{DATA}$ = experimentally measured velocity at y_n

$\bar{u}_{ANALYTICAL}$ = analytical velocity profile at y_n

U_e = freestream velocity .

The best analytical fit to a given experimental profile is defined as that set of model parameter values which minimizes ϵ as defined by (3.1). Previous prediction techniques such as those presented in Scharnhorst et al. (1977) and those used in the Stanford Conference (Coles & Hirst, 1969) utilize the standard error criterion of (3.1) as an objective basis of comparison. The particular optimization method used in this study is presented in the next subsection.

3.2 The Optimization Method - Direct Search

A direct search minimization procedure was used to optimize the composite velocity profile. This technique is simple to use since it only requires values of the objective function and not gradients to carry out the optimization search. The nature of the problem is such that gradients of the objective function cannot be computed analytically and can only readily be evaluated by numerical differentiation. Although the direct search procedure becomes very time consuming when the number of optimization variables is large, it was used here with good success since the maximum number of variables is three. The basic procedure in the direct search minimization was to vary one model parameter such that the least squares error objective function would continuously decrease while holding the other

parameters constant. Each model parameter is varied in turn so that at any stage in the optimization procedure, a one-dimensional search is made for the minimum in that direction. The method used here is somewhat similar to the direct search method of Hooke and Jeeves which is described in Himmeblau (1972) p. 142. The specific logic involved is as follows.

The optimization scheme starts with initial values for the model parameters which must be provided to the subroutine as well as a vector of initial incremental step sizes for the parameters. This initial location is established as a base point. To initiate a search, the objective function $f^{o}(x)$ is evaluated at this base point and one parameter x_1 is then incremented by the specified step size Δx_1. Suppose first that the objective function decreases. The parameter x_1 is incremented continually according to $x_1^{(i+1)} = x_1^{(i)} + \Delta x_1$ and the objective function $f^{(i+1)} = f(x_1^{(i+1)})$ is computed. This process continues for i = 0, 1, 2, 3, ... as long as $f^{(i)}$ continually decreases. Eventually, at a certain step, say step k, the objective function will increase and $f^{(k+1)} > f^{(k)}$. At this stage, a local minimum in the x_1 direction has been bracketed in the range $x_1^{(k-1)} \leq x_1^{(k)} \leq x_1^{(k+1)}$. To further refine the location of this minimum, a quadratic interpolation polynomial, $f = Ax_1^2 + Bx_1 + C$ is used, where A, B, and C are

determined by solving the set of equations:

$$f^{(i)} = Ax_1^{(i)2} + Bx_1^{(i)} + C \qquad (3.2)$$

where

$$i = k\text{-}1,\ k,\ \text{and}\ k+1 \quad .$$

This interpolation polynomial produces a local minimum in the x_1 direction at $x_1^* = -B/2A$. In certain cases, this interpolation scheme may produce a value of x_1^* which is not close to the midpoint of the interval $x_1^{(k)}$ or an objective function which $f^{(*)}$ is not close to $f^{(k)}$. When this situation occurs, then three of the values x_1^*, $x_1^{(k-1)}$, $x_1^{(k)}$, and $x_1^{(k+1)}$ which have the lowest objective function are relabeled as $x_1^{(i-1)}$, $x_1^{(i)}$, and $x_1^{(i+1)}$ and another quadratic interpolation polynomial is fit through these values to obtain a new minimum x_1^*. The interpolation scheme is repeated until a specified convergence criteria is met between the values of x_1^* and $x_1^{(k)}$ or $f^{(x)}$ and $f^{(k)}$. After convergence in the x_1 parameter, the new value of x_1 is retained as the base point; the next parameter x_2 is incremented by the specified step size Δx_2, and the search procedure repeats until all the independent parameters have been changed.

In the second place suppose that an increase in the objective function is realized for the initial step of a model

parameter (for example, x) from its base point. When this situation occurs, the search direction is immediately changed to the negative direction and the program procedure continues as previously stated. In the event that the objective function increases for the first step in the negative direction as well, the program enters into the quadratic interpolating routine since the local minimum has been bracketed in the range $x_1-\Delta x_1 \leq x_1 \leq x_1 + \Delta x_1$. After the local minimum has been refined, a one-dimensional search is carried out for the next variable.

After a one-dimensional search for each variable has been carried out by the above procedure, a new base point is established and a convergence test is performed in which the optimization function values for the last two base points are compared. If these two values differ by an amount less than a specified criterion, a minimum has been found and the program terminates. If the convergence criterion is not met, the step sizes Δx_i of the search are reduced ten percent and the search procedure starts anew from the current base point.

The direct search program contains two types of error flags. The first type of error flag is encountered when the number of combined step and interpolation iterations reaches a specified maximum value. This error flag then terminates the optimization routine and returns to the prediction code

with the latest values for the optimized parameters. The second type of error flag occurs in the quadratic interpolation scheme when the value of the A coefficient of the quadratic polynomial is identically zero. This flag prevents a computation error in the interpolation process and terminates the direct search program. One variable returned by the subroutine is the error variable IER; values IER= 1 and IER = 2 indicate errors of the first and second type respectively. A value IER = 0 indicates a successful search has been completed.

4. TURBULENT BOUNDARY LAYER PROFILE REPRESENTATION

4.1 Introduction

In order to obtain a velocity profile representation for a given set of velocity profile data, one or more of the composite profile parameters S, κ, and K can be altered in several combinations. Each such combination defines a different method of profile representation; if a parameter is not optimized, it must be assigned a universal value. In the study of Scharnhorst (1978), one method considered was to take κ=0.41 (the generally accepted universal value for the von Karman constant) and S=10.4965; this value of S is the value which with κ=0.41 produces a value of C_i = 5.1 in equations (2.76) and (2.77); again C_i = 5.1 is a generally accepted value. Scharnhorst (1978) then carried out a one parameter optimization on K over a wide range of pressure gradient data; the results of this optimization were not encouraging. The principal difficulty was that the analytical profile tended to skew through the data in the logarithmic zone. This difficulty was noted by Scharnhorst (1978) and is illustrated in Figure 4.1; in this figure the results of a one parameter optimization on K (with κ=0.41, S=10.4965) are illustrated for three stations of the data of Anersen et al (1972). These stations are labeled 8109, 8209, and 8309 and are the last measured data stations in equilibrium flows for zero, moderate and strong

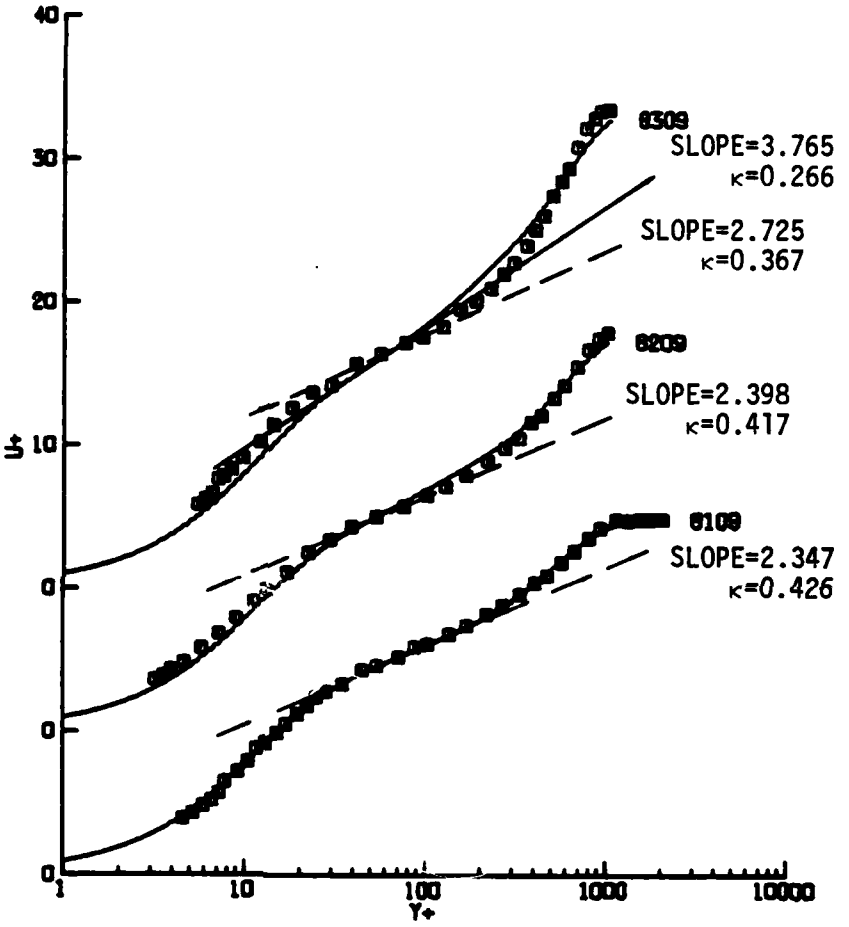

FIGURE 4.1 Velocity profile comparisons for one parameter optimization on K (with κ=0.41, S=10.4965) for three data stations of Andersen et al. (1972). Profiles are for a zero, mild adverse and strong adverse pressure gradient flow; note procedure is less satisfactory with increasing pressure gradient.

adverse pressure gradient flows respectively. It may be observed from Figure 4.1 that the theoretical profile represents the constant pressure profile well in the overlap zone but is increasingly less satisfactory there as the pressure gradient becomes larger. It may be observed from Figure 4.1 that for stations 8209 and 8309, a larger value of κ appears to be indicated in order to decrease the slope of the profile to conform to the data.

However, there are two main difficulties associated with the fitting problem and it is worthwhile to discuss these here before proceding further. The first problem has been termed a "low Reynolds" number effect by Scharnhorst (1978) and is associated with a failure of the composite analytical profile to adequately delineate various regions of the boundary layer. To understand this last statement, consider profile 8309 in Figure 4.1; the solid straight line is apparently tangent to the curve in the overlap zone of the profile. The inverse of the slope of this straight line may be obtained graphically and is indicated on the figure as κ=0.266; however, the value of κ used to obtain the profile in the figure was κ=0.41. The reason for this difficulty may be clearly observed in Figure 4.2 which illustrates composite similarity profiles for two values of the Reynolds number based upon the displacement thickness, δ^*, for fixed values of β_c = 0, K = 0.016, and κ = 0.41. In preparing this figure,

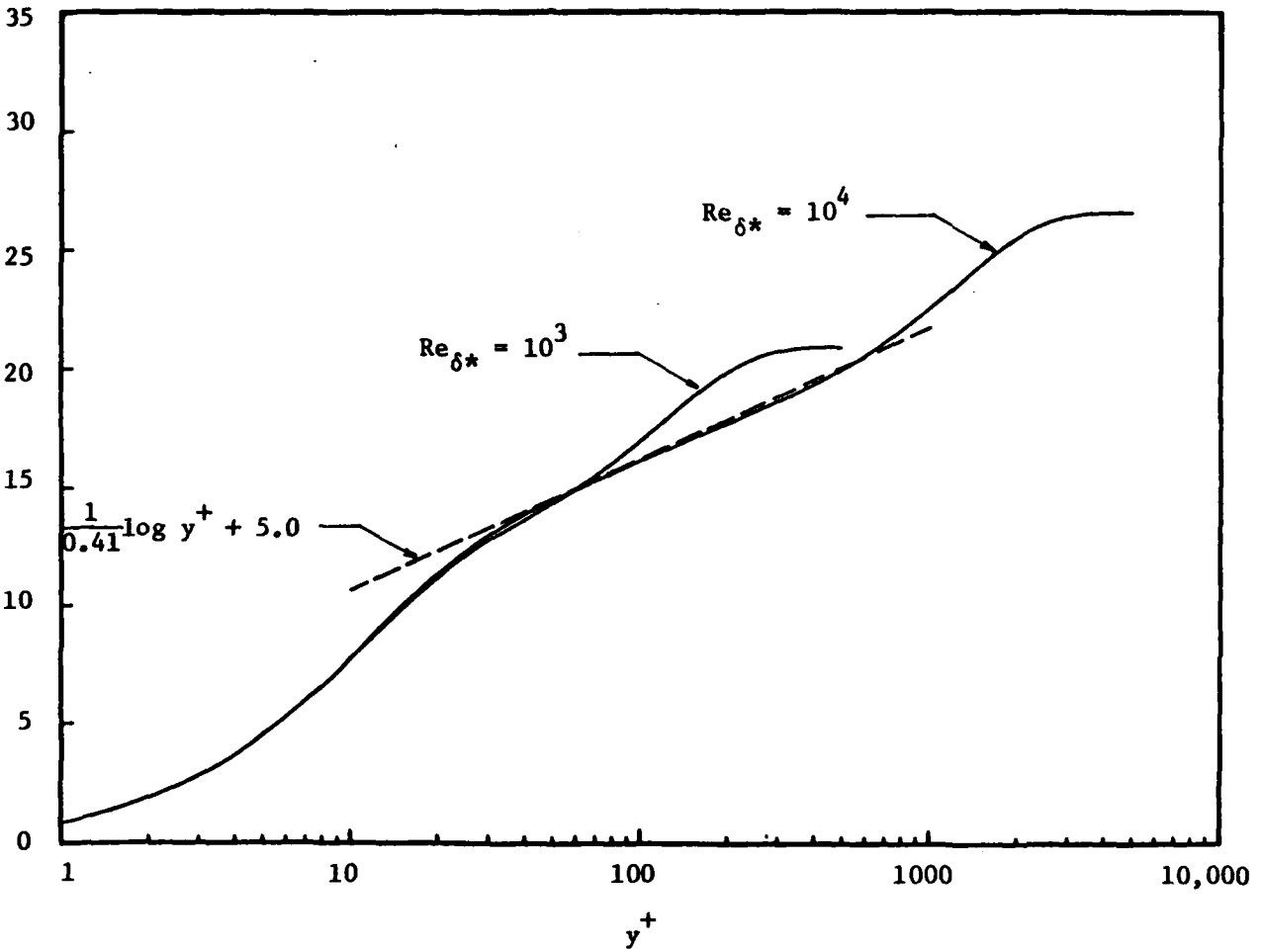

Figure 4.2 Composite similarity profile for S = 10.4965, K = 0.016, κ = 0.41 and β_c = 0.

a value of Re δ^* = 10^3 was chosen since it is typical of practical flows that occur in engineering practice. For $Re_\delta{}^*$ = 10^3 the range of y^+ that exhibits logarithmic behavior is apparently relatively short and the slope of the analytical profile in this region appears to be greater than the value $1/\kappa$. The reason for this behavior is associated with the value of $Re_\delta{}^*$ which relates the inner variable y^+ to the outer variable η by $y^+ = Re_\delta{}^* \eta$. For $Re_\delta{}^*$ = 10^3, a value of y^+ = 100 would correspond to an outer variable value of η=0.1; for this reason, the apparent range of logarithmic behavior in Figure 4.2 for $Re_\delta{}^*$ = 10^3 is relatively short and significant portions of the inner and outer regions blend together in the overlap zone. To show the effect on the profile as the Reynolds number becomes larger, a composite similarity profile is also presented in Figure 4.2 for a value of $Re_\delta{}^*$ arbitrarily increased to 10^4. It may be observed that a logarithmic region emerges over a wider y^+ range and that the composite similarity profile corresponds on the graph more closely with the input log-law behavior.

A second difficulty associated with the fitting of the composite profile is encountered with moderate to strong pressure gradient flows where β_c is O(1). It may be observed in the series solution for the outer profile given in equation (A.4)

that for all $\beta_c \neq 0$, the series contains terms of the form $a_i \eta^i \log \eta$ in addition to the purely logarithmic term $(1/\kappa)\log\eta$; two points about these terms are germane. In the first place, it may easily be verified that such terms arise in the series because of the pressure gradient term in the outer layer equation and are not associated with the choice of turbulence model per se. Secondly, although $\eta^i \log\eta \to 0$ as $\eta \to 0$ for all $i > 0$, such terms do give a significant contribution for $\eta \neq 0$ and the purely logarithmic behavior of $(1/\kappa)\log \eta$ will only be realized for very small η. As previously indicated, for low Re_δ^*, very small values of η will correspond to moderate (but not large) values of y^+ and the logarithmic portion of the analytical profile becomes obscure. As β_c increases the difficulty becomes more severe since it may easily be verified from equation (A.4) that the a_i become increasingly larger as β_c increases. This effect further causes the composite profile to deviate from logarithmic behavior for small η.

The failure of the composite profile to reflect the true input logarithmic behavior for low Reynolds number on a graph is of some concern since the values of Re_δ^* which are characteristic of many experiments are $O(10^3)$ or $O(10^4)$. To attempt to overcome these problems, Scharnhorst (1978) suggested two approaches. In the first of these, a full three parameter

optimization of S, κ, and K was carried out. Generally this procedure produces very good representations of the data; however, as Scharnhorst (1978) points out, the parameters (S,κ,K) tend to lose physical significance in such method in two ways.

First the input value of κ used to produce the profile is not the apparent value that would be calculated from a graph of the profile; this point has been illustrated in Figure 4.1. Secondly, Scharnhorst (1978), upon plotting the values of S obtained for profiles with various values of β_c, observed a trend for S to remain approximately constant or to actually slightly decrease with increasing β_c. This trend is opposite to the experiments (Kline, et al. 1967) which suggest that S should increase with increasing β_c.

The second approach was suggested by Scharnhorst (1978) as one possible way of overcoming the problems of the three parameter optimization and was attempted here. The main ideas are that the parameter K primarily influences the quality of the fit in the outer region while the parameter S mainly influences the inner region; on the other hand, κ influences the slope of the profile in the overlap zone and consequently has an important effect in both regions. The difficulties associated with the strong influence of varying κ and also with fitting this type of profile have been discussed by Scharnhorst (1978) and Weigand

(1978); one approach found to be acceptable for heat transfer profiles (Wiegand, 1978) is to perform a one parameter optimization on K holding κ fixed; once the optimization had been complete, a new value of κ is obtained from a graph of the data in inner region coordinates; note that in the optimization u_τ will vary and hence the graph of u^+ versus y^+ will change. This graphical iteration process starts with a value κ=0.41 and continually obtains new values of κ from the slope of the data points in the logarithmic region of the velocity profile. This approach is denoted by method 1 in this study and the least square curve fit error results of the first iteration are presented in Table 4.1. First iteration curve fits for the last data station of the zero and favorable pressure gradients of Andersen, et al. (1972) are shown in Figure 4.1. Unfortunately method 1 failed for successive graphical iterations since the new values of κ from the slope of the logarithmic region do not provide improved curve fits; in fact, the values of κ taken from the data give a lower value of κ than 0.41 although a larger value of κ is suggested upon comparison of the data and the analytic profile. The lines drawn tangent to the data in the logarithmic zone are depicted in figure 4.1 as broken lines. The failure of this procedure is again due to the low Reynolds number effect for large β_c. In the next section, several other methods are discussed in an effort to obtain improved composite profile data comparisons.

4.2 Composite Profile Data Comparisons

Composite similarity profile representations were obtained using several methods in which certain model parameters were optimized using the direct search technique while holding others constant. The five methods considered in this study for profile representations are:

1. Method 1 - one parameter optimization on K while holding S = 10.4965 and κ = 0.41 constant;
2. Method 2 - two parameter optimization on κ and K while holding S = 10.4965 constant;
3. Method 3 - two parameter optimization on S and K while holding κ = 0.41 constant;
4. Method 4 - three parameter optimization on S, κ, and K;
5. Method 5 - two parameter optimization on S and K while holding κ = 0.46.

To determine which method offers the best profile representations, each method was run with the non-transpired zero, mild, and strong adverse pressure gradient data of Andersen, et al. (1972)(labeled 8100, 8200, and 8300, respectively) and the favorable pressure gradient data of Herring and Norbury (labeled 2700 after Coles & Hirst, 1969). These data sets were chosen for several reasons. First, in all data sets there is a relatively large number of points in the inner layer and this is important in assessing the performance of the unsteady wall layer model. In the second

place, these data sets reflect a wide variety of pressure gradients for equilibrium mainstream velocity distributions. Thirdly, these data sets are relatively recent and are believed to be very reliable. The least squares error ε is presented in Table 4.1 for each of the five optimization methods. The values of $\bar{\varepsilon}$ in parentheses represent recalculated values which neglect the third and fourth data stations for the Herring & Norbury (Coles & Hirst, 1969) 2700 flow and the first two data stations for the Andersen, et al. (1972) 8100, 8200, and 8300 flows. These neglected data stations generally correspond to upstream stations which are suspected of not being representative of equilibrium behavior. The recalculated $\bar{\varepsilon}$ values are observed to have a value close to that for the average ε representing all data stations except for the 2700 series in which a substantial improvement is noted.

By observing the curve fit error for the mild adverse pressure gradient (8200 series) in Table 4.1, it is apparent that substantial improvements in the quality of the fits can be realized by varying more than one parameter. The best curve fits are obtained with methods 2 and 4 in the sense that the lowest least squares errors are obtained with these methods. A similar trend may be observed for the strong adverse pressure gradient (8300 series). Note that the RMS error increases in

TABLE 4.1

ERROR CRITERIA $\bar{\epsilon}$ FOR COMPOSITE

PROFILE OPTIMIZATIONS

FLOW	METHOD 1	METHOD 2	METHOD 3	METHOD 4	METHOD 5
2700 - Herring & Norbury; Favorable Gradient	.008317 (.006434)+	.005700 (.004949)	.006993 (.005156)	.004696 (.004312)	.006241 (.005464)
8100 - Andersen, et al. Constant Pressure	.010344 (.009368)	.008359 (.008115)	.007356 (.007426)	.007000 (.007281)	.007534 (.007359)
8200 - Andersen, et al. Adverse Gradient	.015441 (.015654)	.008198 (.007918)	.010854 (.011532)	.007400 (.007493)	.008826 (.008884)
8300 - Anderson, et al. Adverse Gradient	.025740 (.027232)	.009783 (.010114)	.017472 (.019606)	.008447 (.008975)	.013426 (.014738)

+The numbers in parentheses represent the values of $\bar{\epsilon}$ neglecting the third & fourth stations for 2700 and the first two stations for 8100, 8200, and 8300.

the range 50-70% for methods 1, 3 and 5 in going from the mild to the strong adverse pressure gradient case; for methods 2 and 4, the percentage increase is 19 and 14 percent respectively. The 8300 series is the most difficult case for profile representation because of the low Reynolds number effects and pressure gradient effects which have increasing importance for larger β_c as discussed in §4.1. On the basis of the results in Tables 4.1, methods 1, 3, and 5 may be ruled out as effective parameter adjusting methods.

To further assess which of the surviving methods offers the best profile representation, the complete profile optimization results for methods 2 and 4 are given in Tables 4.2 through 4.9 along with the corresponding profile representations in Figures 4.3 through 4.10. Evidently, the S, κ, and K optimization technique of method 4 has the lowest average root-mean-square error, $\bar{\varepsilon}$; however, this result is not totally unexpected since the adjustment of all three parameters offers more flexibility in curve fitting for both the inner and outer regions. Method 2 (κ, K optimization with constant S = 10.4965) offers a close second choice in the selection of a profile representation method which suggests that the variation of the S value does not drastically change the quality of the curve fits.

An important observation which can be made from the results of the three-parameter fits of method 4 is that the composite

HERRING AND NORBURY, BETA -.35
(ENGLISH UNITS)

NU= .173000E-03

EXPERIMENTAL VALUES

ID	XSTA	UE	UTAU	DUEDX	BETA	DELTA	DELTA*	THETA	SHAPE
2701	0.000	76.50	3.1490	2.650	-.2111	.8500	.1239	.0921	1.3453
2702	1.000	79.80	3.2800	4.900	-.3003	.9000	.1200	.0960	1.3333
2703	2.000	84.60	3.5500	6.130	-.3096	1.0000	.1136	.0875	1.2903
2704	3.000	90.50	3.7900	6.200	-.3598	1.0000	.1110	.0856	1.2967
2705	4.000	97.10	4.0410	6.250	-.3413	1.0000	.1102	.0845	1.3041
2706	5.000	103.60	4.2700	6.250	-.3326	1.0000	.1124	.0860	1.3070

UNSTEADY WALL + SIMILARITY MODEL - FULL PROFILE 2 PARAMETER FIT

ID	BETA	UTAU	S	K	KAPPA	EPSILON	T0+	CI
2701	-.1813	3.390	10.497	.017733	.4015	.006124	.002030	5.647
2702	-.3419	3.493	10.497	.014732	.4400	.005076	.003707	5.370
2703	-.2931	4.093	10.497	.023010	.5554	.006934	.000500	6.130
2704	-.2724	4.365	10.497	.023599	.5601	.007509	.000450	6.164
2705	-.3103	4.105	10.497	.017656	.4122	.004203	.007600	5.023
2706	-.3505	4.113	10.497	.014059	.3416	.003555	.030720	4.116

MEAN EPSILON OVER 6 STATIONS = .005700

TABLE 4.2 Results of Method 2 two parameter fits of the composite similarity profile to the favorable pressure gradient data of Herring and Norbury (Coles and Hirst, 1969).

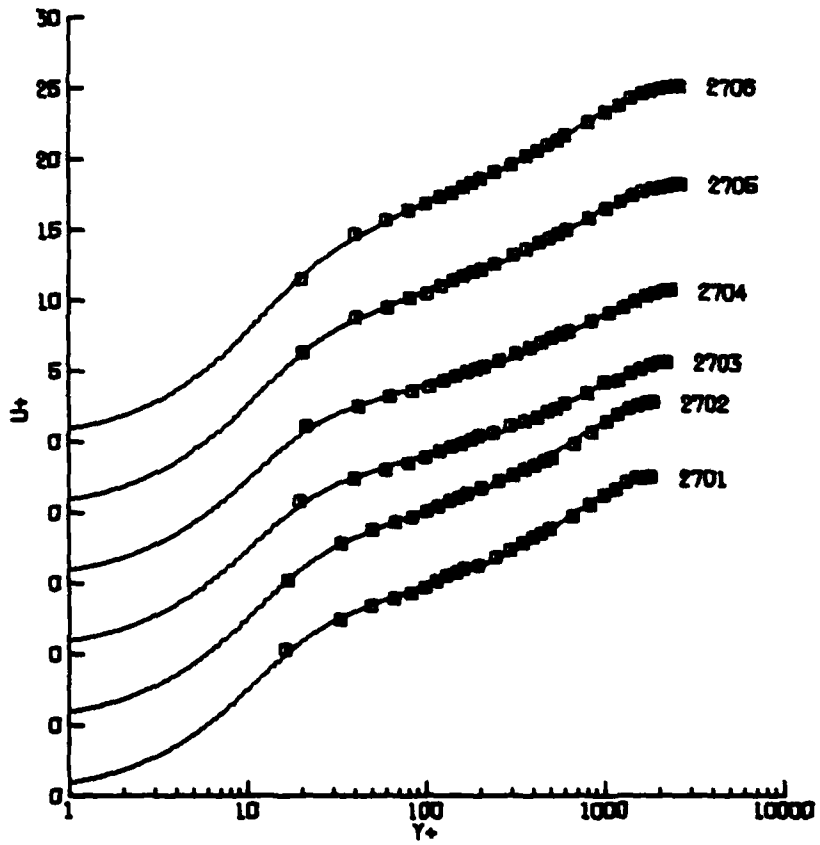

Figure 4.3 Velocity profile comparisons for two parameter optimization on κ and K (with S = 10.4965) for favorable pressure gradient data of Herring and Norbury (1969).

ANDERSEN, KAYS AND MOFFAT - ZERO P. G. - 120771-1
(ENGLISH UNITS)

NU= .159000E-03

EXPERIMENTAL VALUES

ID	XSTA	UE	UTAU	DUEDX	BETA	DELTA	DELTA*	THETA	SHAPE
8101	.167	31.21	1.5574	.009	-.0005	.2071	.0584	.0328	1.5366
8102	.833	31.13	1.4667	.008	-.0007	.4225	.0772	.0521	1.4818
8103	1.833	31.14	1.4000	.006	-.0008	.6242	.1135	.0760	1.4779
8104	2.833	31.05	1.3534	.003	-.0007	.7854	.1412	.0977	1.4452
8105	3.833	31.04	1.3206	.001	-.0002	.9590	.1709	.1185	1.4422
8106	4.833	31.13	1.2985	-.002	.0005	1.1065	.1968	.1375	1.4313
8107	5.833	31.04	1.2723	-.005	.0020	1.2755	.2255	.1584	1.4236
8108	6.833	31.07	1.2544	-.009	.0038	1.4808	.2533	.1794	1.4119
8109	7.500	31.06	1.2463	-.012	.0053	1.5810	.2670	.1902	1.4038

UNSTEADY WALL + SIMILARITY MODEL - FULL PROFILE 2 PARAMETER FIT

ID	BETA	UTAU	S	K	KAPPA	EPSILON	TO+	CI
8101	-.0004	1.635	10.497	.020123	.4217	.009867	.006384	5.122
8102	-.0006	1.629	10.497	.022947	.6183	.009361	.000153	6.461
8103	-.0009	1.355	10.497	.016627	.3635	.009632	.019893	4.437
8104	-.0007	1.333	10.497	.016573	.3815	.006712	.013963	4.672
8105	-.0002	1.294	10.497	.015173	.3839	.006113	.013317	4.781
8106	.0007	1.244	10.497	.015000	.3518	.012026	.025109	4.270
8107	.0020	1.275	10.497	.014675	.4127	.007783	.007606	5.020
8108	.0041	1.220	10.497	.014434	.3695	.007982	.017609	4.517
8109	.0054	1.240	10.497	.014759	.3958	.005757	.010720	4.834

MEAN EPSILON OVER 9 STATIONS = .008359

TABLE 4.3 Results of Method 2 two parameter fits of the composite similarity profile to the constant pressure data of Andersen, et al. (1972).

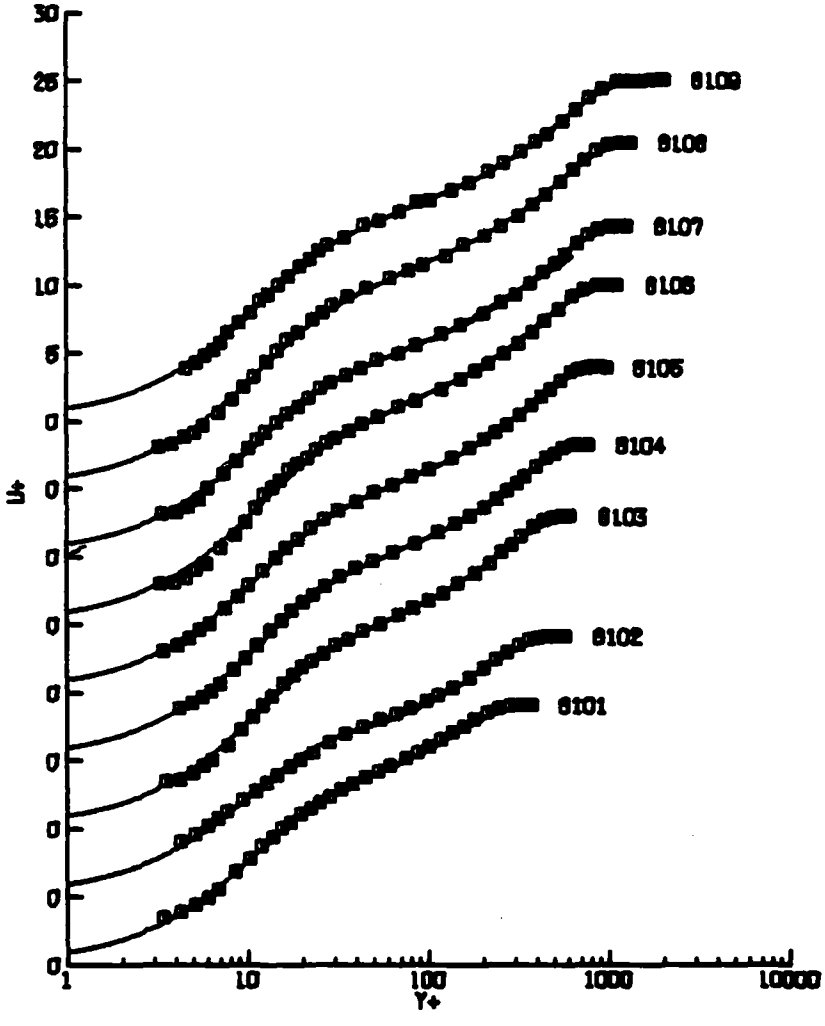

Figure 4.4 Velocity profile comparisons for two parameter optimization on κ and K (with S = 10.4965) for constant pressure data of Andersen, et al. (1972).

ANDERSEN,KAYS+MOFFAT MILD P.G. 71571-5
(ENGLISH UNITS)

NU= .166088E-03

EXPERIMENTAL VALUES

ID	XSTA	UE	UTAU	DUEDX	BETA	DELTA	DELTA*	THETA	SHAPE
8201	.167	29.69	1.5468	-2.448	.1484	.3881	.0556	.0357	1.5574
8202	.833	26.93	1.1980	-3.798	.6744	.5179	.1138	.0718	1.5850
8203	1.833	24.57	1.0108	-1.760	.6839	.8628	.1936	.1238	1.5638
8204	2.833	23.26	.9188	-1.138	.6919	1.1752	.2616	.1700	1.5388
8205	3.833	22.27	.8480	-.820	.7102	1.5029	.3356	.2176	1.5423
8206	4.833	21.36	.7998	-.630	.6910	1.7870	.3934	.2592	1.5177
8207	5.833	20.74	.7658	-.518	.6343	2.1211	.4618	.3049	1.5128
8208	6.833	20.35	.7428	-.438	.6765	2.4043	.5188	.3419	1.4948
8209	7.500	20.05	.7260	-.410	.7082	2.5781	.5443	.3656	1.4904

UNSTEADY WALL + SIMILARITY MODEL - FULL PROFILE 2 PARAMETER FIT

ID	BETA	UTAU	S	K	KAPPA	EPSILON	TO+	CI
8201	.1416	1.540	10.497	.027685	.4609	.010763	.002579	5.548
8202	.6657	1.206	10.497	.021323	.5695	.007598	.000384	6.216
8203	.6590	1.020	10.497	.017896	.5520	.007779	.000534	6.110
8204	.6517	.930	10.497	.016974	.5236	.008380	.000912	5.944
8205	.7489	.826	10.497	.015412	.4502	.011114	.003690	5.390
8206	.6396	.831	10.497	.016084	.5131	.007264	.001112	5.875
8207	.6520	.789	10.497	.015453	.5065	.007322	.001268	5.830
8208	.6027	.786	10.497	.016124	.5202	.006670	.000972	5.922
8209	.6242	.773	10.497	.016361	.5267	.006894	.000861	5.964

MEAN EPSILON OVER 9 STATIONS = .008198

TABLE 4.4 Results of Method 2 two parameter fits of the composite similarity profile to the mild adverse pressure gradient data of Andersen, et al. (1972).

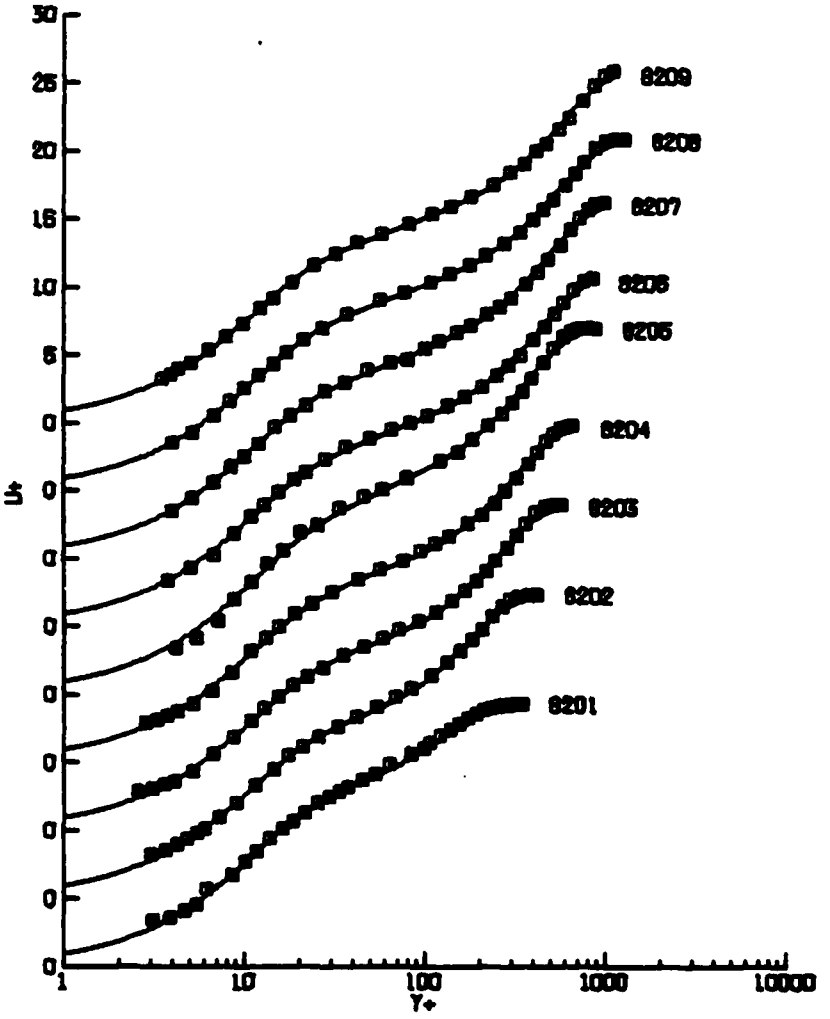

Figure 4.5 Velocity profile comparisons for two parameter optimization on κ and K (with S = 10.4965) for mild adverse pressure gradient of Andersen et al. (1972).

ANDERSEN,KAYS MOFFAT STRONG P.G. 110971
(ENGLISH UNITS)

NU= .161000E-03

EXPERIMENTAL VALUES

ID	XSTA	UE	UTAU	DUEDX	BETA	DELTA	DELTA*	THETA	SHAPE
8301	.167	29.13	1.5110	-3.680	.2137	.3064	.0561	.0359	1.5627
8302	.833	25.70	1.0720	-5.210	1.2011	.5366	.1237	.0770	1.6065
8303	1.833	22.31	.8010	-2.170	1.5570	.9542	.2470	.1496	1.6564
8304	-.833	28.53	.7080	-1.320	1.6323	1.3935	.3628	.2195	1.6528
8305	3.833	19.39	.6550	-.930	1.6260	1.8038	.4663	.2836	1.6442
8306	4.833	18.55	.6150	-.700	1.5739	2.1736	.5497	.3486	1.6139
8307	5.833	17.97	.5800	-.570	1.5433	2.5570	.6291	.3951	1.5923
8308	6.833	17.42	.5590	-.470	1.5819	2.9793	.7263	.4591	1.5820
8309	7.500	17.10	.5430	-.440	1.7585	3.3669	.8244	.5174	1.5934

UNSTEADY WALL + SIMILARITY MODEL - FULL PROFILE 2 PARAMETER FIT

ID	BETA	UTAU	S	K	KAPPA	EPSILON	T0+	CI
8301	.2250	1.492	10.497	.030222	.4604	.010134	.003037	5.470
8302	1.0555	1.144	10.497	.024123	.6095	.007120	.000840	6.755
8303	1.4029	.844	10.497	.017051	.6257	.009002	.000133	6.495
8304	1.5043	.730	10.497	.015569	.6170	.010466	.000157	6.455
8305	1.6103	.650	10.497	.014094	.5555	.010621	.000499	5.130
8306	1.4646	.637	10.497	.015223	.5477	.011766	.000570	6.093
8307	1.3408	.633	10.497	.015429	.5706	.000432	.000323	6.265
8308	1.3766	.600	10.497	.015450	.5527	.011297	.000526	6.122
8309	1.5339	.580	10.497	.015270	.5833	.009211	.000296	6.290

MEAN EPSILON OVER 9 STATIONS = .009703

TABLE 4.5 Results of Method 2 two parameter fits of the composite similarity profile to the strong adverse pressure gradient data of Andersen, et al. (1972).

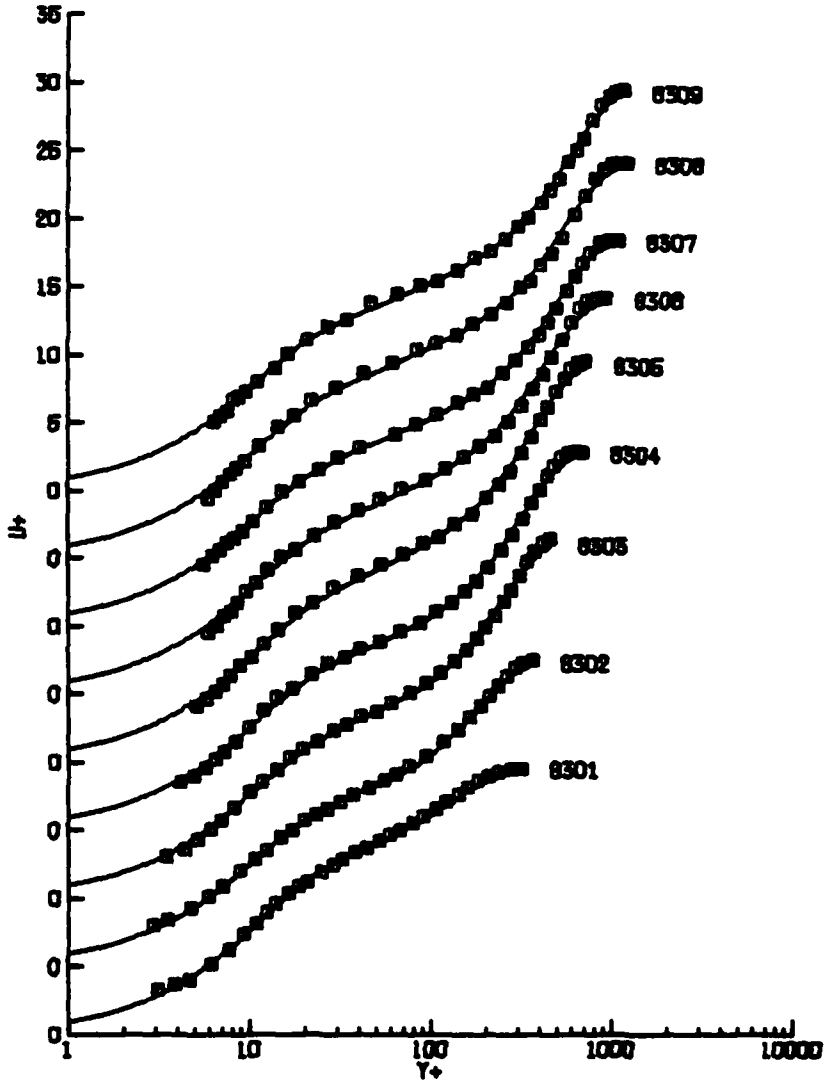

Figure 4.6 Velocity profile comparisons for two parameter optimization on κ and K (with S = 10.4965) for strong adverse pressure gradient of Andersen et al. (1972).

HERRING AND NORBURY, BETA -.35
(ENGLISH UNITS)

NU= .173000E-03

EXPERIMENTAL VALUES

ID	XSTA	UE	UTAU	DUEDX	BETA	DELTA	DELTA*	THETA	SHAPE
2701	0.000	76.50	3.1490	2.650	-.2111	.8500	.1239	.0921	1.3453
2702	1.000	79.80	3.2800	4.900	-.3883	.9000	.1280	.0960	1.3333
2703	2.000	84.60	3.5500	6.130	-.3896	1.0000	.1136	.0875	1.2983
2704	3.000	90.50	3.7980	6.200	-.3590	1.0000	.1110	.0856	1.2967
2705	4.000	97.10	4.0410	6.250	-.3413	1.0000	.1102	.0845	1.3041
2706	5.000	103.60	4.2700	6.250	-.3326	1.0000	.1124	.0860	1.3070

UNSTEADY WALL + SIMILARITY MODEL - FULL PROFILE 3 PARAMETER FIT

ID	BETA	UTAU	S	K	KAPPA	EPSILON	TO+	CI
2701	-.1565	3.658	8.099	.021562	.4562	.004135	.014889	3.865
2702	-.3304	3.553	9.771	.015576	.4361	.005726	.007509	4.778
2703	-.2388	4.534	7.976	.031225	.5445	.005055	.004308	4.334
2704	-.2014	5.076	7.347	.036314	.5773	.005871	.004402	4.073
2705	-.3119	4.227	10.088	.018241	.4079	.004107	.010497	4.709
2706	-.3731	4.032	11.436	.013087	.3490	.003280	.017001	4.826

MEAN EPSILON OVER 6 STATIONS = .004696

TABLE 4.6 Results of Method 4 three parameter fits of the composite similarity profile to the favorable pressure gradient data of Herring and Norbury (Coles and Hirst, 1969).

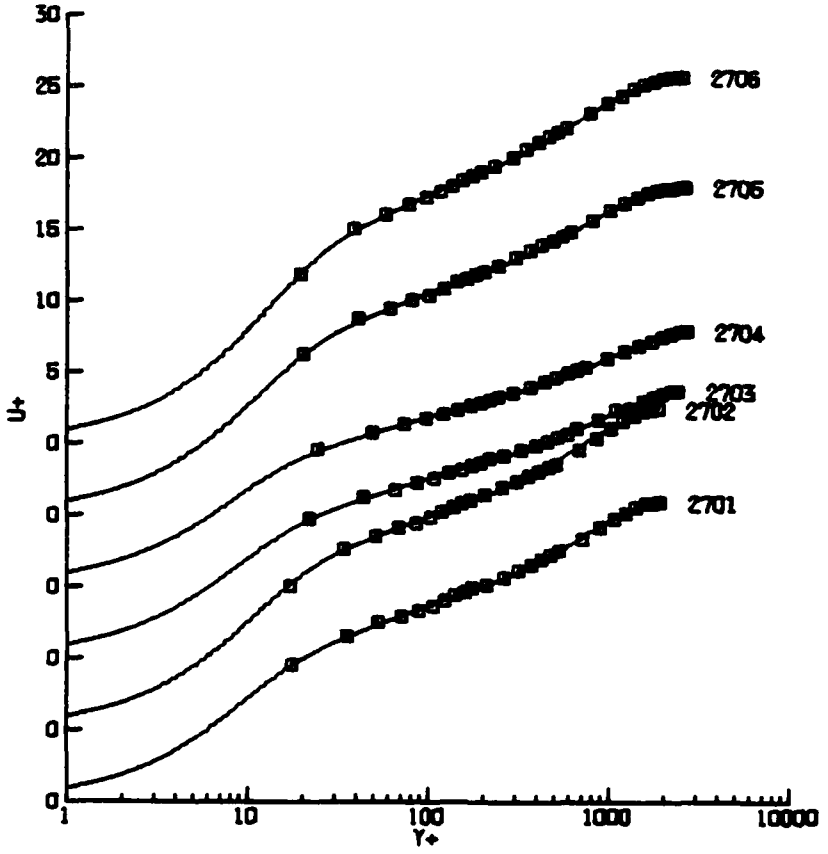

Figure 4.7 Velocity profile comparisons for three parameter optimization on S, κ and K for favorable pressure gradient data of Herring and Norbury (1969).

ANDERSEN, KAYS AND MOFFAT - ZERO P. G. - 120771-1
(ENGLISH UNITS)

NU= .159000E-03

EXPERIMENTAL VALUES

ID	XSTA	UE	UTAU	DUEDX	BETA	DELTA	DELTA*	THETA	SHAPE
8101	.167	31.21	1.5574	.009	-.0005	.2871	.0504	.0328	1.5366
8102	.833	31.13	1.4667	.008	-.0007	.4225	.0772	.0521	1.4818
8103	1.833	31.14	1.4000	.006	-.0008	.6242	.1135	.0768	1.4779
8104	2.833	31.05	1.3534	.003	-.0007	.7854	.1412	.0977	1.4457
8105	3.833	31.04	1.3206	.001	-.0002	.9590	.1709	.1185	1.4422
8106	4.833	31.13	1.2985	-.002	.0006	1.1065	.1968	.1375	1.4313
8107	5.833	31.04	1.2723	-.005	.0020	1.2755	.2255	.1584	1.4236
8108	6.833	31.07	1.2544	-.009	.0038	1.4608	.2533	.1794	1.4119
8109	7.500	31.06	1.2463	-.012	.0053	1.5810	.2670	.1902	1.4038

UNSTEADY WALL + SIMILARITY MODEL - FULL PROFILE 3 PARAMETER FIT

ID	BETA	UTAU	S	K	KAPPA	EPSILON	TD+	CI
8101	-.0004	1.630	8.124	.026616	.3124	.006755	.146708	2.260
8102	-.0006	1.637	7.101	.022908	.3750	.005277	.086508	2.551
8103	-.0009	1.355	11.861	.016605	.4366	.009099	.002038	6.217
8104	-.0007	1.330	11.810	.016324	.4495	.005979	.001620	6.291
8105	-.0002	1.291	11.302	.014987	.4192	.005812	.004181	5.638
8106	.0007	1.237	13.133	.014202	.4773	.010982	.000357	7.488
8107	.0020	1.273	10.943	.014450	.4329	.007684	.003927	5.533
8108	.0041	1.209	12.499	.013703	.4508	.006053	.001008	6.789
8109	.0054	1.235	11.270	.014422	.4241	.005358	.003849	5.668

MEAN EPSILON OVER 9 STATIONS = .007000

TABLE 4.7 Results of method 4 three parameter fits of the composite similarity profile to the constant pressure data of Andersen, et al. (1972).

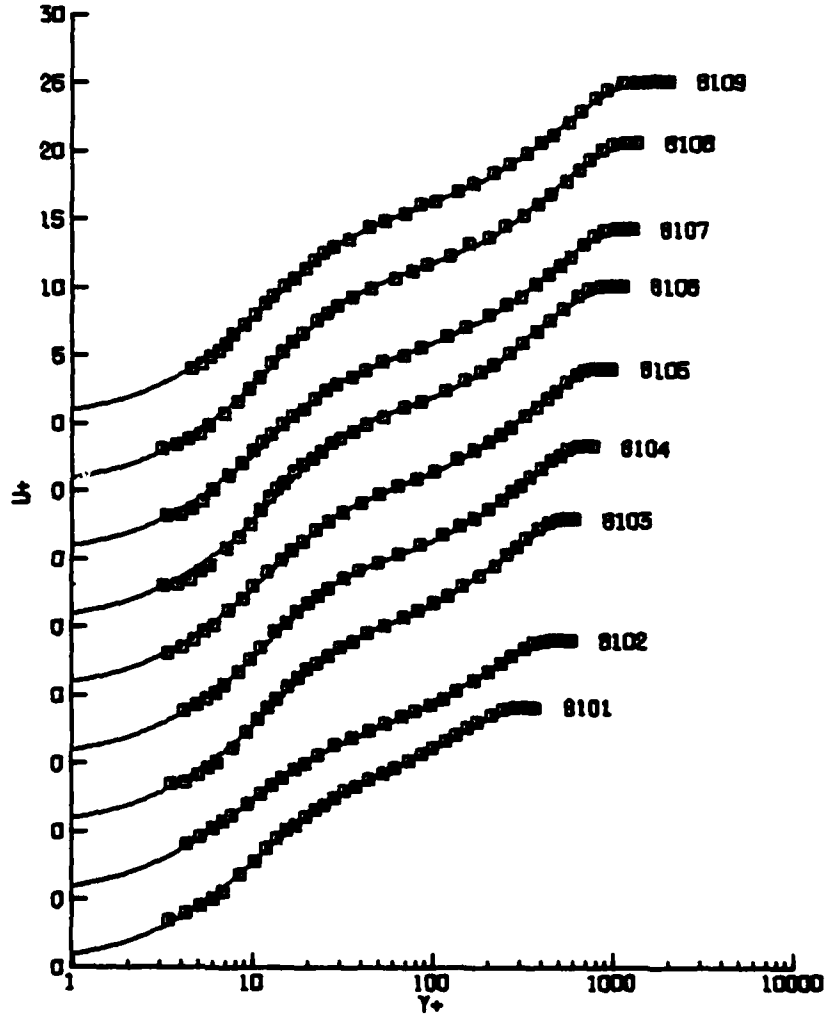

Figure 4.8 Velocity profile comparisons for three parameter optimization on S, κ and K for constant pressure data of Andersen et al. (1972).

ANDERSEN, KAYS AND MOFFAT MILD P.G. 71571-5
(ENGLISH UNITS)

NU= .166080E-03

EXPERIMENTAL VALUES

ID	XSTA	UE	UTAU	DUEDX	BETA	DELTA	DELTA*	THETA	SHAPE
8201	.167	29.69	1.5460	-2.440	.1404	.3081	.0556	.0357	1.5574
8202	.833	26.93	1.1980	-3.790	.6744	.5179	.1138	.0718	1.5850
8203	1.833	24.57	1.0100	-1.760	.6839	.8628	.1936	.1238	1.5638
8204	2.833	23.26	.9100	-1.130	.6919	1.1752	.2616	.1700	1.5388
8205	3.833	22.27	.8480	-.820	.7102	1.5029	.3356	.2176	1.5423
8206	4.833	21.36	.7990	-.630	.6910	1.7870	.3934	.2592	1.5177
8207	5.833	20.74	.7650	-.510	.6943	2.1211	.4610	.3049	1.5120
8208	6.833	20.35	.7420	-.430	.6765	2.4043	.5108	.3419	1.4940
8209	7.500	20.05	.7260	-.410	.7082	2.5701	.5449	.3656	1.4904

UNSTEADY WALL + SIMILARITY MODEL - FULL PROFILE 3 PARAMETER FIT

ID	BETA	UTAU	S	K	KAPPA	EPSILON	TO+	CI
8201	.1439	1.527	7.127	.026009	.3082	.007151	.234016	1.678
8202	.6663	1.205	9.314	.021261	.4796	.007001	.004667	4.828
8203	.6597	1.028	10.494	.017897	.5518	.007779	.000536	6.115
8204	.6553	.935	11.018	.016858	.5594	.008265	.000303	6.537
8205	.7693	.815	12.838	.014944	.5854	.009418	.000037	8.034
8206	.6539	.821	11.740	.015701	.5896	.006411	.000089	7.236
8207	.6572	.786	10.912	.015321	.5268	.007226	.000626	6.260
8208	.6094	.782	11.066	.015895	.5506	.006474	.000347	6.519
8209	.6261	.772	10.661	.016275	.5354	.006875	.000642	6.136

MEAN EPSILON OVER 9 STATIONS = .007400

TABLE 4.8 Results of method 4 three parameter fits of the composite similarity profile to the mild adverse pressure gradient data of Andersen, et al. (1972).

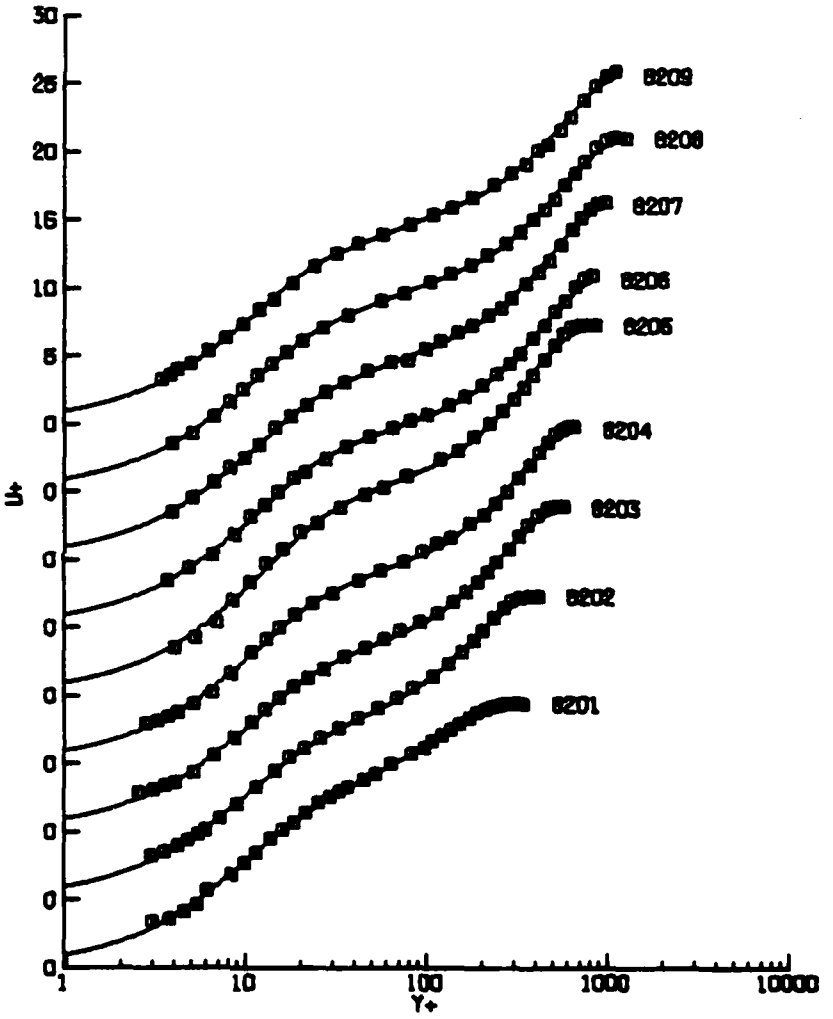

Figure 4.9 Velocity profile comparisons for three parameter optimization on S, κ and K for mild adverse pressure gradient data of Andersen et al. (1972).

ANDERSEN,KAYS AND MOFFAT STRONG P.G. 110971
(ENGLISH UNITS)

NU= .161000E-03

EXPERIMENTAL VALUES

ID	XSTA	UE	UTAU	DUEDX	BETA	DELTA	DELTA*	THETA	SHAPE
8301	.167	29.13	1.5110	-3.680	.2197	.3064	.0561	.0359	1.5627
8302	.833	25.70	1.0720	-5.210	1.2011	.5366	.1237	.0770	1.6065
8303	1.833	22.31	.8010	-2.170	1.5570	.9542	.2478	.1496	1.6564
8304	-.833	20.53	.7080	-1.120	1.6323	1.3935	.3624	.2195	1.6528
8305	3.833	19.39	.6550	-.930	1.6260	1.8038	.4663	.2836	1.6442
8306	4.833	18.55	.6150	-.780	1.5739	2.1736	.5497	.3406	1.6139
8307	5.833	17.97	.5840	-.670	1.5433	2.5570	.6291	.3951	1.5923
8308	6.833	17.42	.5590	-.470	1.5819	2.9793	.7263	.4591	1.5820
8309	7.500	17.10	.5430	-.440	1.7505	3.3669	.8244	.5174	1.5934

UNSTEADY WALL + SIMILARITY MODEL - FULL PROFILE 3 PARAMETER FIT

ID	BETA	UTAU	S	K	KAPPA	EPSILON	TO+	CI
8301	.2264	1.487	7.969	.028629	.3300	.007422	.102317	2.573
8302	1.0436	1.158	8.937	.024318	.5498	.005783	.001897	5.011
8303	1.4145	.841	11.379	.016937	.7162	.008707	.000009	7.520
8304	1.5347	.731	12.152	.015334	.7982	.009509	.000001	8.363
8305	1.6735	.647	12.994	.014548	.7555	.008587	.000001	9.909
8306	1.5137	.627	12.485	.014824	.6796	.010374	.000005	9.226
8307	1.3646	.627	11.423	.015185	.6368	.008008	.000045	7.233
8308	1.4371	.587	12.728	.014929	.6957	.009354	.000003	8.473
8309	1.5861	.571	11.895	.014894	.6654	.008282	.000016	7.715

MEAN EPSILON OVER 9 STATIONS = .008447

TABLE 4.9 Results of method 4 three parameter fits of the composite similarity profile to the strong adverse pressure gradient data of Andersen, et al. (1972).

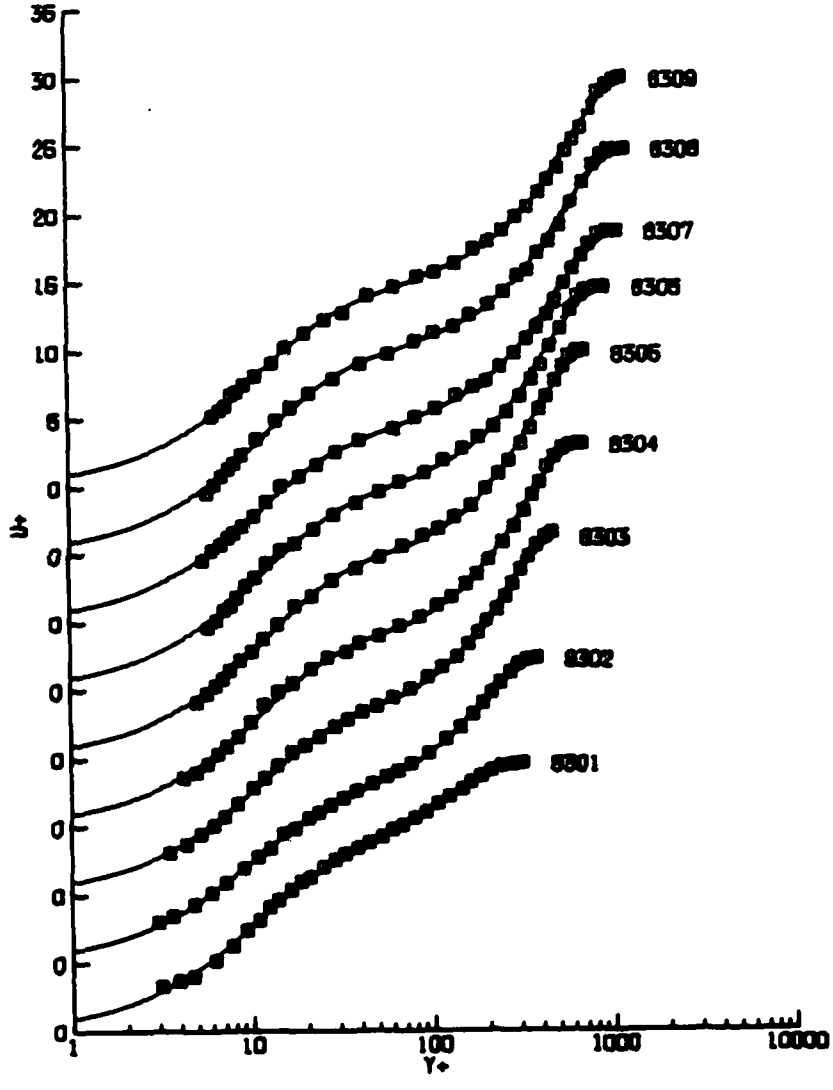

Figure 4.10 Velocity profile comparisons for three parameter optimization on S, κ and K for strong adverse pressure gradient data of Andersen, et al. (1972).

similarity profile encounters difficulty in fitting velocity profiles measured in strong adverse pressure gradient flows. An increase in $\bar{\epsilon}$ with pressure gradient can be observed in Table 4.1; this is not entirely unexpected for two reasons. First, true self-similar behavior is not anticipated in situations with large adverse pressure gradients since boundary layer separation may occur before similarity is achieved; consequently, it may be that the model is not an appropriate one for large adverse pressure gradients. In the second place, there is a significant departure of the composite profile from logarithmic behavior in the overlap region for β_c O(1) due to the low Reynolds number effect and the β_c effect in the series solution as discussed in section 4.1. The effects of increasing β_c in the series solution may be offset by increasing κ, thereby reducing the magnitude of the a_i and b_i coefficients in equation (A.4) (see Appendix A). This cancelation effect may be observed in the results of the three-parameter fits in Tables 4.6 to 4.9 which reveal that the optimized values of κ increase with β_c. As a result, it may be concluded that the three parameter optimization process adjusts the parameters of the composite similarity profile to correct an undesirable low Reynolds number effect or large β_c effect in the series solution. However, the optimized value of κ is no longer associated with the apparent inverse

slope in the logarithmic portion of the profile as taken from a graph of the profile.

To summarize the investigation of all the optimization methods, it was found that a significant reduction in error of the profile fits is realized by optimizing all three parameters of the profile, namely S, κ, and K. However, the three parameter optimization masks any physical interpretation originally associated with the parameters to counteract the low Reynolds number and large β_c effects. Thus, the parameters S, κ, and K become simply profile parameters which are adjusted to obtain a close representation of measured data. The objective now is to obtain correlations for these parameters based upon the four equilibrium flows of 2700, 8100, 8200, and 8300 in order to provide the basis for a prediction scheme.

4.3 Parameter Correlations

In order to develop a profile prediction method, optimized parameter values were obtained for the three parameter optimization of method 4 and the two parameter optimization of method 2. Both optimization methods used the negative pressure gradient flow of Herring and Norbury labeled 2700 and the three Andersen, et al. (1972) flows, 8100, 8200, and 8300 which cover a range of β_c from about -0.4 to 1.5. The results of the optimized

data fits for the three parameter optimization of method 4 were then plotted versus the pressure gradient β_c as shown in Figure 4.11. The first two data stations of flows 8100, 8200, and 8300, and the third and fourth data stations of flow 2700 were not included in the correlations because of the observed form of the experimental velocity profiles which did not appear to exhibit self-similar behavior; this is reflected in the fact that the results for these eight data stations showed a substantial deviation from the straight line correlations in figure 4.11. Prospective correlations which could be used in a prediction procedure were obtained by fitting a least squares straight line and quadratic curve through the optimized parameter values represented by the solid symbols. The resulting correlations for the three parameter optimization of method 4 are given in Table 4.10. The RMS curve fit error for the correlations show that the quadratic curve fits give only a very slight improvement over the linear curve fits. The three parameter optimization correlations indicate that K is nearly constant; most of the variation occurs in κ which in effect offsets the influence of β_c in the series solution for the outer layer mode. A slight variation occurs in the S correlation which is contradictory to the experimentally observed trend for the dimensionless time period between bursts. The correlation indicates that S increases slightly with pressure gradient while the visual observations of Kline, et al. (1967)

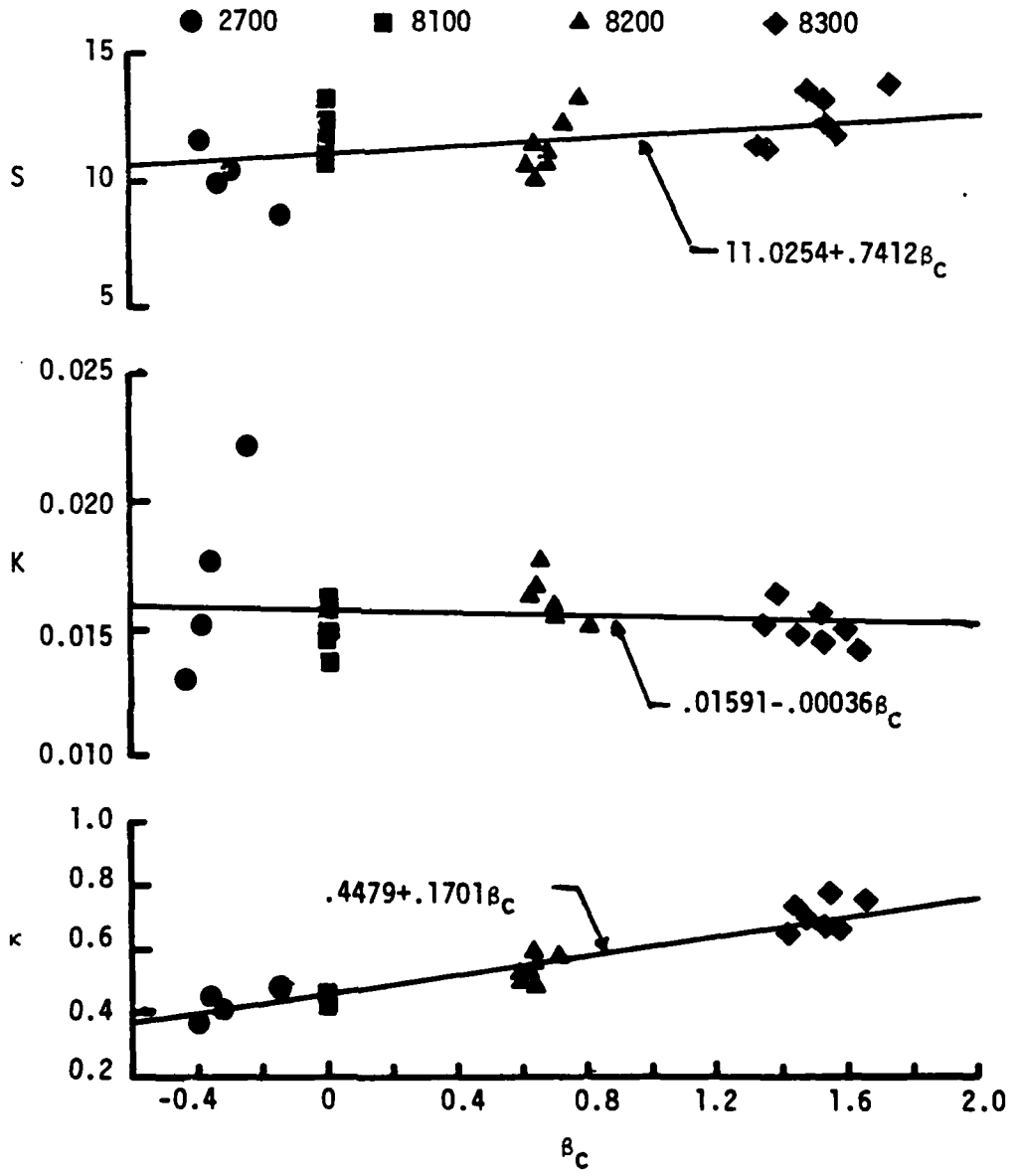

FIGURE 4-11 Parameter correlations obtained from three-parameter fits of the composite similarity profile to four sets of data.

TABLE 4.10

LEAST SQUARES CURVE FITS

OPTIMIZATION METHOD	LINEAR	QUADRATIC
2	$\kappa = .41627 + .11011\beta_c$ (.10283)*	$\kappa = .41662 + .11736\beta_c - .005643\beta^2_c$ (.10274)
	$K = .015774 + .0000219\beta_c$ (.06164)	$K = .014822 + .001021\beta_c - .0007784\beta^2_c$ (.05979)
4	$S = 11.0254 + .74122\beta_c$ (.09349)	$S = 11.0246 + .7111\beta_c + .0228\beta^2_c$ (.09349)
	$\kappa = .44788 + .17013\beta_c$ (.07387)	$\kappa = .44745 + .15308\beta_c + .012900\beta^2_c$ (.07304)
	$K = .015909 - .000358\beta_c$ (.09949)	$K = .015927 + .000396\beta_c - .000571\beta^2_c$ (.09878)

*The numbers in parenthesis are RMS errors.

show that S decreases with increasing pressure gradient. This contradiction is explained by recalling that the three parameter optimization tends to mask any physical significance that may originally have been attributed to the model parameters. Another point which concerns the value of S is worthy of mention; in the wall-layer the data exhibits a rapid profile variation which may give rise to an unnatural weight in the least-squares error calculation. In addition, wall-layer data points also have been shown to exhibit velocity measurements which are dependent upon the pitot probe tip geometry (Andersen, Kays & Moffat, 1972). All of these factors contribute to the conclusion that the slight trend in S with pressure gradient obtained with the three parameter optimizations may not be significant.

The correlation for κ indicates that there is a substantial influence of pressure gradient on the value of κ; this is partly due to the influence of β_c in the series solution which is offset in the optimization by increasing the κ value for larger β_c. Because of this effect and the Reynolds number effect discussed previously, the values for κ obtained from the correlations presented in Table 4.10 cannot be directly associated with the inverse slope of the logarithmic region on a graph for profiles with displacement thickness Reynolds numbers $O(10^3)$. The curve fit data for the κ correlation of the three parameter optimization

exhibits the least scatter (lowest RMS error) of the S, κ, and K correlations which tend to strengthen its reliability for use in a profile prediction scheme.

As a point of interest, correlations based on the two parameter optimizations are also included in Table 4.10. It may be observed that these correlations show the same trends as the results based on the three parameter optimizations of method 4. Note that the dependence of K on β_c is weak while the dependence of κ on β_c is strong; for method 2 the RMS is larger than for the results based on method 4. Since a lower RMS is also observed in the actual profile fits using method 4, this procedure is considered somewhat superior to method 2 and the correlations in Table 4.10 based on method 4 are recommended.

5. MAINSTREAM TURBULENCE

5.1 Introduction

The influence of mainstream turbulence on a fully developed turbulent boundary layer flow with zero pressure gradient has been studied by a number of investigators. The experimental investigations of Kline et al. (1960), Kestin (1966), Huffman et al. (1972), Charnay et al. (1971) and others, indicate that mainstream turbulence affects the turbulent boundary layer velocity profile in many ways. In particular, a thickening of the boundary layer with increasing mainstream turbulence level is observed along with a progressive increase in skin friction. A general change in the shape of the non-dimensionalized mean velocity profile has also been documented in which there is a marked reduction in the "wake" component of the outer layer as the mainstream turbulence level increases. Finally, in a thermal boundary layer, the heat transfer at the wall increases progressively with increasing mainstream turbulence. To consider the possibility of including the effects of mainstream turbulence level into a boundary layer prediction method, it is appropriate to first examine the turbulent boundary layer momentum equation.

The continuity and momentum equations governing nominally steady turbulent boundary layers have been given in equations (2.1) and (2.2) in connection with the conventional type of

turbulent boundary layer; these equations still apply when the mainstream is turbulent. Moreover, the boundary conditions in equations (2.7) and (2.8) for the mean profile are still correct. The single turbulence input to the equations is the Reynolds stress term $\overline{-u'v'}$; unfortunately it is not possible to incorporate the fact that mainstream turbulence is present in the Reynolds stress other than through a correlation. To understand the reason for this, consider the turbulence kinetic energy $\bar{q}^2$ defined as,

$$\bar{q}^2 = \overline{u'^2} + \overline{v'^2} + \overline{w'^2} \tag{5.1}$$

where $\overline{u'^2}$, $\overline{v'^2}$ and $\overline{w'^2}$ are the turbulence intensities. For a laminar mainstream flow $\overline{q^2}$ approaches zero at the boundary layer edge but for mainstream turbulence

$$\overline{q^2} \to \overline{q_e^2} \text{ as } y \to \infty; \tag{5.2}$$

The mainstream turbulence level T_u is defined by

$$T_u^2 = \frac{1}{3} \frac{\overline{q_e^2}}{u_e^2(x)} \quad , \tag{5.3}$$

where U_e is the local mean mainstream velocity. For simplicity, assume that the mainstream turbulence is isotropic, viz.

$$\overline{u'^2} = \overline{v'^2} = \overline{w'^2} \text{ as } y \to \infty \; ; \tag{5.4}$$

consequently,

$$\overline{u'^2},\ \overline{v'^2},\ \overline{w'^2} \to T_u^2,\ \ldots\ ,\ \text{as}\ y \to \infty. \qquad (5.5)$$

However, $\overline{u'v'} \to 0$ at the boundary layer edge just as for the normal type boundary layer.

It should be remarked that the momentum equation (2.2) does not contain the intensities $\overline{u'^2}$, $\overline{v'^2}$ since these terms are of lower order; even if these terms were retained in equation (2.2), the dilemma is still not resolved since the intensities appear as the difference $(\overline{u'^2}-\overline{v'^2})$ which still must vanish at the boundary layer edge for isotropic mainstream turbulence.

Since it is not possible to incorporate the fact that mainstream turbulence is present in the boundary conditions for either the mean profile or the turbulence terms, the other possibility of developing a correlation for the eddy viscosity model parameters is investigated here. In particular, the eddy viscosity formula in equation (2.55) contains the parameters K and κ and here possible trends for these parameters with T_u will be considered. In addition, a possible trend in the inner region profile parameter S will be investigated. Again, this is carried out by a systematic adjustment of these parameters to obtain a best fit to data in an equilibrium flow but now with various levels of mainstream turbulence. The ultimate objective here is to provide correlations for these parameters which could be used in a prediction method.

AD-A115 151 LEHIGH UNIV BETHLEHEM PA DEPT OF MECHANICAL ENGINEE--ETC F/G 20/4
AN OPTIMIZATION TECHNIQUE FOR THE DEVELOPMENT OF TWO-DIMENSIONA--ETC(U)
MAR 82 L J YUMAS, J D WALKER F49620-78-C-0071
UNCLASSIFIED TR-FM-82-1 AFOSR-TR-82-0417 NL

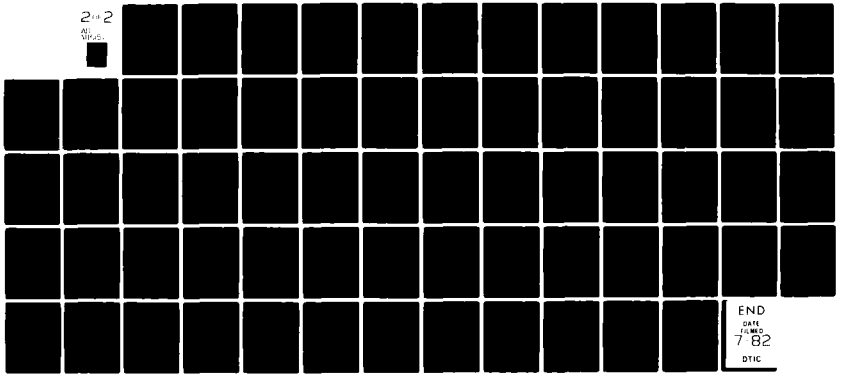

END
DATE FILMED
7 82
DTIC

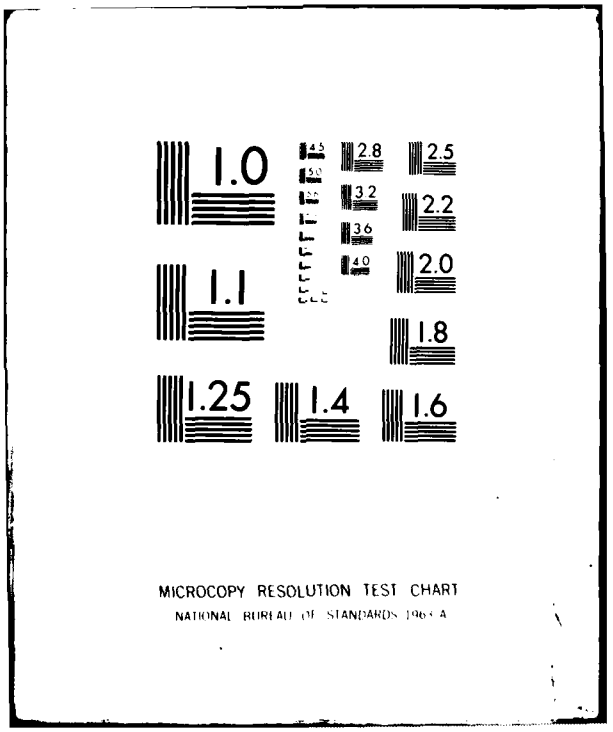
1.0
1.1
1.25
1.4
1.6
1.8
2.0
2.2
2.5
2.8
3.2
3.6
4.0
MICROCOPY RESOLUTION TEST CHART
NATIONAL BUREAU OF STANDARDS 1963 A

The data used for composite profile representations was obtained from the United Technologies Research Center boundary layer wind tunnel (Blair and Werle, 1980). Several turbulent boundary layer mean velocity profile data sets were available for zero pressure gradient flows with mainstream turbulence intensities ranging from 0.2% to 6.4%. These data sets have a large number of points that provide a good data base for profile fits and represent the best available test data at this time which reflects the effect of mainstream turbulence.

5.2 Composite Profile Data Comparisons

Composite similarity profile representations were obtained for two methods in which one or two model parameters were optimized using the direct search technique while holding others constant. The first profile optimization method used to represent turbulent boundary layer velocity profile data with mainstream turbulence was a one parameter optimization in K with constant values S = 11.025 and κ = 0.44789. These constant S and κ values correspond to the values taken from the three parameter optimization correlations in §4.3 for zero pressure gradient. Results of this method are presented in Tables 5.1 through 5.3 along with the corresponding profile representations in Figures 5.1 through 5.3; note that the 18 data stations used

UT MAINSTREAM TURBULENCE TEST DATA
(ENGLISH UNITS)

EXPERIMENTAL VALUES

ID	XSTA	UE	UTAU	NU	BETA	DELTA	DELTA*	THETA	TU
1001	40.300	98.76	4.0294	.0001673	0.000	.5900	.0824	.0573	.0020
1002	84.100	99.39	3.7384	.0001710	0.000	1.1600	.1672	.1185	.0020
1003	94.100	98.70	3.7216	.0001737	0.000	1.3500	.1765	.1242	.0084
1004	76.300	98.67	3.7708	.0001740	0.000	1.2000	.1603	.1126	.0090
1005	36.200	98.79	4.0759	.0001715	0.000	.6000	.0794	.0542	.0100
1006	28.230	98.58	4.5485	.0001700	0.000	.3800	.0397	.0265	.0110

UNSTEADY WALL + SIMILARITY MODEL - FULL PROFILE 1 PARAMETER FIT

ID	BETA	UTAU	S	K	KAPPA	EPSILON	T0+	CI
1001	0.0000	4.159	11.025	.018410	.4479	.010006	.002762	5.731
1002	0.0000	3.851	11.025	.015374	.4479	.008218	.002762	5.731
1003	0.0000	3.838	11.025	.015939	.4479	.007677	.002762	5.731
1004	0.0000	3.890	11.025	.016966	.4479	.009648	.002762	5.731
1005	0.0000	4.189	11.025	.018591	.4479	.008480	.002762	5.731
1006	0.0000	4.658	11.025	.027508	.4479	.018923	.002762	5.731

MEAN EPSILON OVER 6 STATIONS = .009145

TABLE 5.1 Results of one parameter fits of the composite similarity profile to mainstream turbulence data.

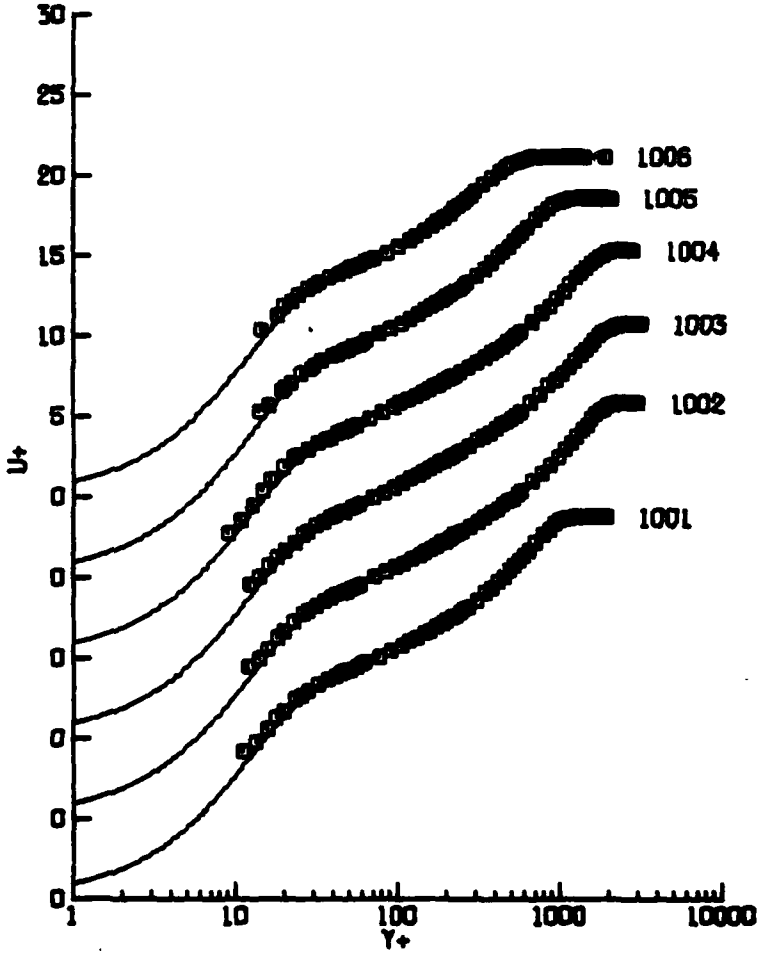

FIGURE 5.1 Velocity profile comparisons for one parameter optimization on K (with S=11.025 and κ=0.44789) for mainstream turbulence flow.

UT MAINSTREAM TURBULENCE TEST DATA
(ENGLISH UNITS)

EXPERIMENTAL VALUES

ID	XSTA	UE	UTAU	NU	BETA	DELTA	DELTA*	THETA	TU
1007	84.100	99.03	3.7488	.0001741	0.000	1.6200	.1905	.1363	.0145
1008	68.300	99.03	3.8159	.0001734	0.000	1.3700	.1589	.1133	.0150
1009	28.100	98.59	4.1259	.0001696	0.000	.6200	.0732	.0506	.0200
1010	20.210	98.49	4.3119	.0001686	0.000	.4700	.0532	.0363	.0210
1011	84.200	99.51	3.8924	.0001761	0.000	2.4000	.1973	.1484	.0300
1012	60.100	98.74	3.9848	.0001728	0.000	1.9000	.1517	.1146	.0340

UNSTEADY WALL + SIMILARITY MODEL - FULL PROFILE 1 PARAMETER FIT

ID	BETA	UTAU	S	K	KAPPA	EPSILON	T0+	CI
1007	0.0000	3.852	11.025	.017269	.4479	.006497	.002762	5.731
1008	0.0000	3.933	11.025	.018140	.4479	.008645	.002762	5.731
1009	0.0000	4.249	11.025	.020266	.4479	.008749	.002762	5.731
1010	0.0000	4.424	11.025	.022412	.4479	.008334	.002762	5.731
1011	0.0000	4.012	11.025	.025874	.4479	.008789	.002762	5.731
1012	0.0000	4.123	11.025	.030230	.4479	.010836	.002762	5.731

MEAN EPSILON OVER 6 STATIONS = .009642

TABLE 5.2 Results of one parameter fits of the composite similarity profile to mainstream turbulence data.

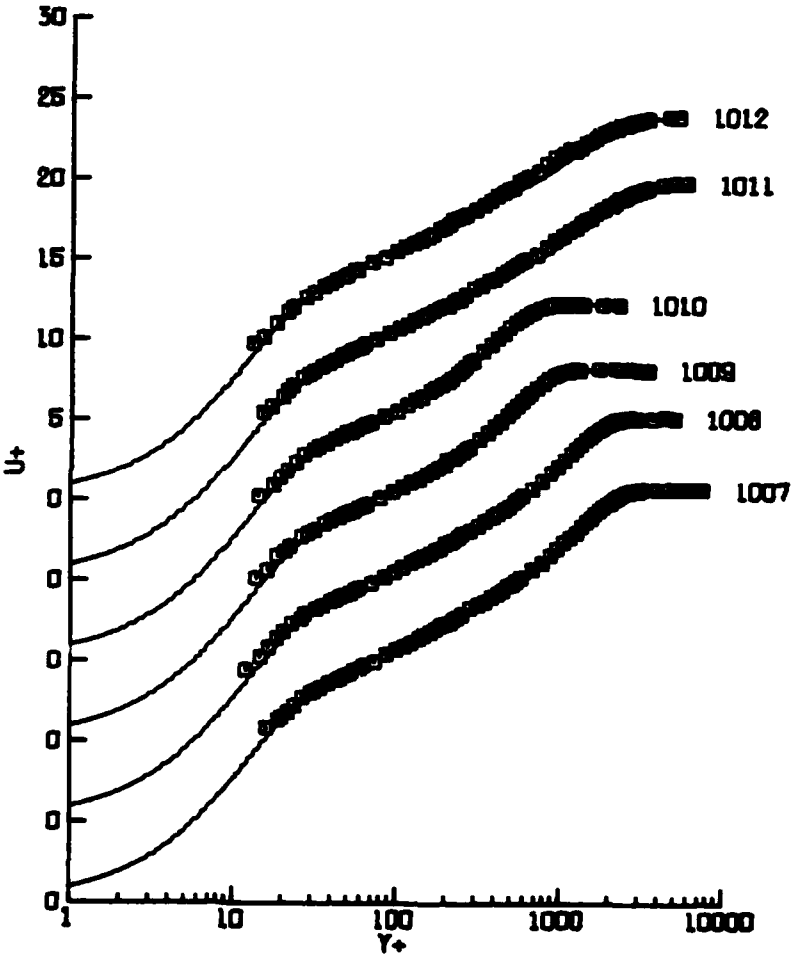

FIGURE 5.2 Velocity profile comparisons for one parameter optimization on K (with S=11.025 and κ=0.44789) for mainstream turbulence flow.

UT MAINSTREAM TURBULENCE TEST DATA
(ENGLISH UNITS)

EXPERIMENTAL VALUES

ID	XSTA	UE	UTAU	NU	BETA	DELTA	DELTA*	THETA	TU
1013	84.000	100.64	3.9886	.0001753	0.000	2.6000	.1795	.1360	.0350
1014	12.150	100.70	4.7077	.0001713	0.000	.4480	.0402	.0288	.0400
1015	28.200	99.59	4.2230	.0001785	0.000	1.1000	.0847	.0620	.0440
1016	28.100	100.59	4.3571	.0001729	0.000	.8100	.0744	.0542	.0530
1017	12.000	99.11	4.6603	.0001683	0.000	.4100	.0384	.0272	.0540
1018	12.150	100.57	4.7789	.0001711	0.000	.4100	.0356	.0252	.0640

UNSTEADY WALL + SIMILARITY MODEL - FULL PROFILE 1 PARAMETER FIT

ID	BETA	UTAU	S	K	KAPPA	EPSILON	T0+	CI
1013	0.0000	4.111	11.025	.027794	.4479	.010487	.002762	5.731
1014	0.0000	4.870	11.025	.038243	.4479	.009894	.002762	5.731
1015	0.0000	4.352	11.025	.027307	.4479	.009888	.002762	5.731
1016	0.0000	4.491	11.025	.030326	.4479	.009672	.002762	5.731
1017	0.0000	4.818	11.025	.038499	.4479	.010966	.002762	5.731
1018	0.0000	4.961	11.025	.042216	.4479	.012070	.002762	5.731

MEAN EPSILON OVER 6 STATIONS = .010483

TABLE 5.3 Results of one parameter fits of the composite similarity profile to mainstream turbulence data.

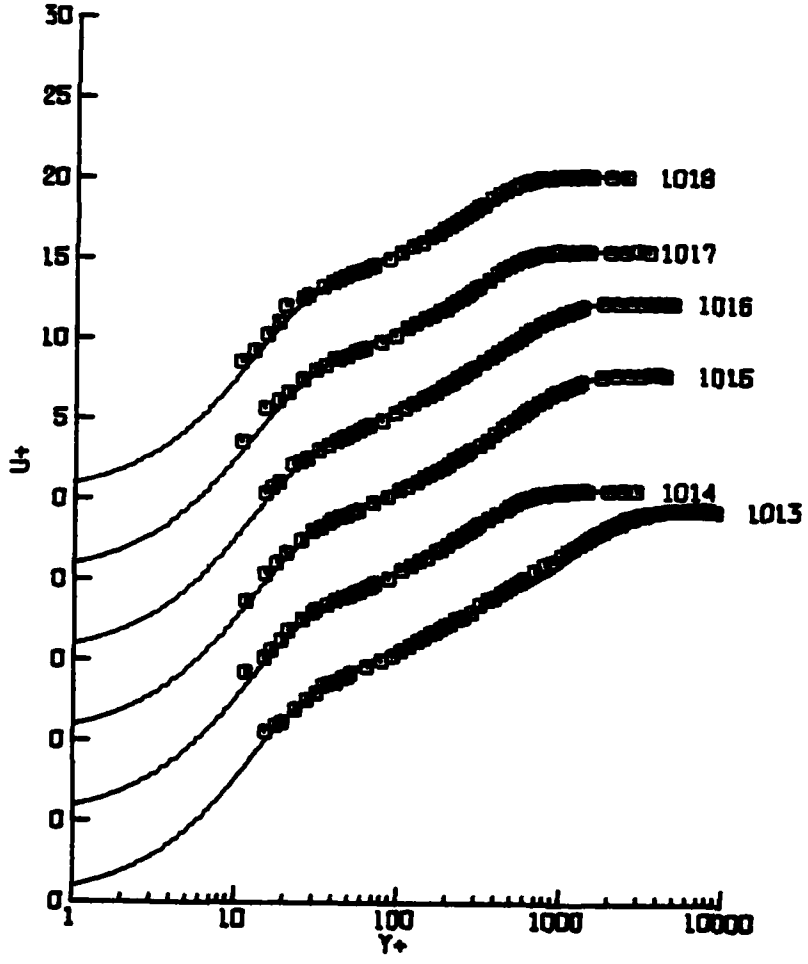

FIGURE 5.3 Velocity profile comparisons for one parameter optimization on K (with S=11.025 and κ=0.44789) for mainstream turbulence flow.

in these profile comparisons have been taken from the study of Blair & Werle (1980)and have been arranged here as a 1000 series in increasing order corresponding to increasing levels of local mainstream turbulence. Consequently the data in this sequence represents a mixture of data stations from the four basic runs with different mainstream turbulence generators which were carried out by Blair & Werle (1980). By observing the least squares error ε tabulated in Tables 5.1 through 5.3 and the velocity profile representations presented in Figures 5.1 through 5.3, it is apparent that the quality of curve fits are acceptable and that the profile model can be used to demonstrate the effects of mainstream turbulence on turbulent velocity profiles with good success. The optimization results indicate that there is a trend in which the value of the K parameter increases with increasing turbulence level Tu. This trend was anticipated in the sense that it was known that increasingly larger mainstream turbulence levels result in a progressively thicker boundary layer; mathematically larger values of K in the eddy viscosity formula give rise to a thicker boundary layer.

A second profile optimization method was considered in an attempt to obtain improved velocity profile fits. This method was initiated to investigate possible changes in both the inner and outer layers of the velocity profile and utilized

a two parameter optimization on S and K with a constant value of $\kappa = 0.44789$; again this value of κ corresponds to the value taken from the three parameter optimization in §4.3. The results of this two parameter optimization are presented in Tables 5.4 through 5.6 along with the corresponding profile representations in Figures 5.4 through 5.6.

An observation which can be made concerning the results of the two parameter optimization is that the least squares error is generally smaller than for the one parameter optimization; but that the improvement in the quality of the curve fits is not dramatic. The reason for this behavior may be explained by close examination of the nature of the curve fits near the wall; in this region there is a greater curve fit error for the one parameter K optimization than for the error associated with the two parameter S and K optimization. The remaining sections of the model velocity profiles for the one and two parameter optimizations are similar and exhibit almost the same curve fit error. In the two parameter fit the value of S adjusts to minimize this error for the data points nearest the wall. Unfortunately these data points are usually the most uncertain; it is also important to note that the S parameter values obtained from the two parameter optimization exhibit a great deal of scatter and any attempt to derive a trend from this

UT MAINSTREAM TURBULENCE TEST DATA
(ENGLISH UNITS)

EXPERIMENTAL VALUES

ID	XSTA	UE	UTAU	NU	BETA	DELTA	DELTA*	THETA	TU
1001	40.300	98.76	4.0294	.0001673	0.000	.5900	.0824	.0573	.0020
1002	84.100	99.39	3.7384	.0001710	0.000	1.1600	.1672	.1185	.0020
1003	84.100	98.70	3.7216	.0001737	0.000	1.3500	.1765	.1242	.0084
1004	76.300	98.67	3.7708	.0001740	0.000	1.2000	.1603	.1126	.0090
1005	36.200	98.79	4.0759	.0001716	0.000	.6000	.0794	.0542	.0100
1006	20.230	98.58	4.5405	.0001780	0.000	.3800	.0397	.0265	.0110

UNSTEADY WALL + SIMILARITY MODEL - FULL PROFILE 2 PARAMETER FIT

ID	BETA	UTAU	S	K	KAPPA	EPSILON	T0+	CI
1001	0.0000	4.476	8.983	.020849	.4479	.006855	.009863	4.365
1002	0.0000	4.096	9.269	.017418	.4479	.006087	.008275	4.551
1003	0.0000	4.187	9.049	.018461	.4479	.005249	.009476	4.408
1004	0.0000	4.133	9.273	.019074	.4479	.006912	.008259	4.553
1005	0.0000	4.551	8.781	.021610	.4479	.005515	.011170	4.234
1006	0.0000	5.123	8.514	.031755	.4479	.007694	.013142	4.064

MEAN EPSILON OVER 6 STATIONS = .006385

TABLE 5.4 Results of two parameter fits of the composite similarity profile to mainstream turbulence data.

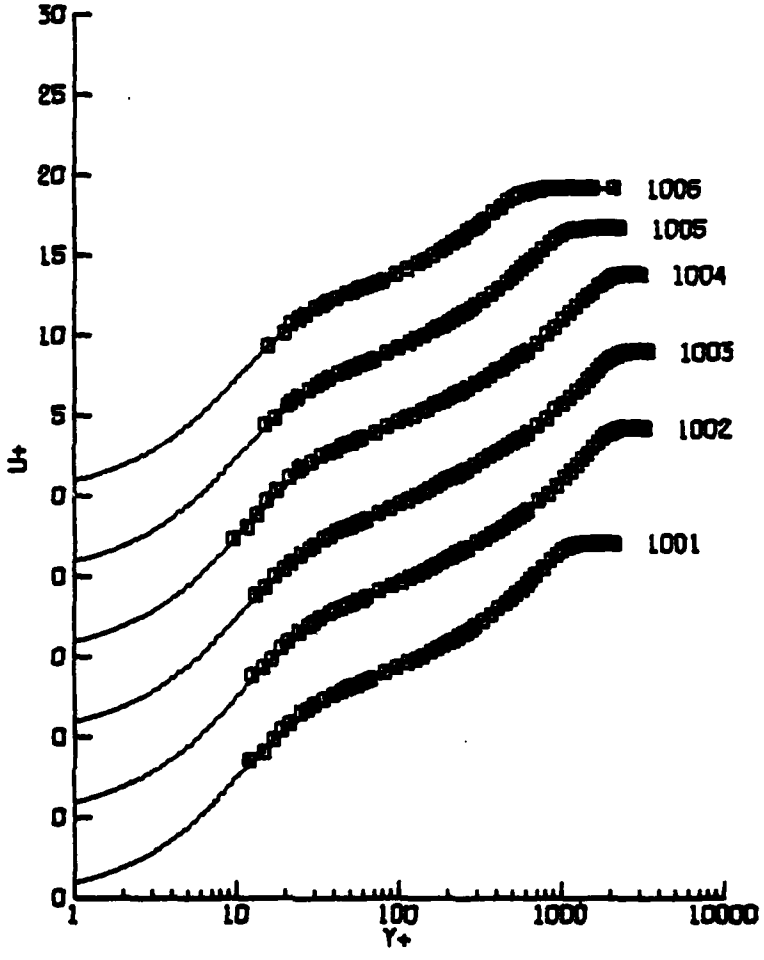

FIGURE 5.4 Velocity profile comparisons for two parameter optimization on S and K (with κ=0.44789) for mainstream turbulence flow.

UT MAINSTREAM TURBULENCE TEST DATA
(ENGLISH UNITS)

EXPERIMENTAL VALUES

ID	XSTA	UE	UTAU	NU	BETA	DELTA	DELTA*	THETA	TU
1007	84.100	99.03	3.7488	.0001741	0.000	1.6200	.1905	.1363	.0145
1008	68.300	99.03	3.8159	.0001734	0.000	1.3700	.1589	.1133	.0150
1009	28.180	98.59	4.1259	.0001696	0.000	.6200	.0732	.0506	.0200
1010	20.210	98.49	4.3119	.0001686	0.000	.4700	.0532	.0363	.0210
1011	84.200	99.51	3.8924	.0001761	0.000	2.4000	.1973	.1484	.0300
1012	60.100	98.74	3.9848	.0001728	0.000	1.9000	.1517	.1146	.0340

UNSTEADY WALL + SIMILARITY MODEL - FULL PROFILE 2 PARAMETER FIT

ID	BETA	UTAU	S	K	KAPPA	EPSILON	T0+	CI
1007	0.0000	4.180	8.746	.020918	.4479	.004514	.011408	4.212
1008	0.0000	4.257	8.792	.021473	.4479	.005439	.011090	4.242
1009	0.0000	4.604	8.852	.023402	.4479	.005797	.010695	4.280
1010	0.0000	4.775	8.980	.025384	.4479	.005800	.009885	4.363
1011	0.0000	4.384	8.515	.033027	.4479	.006574	.013134	4.065
1012	0.0000	4.636	7.725	.041907	.4479	.008186	.021172	3.571

MEAN EPSILON OVER 6 STATIONS = .006052

TABLE 5.5 Results of two parameter fits of the composite similarity profile to mainstream turbulence data.

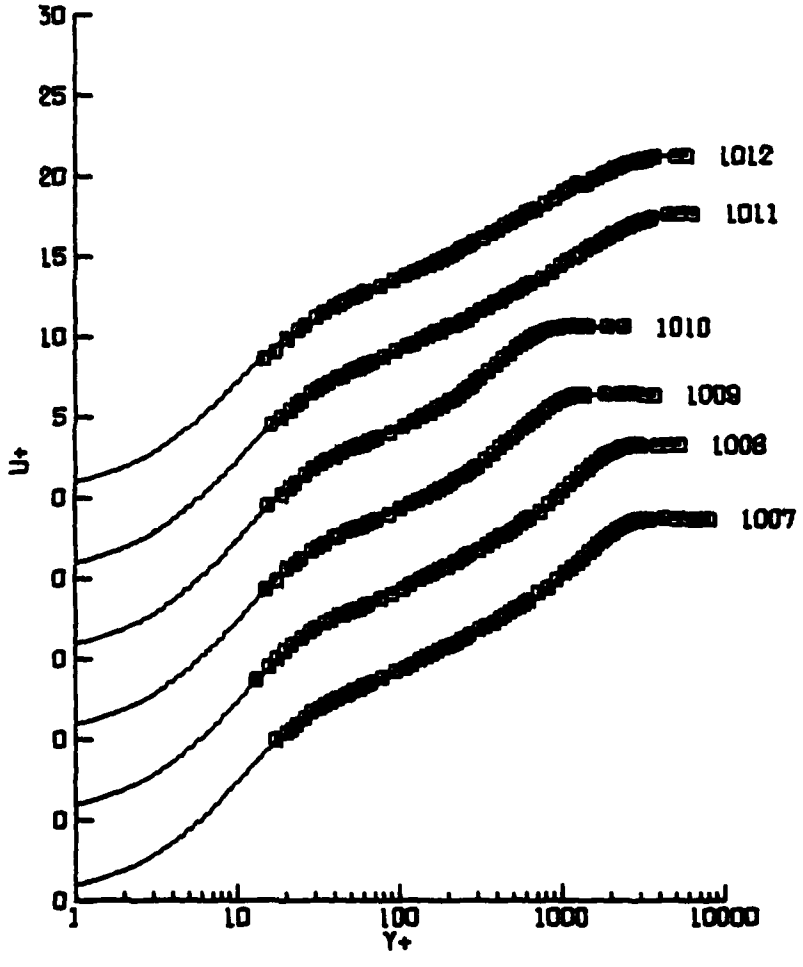

FIGURE 5.5 Velocity profile comparisons for two parameter optimization on S and K (with κ=0.44789) for mainstream turbulence flow.

UT MAINSTREAM TURBULENCE TEST DATA
(ENGLISH UNITS)

EXPERIMENTAL VALUES

ID	XSTA	UE	UTAU	NU	BETA	DELTA	DELTA*	THETA	TU
1013	84.000	100.64	3.9806	.0001759	0.000	2.6000	.1795	.1360	.0350
1014	12.150	100.70	4.7077	.0001713	0.000	.4400	.0402	.0286	.0400
1015	28.200	99.59	4.2230	.0001706	0.000	1.1000	.0847	.0620	.0440
1016	28.100	100.59	4.3571	.0001728	0.000	.8100	.0744	.0542	.0530
1017	12.000	99.11	4.6683	.0001683	0.000	.4100	.0384	.0272	.0540
1018	12.150	100.57	4.7789	.0001711	0.000	.4100	.0356	.0252	.0640

UNSTEADY WALL + SIMILARITY MODEL - FULL PROFILE 2 PARAMETER FIT

ID	BETA	UTAU	S	K	KAPPA	EPSILON	TO+	CI
1013	0.0000	4.730	7.868	.042079	.4479	.007658	.031346	3.174
1014	0.0000	5.284	8.809	.042627	.4479	.006308	.010980	4.252
1015	0.0000	4.603	9.463	.030386	.4479	.008471	.007341	4.679
1016	0.0000	5.004	8.097	.038308	.4479	.007134	.016925	3.801
1017	0.0000	5.270	8.602	.043213	.4479	.006478	.012458	4.120
1018	0.0000	5.342	8.980	.045056	.4479	.008095	.009889	4.363

MEAN EPSILON OVER 6 STATIONS = .007357

TABLE 5.6 Results of two parameter fits of the composite similarity profile to mainstream turbulence data.

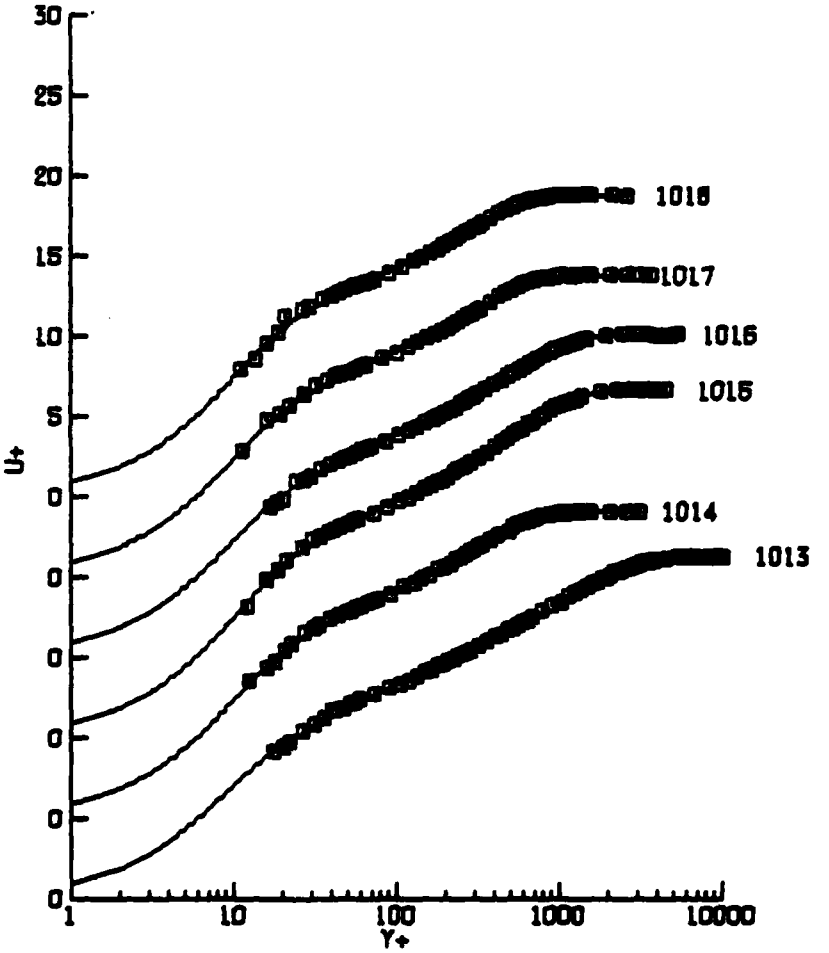

FIGURE 5.6 Velocity profile comparisons for two parameter optimization on S and K (with κ=0.44789) for mainstream turbulence flow.

information was considered to be potentially misleading. Finally, the magnitude of the S parameter for the low turbulence intensity cases did not match the value of S = 11.025 which was obtained from the S correlation of §4.3. All of the above observations suggest that the one parameter K optimization with constant values S = 11.025 and κ = 0.44789 provides the most realistic method for developing velocity profile predictions. The objective now is to obtain a correlation for the K parameter based upon the results of this section.

5.3 Parameter Correlations

In order to develop a profile prediction method optimized parameter values were obtained from the one parameter optimization of K with constant values of S = 11.025 and κ = 0.44789. This optimization method examined eighteen zero pressure gradient data sets with mainstream turbulence levels which cover a range of Tu from 0.002 to 0.0640. The results of the optimized data fits for the K parameter were then plotted versus the turbulence level Tu as shown in Figure 5.7. Prospective correlations which could be used in a prediction procedure were obtained by fitting a least squares straight line and quadratic curve through the optimized parameter values represented by the symbols. The resulting correlations for the one parameter

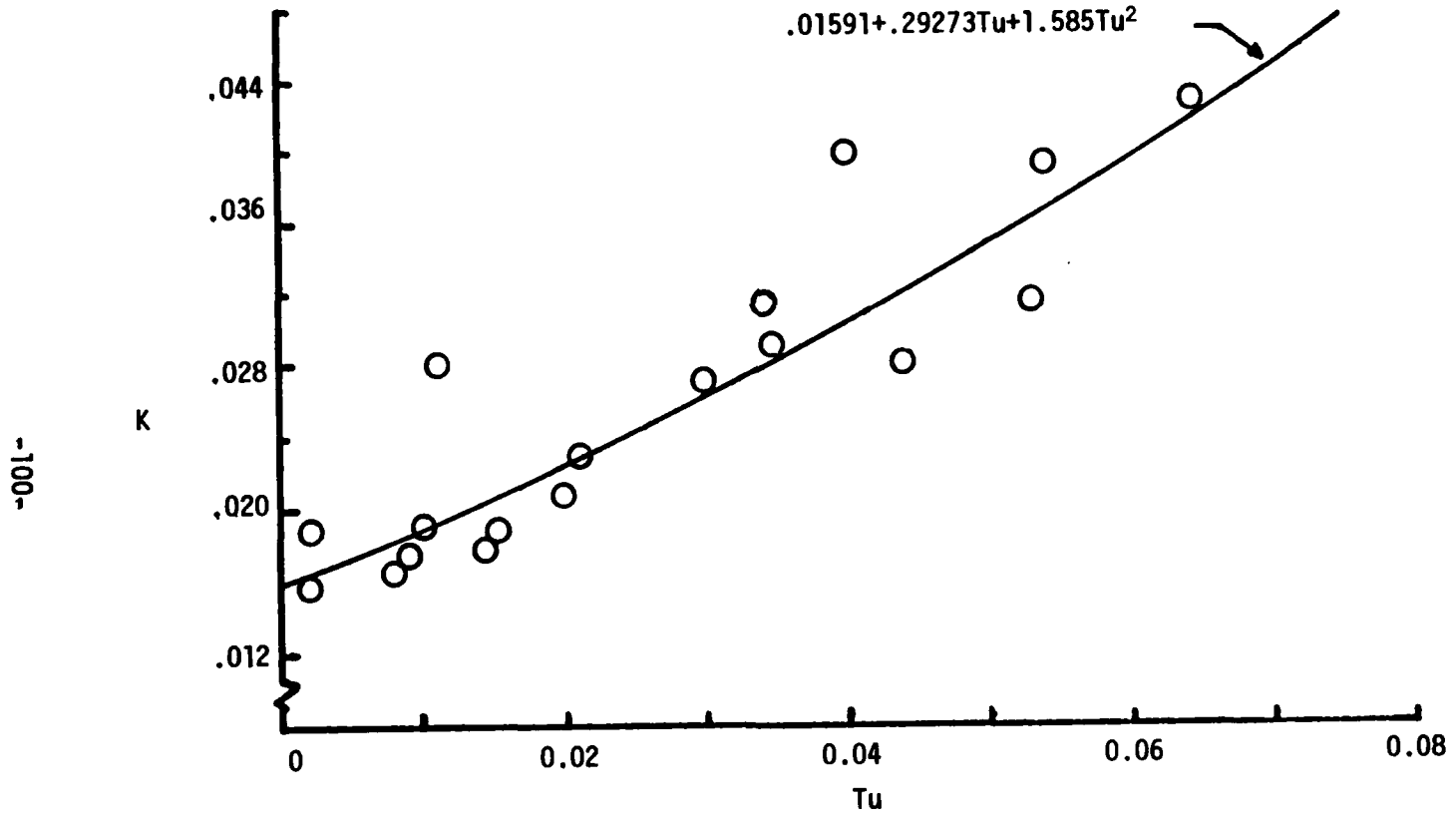

FIGURE 5.7 K parameter correlation obtained from one parameter fits of the composite similarity profile to constant pressure test data with mainstream turbulence.

optimization on K are

$$K = 0.01489 + 0.39285\ Tu \qquad (.0008519) \qquad (5.10)$$

and

$$K = 0.01567 + 0.30941\ Tu + 1.35909\ Tu^2 \quad (.0008462) \quad (5.11)$$

for the linear and quadratic fits respectively. Both correlations represent increasing functions of mainstream turbulence intensity as expected and discussed in section 5.1. The RMS curve fit errors for the correlations are given in parenthesis following the equations. These RMS values indicate that the quadratic curve fit gives only a very slight improvement over the linear fit; however, one feature of the quadratic correlation is that the value of its intercept is close to the value 0.01591 obtained from the three parameter correlation of §4.3 for turbulent boundary layers affected by pressure gradient. This indicates that the prediction methods for pressure gradient effects outlined in §4 and the method for mainstream turbulence are compatible. This compatibility adds to the credibility of the correlations for use in profile prediction. To obtain a correlation that incorporates the zero pressure gradient intercept value of K = 0.01591 from §4,3, the quadratic curve fit of equation (5.11) was rerun with the intercept held at 0.01591. The resulting correlation for the one parameter optimization

on K was

$$K = 0.01591 + .292727Tu + 1.58500Tu^2 \qquad (.0008465) \quad (5.12)$$

where the RMS curve fit error is given in parenthesis. The correlation of equation (5.12) is recommended for prediction purposes to insure complete compatibility.

6. SUMMARY AND CONCLUSIONS

In the present study, a profile model for the mean velocity in a nominally steady two-dimensional turbulent boundary layer has been developed. To obtain this profile, the leading terms in an asymptotic expansion for high Reynolds number for the mean velocity were derived for both the inner and outer layers of the turbulent boundary layer. A self-similar behavior in the velocity was assumed. In the outer layer, a simple eddy viscosity formula was assumed containing two parameters κ and K; the outer layer self-similar profile satisfies an ordinary differential equation which was solved numerically. For the inner layer, an analytical profile model which is based on the observed coherent structure of the time-dependent flow in the wall layer was used; this model contains the parameters κ and S. A composite profile which spans the entire boundary layer was defined and this profile is in general a function of the three parameters (K, κ, S). A computer code was developed for which any or all of the three profile parameters may be varied to obtain a best fit to a given set of experimentally measured profile data; this code is described in Appendix C. A test case for the code is presented in Appendix D.

There are two potential uses for this optimization procedure. In the first of these, a very close representation of a given

set of velocity data may be obtained by carrying out a three parameter optimization using the code described in Appendix C even in situations where the flow does not exhibit self similar behavior. The second use is rather more significant and is associated with the development of the basic model for a boundary-layer prediction method. By carrying out a series of optimization studies for given sets of data, it is demonstrated in §4 and §5 that trends in the optimized values of (s,κ,K) may be observed; from these trends correlations for the model parameters for a physical effect may be obtained. In the present report, two such studies have been carried out and correlations have been developed for the effects of both pressure gradients and mainstream turbulence.

LIST OF REFERENCES

1. Andersen, P.S., Kays, W.M. and Moffat, R.J. (1972). "The Turbulent Boundary Layer on a Porous Plate: An Experimental Study of the Fluid Mechanics for Adverse Free-Stream Pressure Gradients", Mech. Engrg. Rept. HMT-15, Stanford Univ.

2. Blair, M.F., and Werle, M.J. (1980). "The Influence of Free-Stream Turbulence on the Zero Pressure Gradient Fully Turbulent Boundary Layer", Tech. Report R80-914388-12, United Technologies Research Center.

3. Brown, K.C. and Stewartson, K. (1965). "On Similarity Solutions of the Boundary Layer Equations with Algebraic Decay", J. Fluid Mech., 23, pp. 673-687.

4. Cebeci, T. and Smith, A.M.O. (1974). Analysis of Turbulent Boundary Layers, Academic Press, New York.

5. Charnay, G., Compte-Bellot, G., and Mathiew, J. (1971). "Development of a Turbulent Boundary Layer on a Flat Plate in an External Turbulent Flow", AGARD, CP93, Paper No. 27.

6. Clauser, F.H. (1954). "Turbulent Boundary Layers in Adverse Pressure Gradients", J. Aeronaut. Sci., 21, pp. 91-108.

7. Clauser, F.H. (1956). "The Turbulent Boundary Layer", Adv. Appl. Mech. 1, pp. 1-51.

8. Coles, D.E. and Hirst, E.A. (1969). Proceedings, Computation of Turbulent Boundary Layers - 1968, AFOSR-IFP-Stanford Conference, Volume II, Mech. Engrg., Stanford Univ.

9. Corino, E.R. and Brodkey, R.S. (1969). "A Visual Investigation of the Wall Region in Turbulent Flow", J. Fluid Mech., 37, pp. 1-30.

10. Doligalski, T.L., Smith, C.R., and Walker, J.D.A. (1981). "Production Mechanism for Turbulent Boundary-Layer Flows", Viscous Flow Drag Reduction, G.R. Hough (Ed.), Progress in Astronautics and Aeronautics, 72, AIAA.

11. Doligalski, T. and Walker, J.D.A. (1978). "Shear Layer Breakdown due to Vortex Motion", Proc. Workshop on Coherent Structure in Turbulent Boundary Layers, C.R. Smith and D.E. Abbott (Ed.), Lehigh Univ. Press.

12. Fendell, F.E. (1972). "Singular Perturbation and Turbulent Shear Flow Near Walls", J. Astronaut. Sci., 20, pp. 129-165.

13. Himmelblau, D.M. (1972). Applied Nonlinear Programming, McGraw-Hill.

14. Huffman, G.D., Zimmerman, D.R., and Bennet, W.A. (1972). "The Effect of Freestream Turbulence Level in Turbulent Boundary Layer Behavior", AGARD AG164, pp. 91-115.

15. Keller, H.B. (1969). "Accurate Difference Methods for Linear Ordinary Differential Equations Subject to Linear Constraints", SIAM J. Numer. Anal., 6, pp. 8-30.

16. Kestin, J. (1966). "The Effect of Free-Stream Turbulence on Heat Transfer Rates", Advances in Heat Transfer, 3, Academic Press, New York, pp. 1-31.

17. Kline, S.J., Lisin, A.V., and Waitman, B.A. (1960). "Preliminary Experimental Investigation of Effect of Free-Stream Turbulence on Turbulent Boundary-Layer Growth", NASA Tech. Note D-368.

18. Kline, S.J., Reynolds, W.C., Schraub, F.A. and Runstadler, P.W. (1967). "The Structure of Turbulent Boundary Layers", J. Fluid Mech. 30, pp. 741-773.

19. Kline, S.J. and Runstadler, P.W. (1959). "Some Preliminary Results of Visual Studies of the Flow Model of the Wall Layers of the Turbulent Boundary Layer", Trans. ASME, (Ser. E), J. of Appl. Mech., 2, pp. 166-170.

20. Leibovich, S. (1967a). "On the Differential Equation Governing the Rear Stagnation Point in Magnetohydrodynamics and Goldstein's 'Backward' Boundary Layers", Proc. Cam. Phil. Soc., 63, pp. 1327-1330.

21. Leibovich, S. (1967b). "Magnetohydrodynamic Flow at a Rear Stagnation Point", J. Fluid Mech., 29, pp. 401-413.

22. Mellor, G.L. (1972). "The Large Reynolds Number, Asymptotic Theory of Turbulent Boundary Layers", Int. J. Engrg. Sci., 10, pp. 851-873.

23. Mellor, G.L. and Gibson, D.M. (1966). "Equilibrium Turbulent Boundary Layers", J. Fluid Mech., 29, pp. 401-413.

24. Mellor, G.L. and Herring, H.J. (1968). "Two Methods of Calculating Turbulent Boundary-Layer Behavior Based on Numerical Solutions of the Equations of Motion", Proceedings Computation of Turbulent Boundary Layers-1968, AFOSR-IFP-Stanford Conference, Volume I, Mech. Engrg., Stanford Univ.

25. Mellor, G.L. and Herring, H.J. (1969). "A Method for Calculating Compressible Turbulent Boundary Layers", NASA CR-1144.

26. Murthy, S.N.B. (1977). Turbulence in Internal Flows, Turbomachinery and Other Engineering Applications, Hemisphere Publish., Washington.

27. Nychas, S.G., Hershey, H.C., and Brodkey, R.S. (1973). "A Visual Study of Turbulent Shear Flow", J. Fluid Mech., 61, pp. 513-540.

28. Scharnhorst, R.K. (1978). "An Analysis and Prediction of Nominally Steady, Two-Dimensional Constant-Property Turbulent Boundary Layers", Dept. of Mech., Ph.D. Thesis, Purdue Univ.

29. Scharnhorst, R.K., Walker, J.D.A. and Abbott, D.E. (1977). "Comparisons of Theoretical Profiles for a Two-dimensional Time-dependent Turbulent Boundary Layer with Experimental Data", Tech. Report CFMTR-77-1, School of Mech. Engrg., Purdue Univ.

30. Van Driest, E.R. (1956). "On Turbulent Flow Near A Wall", J. Aeronaut. Sci. 23, pp. 1007-1011 and 1036.

31. Van Dyke, M. (1975). Perturbation Methods in Fluid Mechanics, The Parabolic Press, Stanford, CA.

32. Walker, J.D.A. (1978). "The Boundary Layer Due to a Rectilinear Vortex", Proc. Roy. Soc. A359, pp. 167-188.

33. Walker, J.D.A. and Abbott, D.E. (1977). "Implications of the Structure of the Viscous Wall Layer", Turbulence in Internal Flows, Squid Workshop Proc., S.N.B. Murthy, (ed.), Plenum Press.

34. Walker, J.D.A., Abbott, D.E., and Scharnhorst, R.K. (1976). "On the Nominally Steady Two-dimensional Time-Mean Turbulent Boundary Layer", Tech. Report CFMTR-76-1, School of Mech. Engrg., Purdue Univ.

35. Walker, J.D.A. and Scharnhorst, R.K. (1977). "Solutions of the Time-Dependent Wall Layer Flow in a Turbulent Boundary Layer", Recent Advances in Engineering Science, G.D. Sih (ed.), Lehigh Univ. Press, Bethlehem, PA.

36. Walker, J.D.A. and Stenartson, K. (1972). "The Flow Past a Circular Cylinder in a Rotating Frame", Z. Agnew. Math. Phys., 23, pp. 745-752.

37. Weigand, G.G. (1978). "Forced Convection in a Two Dimensional Nominally Steady Turbulent Boundary Layer", Ph.D. Thesis, Purdue Univ., Aug. 1978.

38. Willmarth, W.W. (1975). "Structure of Turbulence in Boundary Layers", Advances in Appl. Mech. 15, pp. 159-254.

APPENDIX A

OUTER LAYER SIMILARITY SOLUTION

A.1 INTRODUCTION

In this section, the outer layer similarity equation

$$\frac{d}{d\eta}\left\{\varepsilon(\eta)\frac{dU_1}{d\eta}\right\} + (1+2\beta_c)\eta\ \frac{dU_1}{d\eta} + 2\beta_c U_1 = 0 \quad , \qquad (A.1)$$

is solved to obtain the outer layer velocity profile. Because of the irregular logarithmic behavior near η=0, two types of solution methods were used and these consist of a series solution for small η and a numerical solution for large η. The matching point where the series and numerical solutions are required to merge smoothly is taken to be $\eta_m = K/2\kappa$.

A.2 SERIES SOLUTION FOR SMALL η

The eddy viscosity function $\varepsilon(\eta)$ was selected such that $\varepsilon(\eta)$ approaches a linear variation $\kappa\eta$ exponentially quickly as η approaches zero. Consequently for small η, the outer layer similarity equation (A.1) becomes

$$\kappa\eta\ \frac{d^2U_1}{d\eta^2} + \{\kappa+(1+2\beta_c)\eta\}\ \frac{dU_1}{d\eta} + 2\beta_c\ U_1 = 0 \ . \qquad (A.2)$$

For equation (A.2), a series solution of the form

$$u_1 = \eta^{\alpha} \sum_{i=0}^{\infty} a_n \eta^i \ , \tag{A.3}$$

is assumed and the indicial equation yields a double root $\alpha=0$. The solution thus takes the form of a regular power series plus a logarithmic term of the form,

$$U_1 = \sum_{n=0}^{\infty} b_n \eta^n + \{ \sum_{n=0}^{\infty} a_n \eta^n \} \log \eta \ , \tag{A.4}$$

with derivatives

$$\frac{dU_1}{d\eta} = \sum_{n=1}^{\infty} h\, b_n \eta^{n-1} + \{ \sum_{n=1}^{\infty} n\, a_n \eta^{n-1} \} \log \eta + \sum_{n=0}^{\infty} a_n \eta^{n-1} \ , \tag{A.5}$$

and

$$\frac{d^2U_1}{d\eta^2} = \sum_{n=2}^{\infty} n(n-1) b_n \eta^{n-2} + \{ \sum_{n=2}^{\infty} n(n-1) a_n \eta^{n-2} \} \log \eta$$

$$+ \sum_{n=1}^{\infty} n\, a_n \eta^{n-2} - \frac{a_0}{\eta^2} + \sum_{n=2}^{\infty} a_n (n-1) \eta^{n-2} \ . \tag{A.6}$$

As $\eta \to 0$, the required behavior for U_1 is given by equation (2.63) and is

$$U_1 \sim \frac{1}{\kappa} \log \eta + C_o \ ; \tag{A.7}$$

therefore

$$a_o = \frac{1}{\kappa} \quad \text{and} \quad b_o = C_o \quad . \tag{A.8}$$

Recursion relations for a_n and b_n are obtained by substitution of U_1 and its derivatives from equations (A.4), (A.5), and (A.6) into equation (A.2). It may easily be shown that

$$a_{n+1} = \frac{-\{2\beta_c + n(1+2\beta_c)\}a_n}{\kappa(n+1)^2} \tag{A.9}$$

and

$$b_{n+1} = \frac{-1}{\kappa(n+1)^2}\left\{\frac{a_n}{n+1}\left[1 - (2\beta_c + n(1+2\beta_c))\right]\right.$$

$$\left. + (2\beta_c + n(1+2\beta_c))b_n\right\} \quad . \tag{A.10}$$

A.3 NUMERICAL SOLUTION OF OUTER REGION FOR LARGE η

A numerical solution to the outer layer similarity equation (A.1) is calculated in the range $\eta_m < \eta < \eta_o$ where η_m is the matching point to the series solution and η_o represents the outer bound of the numerical mesh which is chosen large enough to ensure no significant change in the solution. In order to obtain an accurate numerical solution, a small mesh size is needed near the wall whereas far from the wall, the solution decays rapidly and a larger mesh may be used. For this reason, a numerical method developed by Kellor (1969) which permits a

non-uniform mesh was used in this study; the details of this method will be described here.

The ordinary differential equation to be solved is of the form

$$\frac{d^2U}{d\eta^2} + P(\eta)\frac{dU}{d\eta} + q(\eta)U = 0 , \tag{A.11}$$

where

$$P(\eta) = \frac{1}{\varepsilon(\eta)}\{\frac{d\varepsilon}{d\eta} + (1+2\beta_o)\eta\} , \tag{A.12}$$

$$q(\eta) = \frac{2\beta_c}{\varepsilon(\eta)} \quad . \tag{A.13}$$

Equation (A.11) is reduced to two first order differential equations by the introduction of an auxiliary variable v defined as

$$\frac{du}{d\eta} = V \tag{A.14}$$

which transforms (A.11) to

$$\frac{dV}{d\eta} = -p(\eta)V - q(\eta)u \quad . \tag{A.15}$$

A non-uniform mesh is defined by

$$\eta_j = \eta_{j-1} + h_{j-1} \tag{A.16}$$

where h_{j-1} is the variable mesh length. Equations (A.14) and (A.15) are approximated at the midpoint of η_j and η_{j+1} using a central difference for the first derivative and average values for u and v. As a result, equations (A.14) and (A.15) become,

$$\frac{u_{j+1}-u_j}{h_j} = \frac{1}{2}(v_{j+1} + v_j) \quad , \tag{A.17}$$

and

$$\frac{v_{j+1}-v_j}{h_j} = \frac{-p_{j+\frac{1}{2}}}{2}(v_{j+1}+v_j) - \frac{q_{j+\frac{1}{2}}}{2}(w_{j+1}+w_j) \quad , \tag{A.18}$$

where

$$P_{j+\frac{1}{2}} = P(\eta_j+\frac{h_j}{2}) \text{ and } q_{j+\frac{1}{2}} = q(\eta_j + \frac{h_j}{2}) \quad .$$

The auxiliary variable v_{j+1} is eliminated using equation (A.17) to obtain

$$-2v_j + \frac{2}{h_j}(u_{j+1}-u_j) = -p_{j+\frac{1}{2}}(u_{j+1}-u_j) - \frac{h_j q_{j+\frac{1}{2}}}{2}(u_{j+1}+u_j) \quad . \tag{A.19}$$

A similar procedure is used to approximate (A.14) and (A.15) at the midpoint of η_{j-1} and η_j. Eliminating the variable v_{j-1} in a similar fashion reveals

$$2v_j - \frac{2}{h_{j-1}}(u_j - u_{j-1}) = -P_{j-\frac{1}{2}}(u_j - u_{j-1})$$

$$- \frac{h_{j-1} q_{j-\frac{1}{2}}}{2}(u_j + u_{j-1}) \ . \qquad \text{(A.20)}$$

By adding (A.19) and (A.20) to eliminate v_j, it may be shown that the finite difference equations reduce to the general form

$$b_j \, u_{j+1} + a_j u_j + c_j u_{j-1} = d_j \ , \qquad \text{(A.21)}$$

where

$$a_j = -1-\gamma - \frac{h_j}{2}(P_{j+\frac{1}{2}} - P_{j-\frac{1}{2}}) + \frac{h^2_j}{4}(q_{j+\frac{1}{2}} + \frac{1}{\gamma} q_{j-\frac{1}{2}}) \ ,$$

$$b_j = 1 + \frac{h_j}{2} P_{j+\frac{1}{2}} + \frac{h^2_j}{4} q_{j+\frac{1}{2}} \ ,$$

$$c_j = \gamma - \frac{h_j}{2} P_{j-\frac{1}{2}} + \frac{h^2_j}{4\gamma} q_{j-\frac{1}{2}} \ ,$$

$$d_j = 0 \ ,$$

$$\gamma = \frac{h_j}{h_{j-1}} \ .$$

This general form can be used to generate a system of N-1 finite difference equations for a mesh with j=1,2,3,...,N number of grid points. The system of equations forms a tri-diagonal matrix which can be solved in a direct and efficient manner by using the Thomas algorithm; this

algorithm defines two functions δ_j and F_j in which the system (A.21) may be solved as

$$u_j = F_j\, u_{j+1} + \delta_j\,, \tag{A.22}$$

where

$$\begin{aligned} F_1 &= 0, \qquad F_j = \frac{-b_j}{a_j + C_j F_{j-1}}\,, \\ \delta_1 &= u_1, \qquad \delta_j = \frac{d_j - C_j \delta_{j-1}}{a_j + C_j F_{j-1}}\,, \end{aligned} \tag{A.23}$$

for j=1,2,3,...,N-1. After the arrays F_j and δ_j are calculated, the solution u_j is obtained from (A.22) by back substitution from j=N-1 to j=1.

A.4 SOLUTION PROCEDURE

The procedure used in this study to obtain a smooth match between the series and numerical solutions at the match point η_m is outlined below. Let the solution to equation (A.1) be represented by

$$u = \begin{cases} u_s\,, & 0 < \eta \leq \eta_m \\ u_n\,, & \eta_m \leq \eta < \eta_o \end{cases}$$

where u_s and u_n denote the series and numerical solutions respectively. First, an arbitrary value for the constant C_o

in equation (A.7) is guessed, say $C_o^{(1)}$. From this value, a series solution may now be calculated for $0 < \eta < \eta_m$, say $u_s^{(1)}$. In particular, the series solution is used at the match point to obtain $u_s^{(1)}(\eta_m)$ and its derivative $du_s^{(1)}(\eta_m)/d\eta$. Using $u_s^{(1)}(\eta_m)$, the numerical solution for $\eta_m \leq \eta \leq \eta_o$ is calculated, say $u_n^{(1)}(\eta)$; the derivative $du_1^{(1)}(\eta_m)/d\eta$ is calculated numerically using a six point forward difference formula (Abramowitz & Stegum 1972, p. 914). It is worthwhile to note that at this step the resulting solution will not have a continuous derivative at $\eta=\eta_m$. A second arbitrary value for C_o is guessed, say $C_o^{(2)}$ from which $u_s^{(2)}$ and $u_n^{(2)}$ are calculated using a similar procedure as that stated above. Again, the resulting solution will not have a continuous derivative at $\eta=\eta_m$.

The final solution with a continuous first derivative at $\eta=\eta_m$ is a linear combination of the solutions previously found. Thus,

$$u_s = B_1 u_s^{(1)} + B_2 u_s^{(2)} \text{ for } 0 < \eta \leq \eta_m, \tag{A.24}$$

and

$$u_n = B_1 u_n^{(1)} + B_2 u_n^{(2)} \text{ for } \eta_m \leq \eta \leq \eta_o, \tag{A.25}$$

where B_1 and B_2 are constants. One condition imposed on B_1

and B_2 is

$$B_1 + B_2 = 1 \ , \tag{A.26}$$

in order that u satisfies

$$u \sim \frac{1}{\kappa} \log \eta + C_o \quad \text{as} \quad \eta \to 0 \ .$$

A second condition relating B_1 and B_2 is that the first derivatives of equations (A.24) and (A.25) must be equal at the match point according to

$$B_1 \left\{ \frac{du_s^{(1)}}{d\eta} - \frac{du_n^{(1)}}{d\eta} \right\}_{\eta=\eta_m} + B_2 \left\{ \frac{du_s^{(2)}}{d\eta} - \frac{du_n^{(2)}}{d\eta} \right\}_{\eta=\eta_m} = 0. \tag{A.27}$$

Equations (A.26) and (A.27) can be solved to yield the values of B_1 and B_2. The true value of C_o is thus

$$C_o = B_1 C_o^{(1)} + B_2 C_o^{(2)} \ . \tag{A.28}$$

In this manner, a solution to equation (A.1) is obtained consisting of a series solution for $\eta < \eta_m$ and a numerical solution for $\eta > \eta_m$; this solution and its first derivative are continuous at the matching point $\eta=\eta_m$. Since equation (A.1) is a second order equation all derivatives are therefore continuous at $\eta=\eta_m$.

APPENDIX B

THE Ξ FUNCTION

The Ξ function is defined as

$$\Xi(\eta) = \int_0^{\eta} e^{-x^2} \int_0^{x} e^{y^2} \int_0^{y} e^{-t^2} dt\, dy\, dx \,, \tag{B.1}$$

which satisfies the differential equation

$$\Xi'' + 2\eta\,\Xi = \frac{\sqrt{\pi}}{2} \operatorname{erf}(\eta) \,. \tag{B.2}$$

The following expansion is readily obtained

$$\Xi(\eta) = \frac{e^{-\eta^2}}{4} \sum_{j=1}^{\infty} \frac{2^j \alpha(j) \eta^{2j+1}}{(2j+1)!!} \,, \tag{B.3}$$

where

$$\alpha(j) = \alpha(j-1) + \frac{1}{j} \,, \quad \alpha(1) = 1 \,, \tag{B.4}$$

which is uniformly convergent for all η. An asymptotic expansion used to evaluate $\Xi(\eta)$ as $\eta \to \infty$ is

$$\Xi(\eta) \sim \frac{\sqrt{\pi}}{4} \left\{ \log \eta + \frac{\gamma_o}{2} - \frac{1}{2} \sum_{j=1}^{\infty} \frac{(2j-1)!!}{j 2^j \eta^{2j}} \right\} \,, \tag{B.5}$$

where γ_o is Euler's constant equal to 0.57721566... .

APPENDIX C

THE OPTIMIZATION CODE

```
      PROGRAM MAIN(INPUT,OUTPUT,TAPE5=INPUT,TAPE6=OUTPUT)
      COMMON/VAR/IVAR(3),X0(3)
      EXTERNAL F
C
C * * * THIS IS THE MAIN PROGRAM WHICH INITIATES THE DATA FITTING
C * * * BY CALLING SUBROUTINE PROFIT.
C
C * * * NPAR - NUMBER OF PARAMETERS DESIRED FOR THE PROFILE FIT.
C * * * REFERENCE: AN OPTIMIZATION TECHNIQUE FOR THE DEVELOPMENT
C * * *            OF A TWO-DIMENSIONAL TURBULENT BOUNDARY LAYER
C * * *            MODEL, YUHAS, L.J. MASTER'S THESIS
C * * *            LEHIGH UNIVERSITY
C
C * * * ITERM - MAXIMUM NUMBER OF CYCLES TO BE PERFORMED IN ORSRCH
C               (NORMALLY 50)
C * * * IPRINT=1 IF PRINTING OF INTERMEDIATE RESULTS IN ORSRCH IS
C              DESIRED DURING THE COURSE OF THE OPTIMIZATION.
C            =0 IF NO PRINTING IN ORSRCH IS DESIRED.
C * * * EPS - THE EXIT TOLERANCE IN ORSRCH IF,SAY,EPS=1.E-5 THE
C           ITERATION WILL CONTINUE IN ORSRCH UNTIL THE PARAMETERS
C           BEING OPTIMIZED HAVE CONVERGED TO 5 SIGNIFICANT
C           FIGURES
C
C   THE PARAMETERS CAPK,S,KAPPA TO BE OPTIMIZED ARE INITIALIZED
C   IN THE INPUT
C   IVAR(I)= 0  NOT OPTIMIZED
C          = 1 OPTIMIZED
C   WHERE I = 1 CAPK
C           = 2 S
C           = 3 KAPPA
C
      READ(5,10)(IVAR(I),I=1,3)
      NPAR=0
      DO 30 I=1,3
   30 NPAR=NPAR+IVAR(I)
      READ(5,20)ITERM,IPRINT,EPS,NA
      CALL PROFIT(NPAR,ITERM,IPRINT,EPS,NA)
   10 FORMAT(3I2)
   20 FORMAT(2I4,E6.1,I4)
      STOP
      END
```

```
      SUBROUTINE PROFIT(NPAX,ITERM,IPRINT,EPS,NA)
      DIMENSION ITITLE(5),LUNIT(4),XF(3)
      DIMENSION LSYS(2),IDEN(15),X(15),UE(15),UTAU(15),DUEDX(15),PPLUS(1
     +5),DELTA(15),DELSTR(15),THETA(15),SHAPE(15),EPSI(15),DELT(15)
      DIMENSION PPLUSE(15),UTAUE(15),ES(15),YOPLUS(15),C(15),BETE(15)
      DIMENSION CF(15),CFE(15),CI(15),CAPK(15),XKAP(15),BT(15),TUT(15)
      DIMENSION FS(3),DX(3),DXERR(3),DXF(3),DXERF(3),XN(15)
      COMMON/DATA/NPAR,NOP,XNU,UI,DUIDX,YD(90),UD(90),DLSTR,UA(90),
     +YOPL(1000),UAPL(1000),NPPT
      COMMON/VAR/IVAR(3),XO(3)
      COMMON/UOUT/NO,ETA(400),DETA(400),U(400),ETAM,ETAO,COUT,CIN,
     1S,TNOTP,DELIN,DELOUT,USTAR,BETAC
      EXTERNAL F
      DATA LUNIT/2HFT,2H M,2HIN,2HCM/,LSYS/7HENGLISH,7H METRIC/,EBAR/0./
      DATA HGHT/0.1/
      DATA NPPT/400/
      NO=NA
C
C * * * SUBROUTINE PROFIT READS IN THE EXPERIMENTAL DATA AND
C * * * INITIATES THE OPTIMIZATION AT EACH DATA STATION BY
C * * * CALLING SUBROUTINE ORSRCH
C
C * * * INPUT IDENTIFICATION FOR DATA RUN
C       ID - A FOUR DIGIT NUMBER (USER SUPPLIED) TO IDENTIFY DATA
C       IUNIT - ZERO FOR ENGLISH UNITS,ONE FOR METRIC UNITS
C       ITITLE- TITLE OF DATA SET (50 CHARACTERS MAXIMUM)
C
      READ(5,100)ID,IUNIT,(ITITLE(I),I=1,5)
      IUP1=IUNIT+1
      IUP3=IUNIT+3
      CONV=12.
      IF(IUNIT.EQ.1)CONV=100.
      NPAR=NPAX
C
C * * * XNU - KINEMATIC VISCOSITY
C * * * NSTA - NUMBER OF DATA STATIONS
C
      READ(5,102) NSTA
C
C   INPUT PARAMETERS FOR PLOTTING
C
C * * * NCYC - NO. OF X CYCLES
C * * * NPLTPP - NO. OF ZERO PLOT TICKS ON Y AXIS
C * * * XLC - LENGTH OF EACH CYCLE ON X AXIS
C * * * INCPL - INCREMENT LABELS ON Y AXIS
C * * * NL - NO. OF NON-ZERO TICKS ON Y-AXIS
C * * * XL - LENGTH BETWEEN TICKS ON Y-AXIS
C
      READ(5,90) NCYC,NPLTPP,XLC,XL,NL,INCPL
 90   FORMAT(2I4,2F10.2,2I4)
      DO 10 N=1,NSTA
      ID=ID+1
      IDEN(N)=ID
      WRITE(6,103) (ITITLE(I),I=1,5),ID
C
C * * * X  - LOCAL VALUE OF X-LOCATION ON THE WALL
C * * * UE - LOCAL MAINSTREAM VELOCITY
```

```
C * * * UTAUE - ESTIMATE OR EXPERIMENTALLY QUOTED VALUE OF UTAU
C * * * DELTA - EXPERIMENTAL VALUE OF BOUNDARY LAYER THICKNESS
C * * * DELSTR- EXPERIMENTAL VALUE OF DISPLACEMENT THICKNESS
C * * * THETA - EXPERIMENTAL VALUE OF MOMENTUM THICKNESS
C * * * DUEDX - LOCAL VALUE OF THE MAINSTREAM VELOCITY GRADIENT
C
      READ(5,101)XNU
      XN(N)=XNU
      READ(5,104)X(N),UE(N),UTAUE(N),DELTA(N),DELSTR(N),THETA(N),DUEDX(N
     +),BETE(N)
      READ(5,130) TUT(N)
C
C * * * CFE - EXPERIMENTAL VALUE OF THE SKIN FRICTION COEFFICIENT
C * * * SHAPE-SHAPE FACTOR
C
      CFE(N)=2.*(UTAUE(N)/UE(N))**2
      SHAPE(N)=DELSTR(N)/THETA(N)
C
C * * * IF AN ESTIMATE OF UTAU IS NOT AVAILABLE,THE VALUES OF
C * * * UTAU ARE TO BE READ IN AS ZERO AND AN ESTIMATE FOR
C * * * UTAU IS COMPUTED USING THE LUDWEIG-TILLMAN CORRELATION.
C * * * NOTE THAT THIS IS ONLY USED AS A STARTING ESTIMATE
C * * * FOR UTAU IN THE OPTIMIZATION PROCEDURE.
C
      IF(ABS(UTAUE(N)).GT.1.E-16)GO TO 15
      CFE(N)=0.246*(UE(N)*THETA(N)/(XNU*CONV))**(-0.268)*10.**(-.678*SHA
     +PE(N))
      UTAUE(N)=UE(N)*SQRT(0.5*CFE(N))
   15 CONTINUE
C
C * * * PPLUSE-EXPERIMENTAL VALUE OF THE INNER REGION PRESSURE
C * * *         GRADIENT PARAMETER
C
      PPLUSE(N)=-XNU*UE(N)*DUEDX(N)/(UTAUE(N)**3)
      WRITE(6,105)X(N),LUNIT(IUP1),UE(N),LUNIT(IUP1)
      WRITE(6,106)DUEDX(N),UTAUE(N),LUNIT(IUP1),DELTA(N),LUNIT(IUP3),DEL
     +STR(N),LUNIT(IUP3),THETA(N),LUNIT(IUP3)
C
C * * * YO - Y LOCATIONS OF THE EXPERIMENTAL DATA POINTS
C * * * UO - EXPERIMENTALLY MEASURED MEAN VELOCITY AT YO
C
C     SET UP AXIS FOR PLOTTING
C
      IF(N.GT.NPLTPP) GO TO 26
      IF(N.GT.1) GO TO 25
      CALL PLOT(XLC*NCYC+2.,2.0,-3)
      CALL LOGAX(NCYC,XLC,HGHT)
      CALL SHFTYAX(NL,NPLTPP,XL,INCPL,HGHT)
      GO TO 27
   26 IF(N.GT.NPLTPP+1) GO TO 25
      CALL PLOT(XLC*NCYC+2.,-XL*(NPLTPP-1),-3)
      CALL LOGAX(NCYC,XLC,HGHT)
      CALL SHFTYAX(NL,NSTA-NPLTPP,XL,INCPL,HGHT)
      GO TO 27
   25 CALL PLOT(0.0,XL,-3)
   27 CONTINUE
      READ(5,102) NDP
```

```
      READ(5,99) X0(1),X0(2),X0(3)
 99   FORMAT(3F10.0)
      READ(5,107) (YD(I),I=1,NDP)
      READ(5,107) (UD(I),I=1,NDP)
      WRITE(6,108) NDP,LUNIT(IUP3)
      WRITE(6,109) (YD(I),UD(I),I=1,NDP)
      DO 20 I=1,NDP
20    YD(I)=YD(I)/CONV
      DELTA(N)=DELTA(N)/CONV
      DELSTR=DELSTR(N)/CONV
      USTAR=UTAUE(N)/UE(N)
      UI=UE(N)
      DUIDX=DUEDX(N)
C
C    INITIALIZE STEP SIZES FOR DRSRCH
C
      DX(1)=.001
      DX(2)=0.5
      DX(3)=0.01
      DXERR(1)=0.00001
      DXERR(2)=0.0001
      DXERR(3)=0.0001
C
C     ARRANGE VARIABLES BEING OPTIMIZED
C    IN ORDERED FORM FOR OPTIMIZATION IN DRSRCH.
C
      JC=0
      DO 30 I=1,3
      IF(IVAR(I).EQ.0)GO TO 30
      JC=JC+1
      XF(JC)=X0(I)
      DXF(JC)=DX(I)
      DXERF(JC)=DXERR(I)
 30   CONTINUE
C
C    INITIATE OPTIMIZATION IN DRSRCH
C
      CALL DRSRCH(NPAR,3,F,FF,FS,XF,DXF,DXERF,ITERM,EPS,ITER,
     1IPRINT,IER)
C
C    OPTIMIZATION COMPLETE.  REARRANGE VARIABLES IN CORRECT ORDER.
C
      JC=1
      DO 40 I=1,3
      IF(IVAR(I).EQ.0)GO TO 40
      X0(I)=XF(JC)
      DX(I)=DXF(JC)
      DXERR(I)=DXERF(JC)
      JC=JC+1
 40   CONTINUE
      EPSI(N)=SQRT(FF)
      EBAR=EBAR+EPSI(N)
      DELTA(N)=DELTA(N)*CONV
      CAPK(N)=X0(1)
      ES(N)=X0(2)
      XKAP(N)=X0(3)
      UTAU(N)=USTAR*UE(N)
```

```
      CF(N)=2.*(UTAU(N)/UE(N))**2
      CI(N)=CINF(ES(N),TOPLUS(N),X0(3),0.,1.)
      BT(N)=BETAC
      WRITE(6,110) ITER,EPSI(N),NPAR
      WRITE(6,111) (X0(J),J=1,3),UTAU(N)
      WRITE(6,112)CI(N),TOPLUS(N)
      WRITE(6,113) BETAC
C     MATCH CONDITION CRITERIA FOR INNER AND OUTER REGION VELOCITY PROFILES
      WRITE(6,114)
      WRITE(6,115) ETAM,N0,ETA0
C     INNER AND OUTER LENGTH SCALES
      WRITE(6,200)
      WRITE(6.201) DELIN,DELOUT
      WRITE(6,116)
         DO  50 I=1,NDP
            YP=YD(I)/DELIN
            UDP=UD(I)/USTAR
            UAP=UA(I)/USTAR
            UDPMUAP=UDP-UAP
   50    WRITE (6,117) YP,UD(I),UDP,UA(I),UAP,UDPMUAP
C
C     SET UP FOR PLOTTING
C     COMPUTE ENOUGH PLOT POINTS FOR A SMOOTH CURVE
C     FOR ETA LESS THAN ETAM
C
      NNPTS=400
      ETPL=ETAM-1.*DELIN/DELOUT
      DELP=ETPL/FLOAT(NNPTS)
      YDPL(1)=1.000*DELIN
      DO 55 I=1,NNPTS
      IF(I.EQ.1) GO TO 54
      YDPL(I)=YDPL(I-1)+DELP*DELOUT
 54   YDL=YDPL(I)/DELIN
      ETAD=YDPL(I)/DELOUT
      CALL U1SER(XKAP(N),BETAC,COUT,ETAD,U1,U1D,EPS)
      WAKE=U1-ALOG(ETAD)/XKAP(N)-COUT
      UAPL(I)=USTAR*(UP(YDL,S,TNOTP,CIN,XKAP(N),0.)+WAKE)
 55   CONTINUE
      DO 56 I=1,NNPTS
      YDPL(I)=(FLOAT(NCYC)*XLC)/ALOG(10.**FLOAT(NCYC))*(ALOG(YDPL(I)/DEL
     1IN))
      UAPL(I)=XL*NL*UAPL(I)/(NL*INCPL*USTAR)
 56   CONTINUE
C
C     FOR ETA GREATER THAN ETA MATCH, USE THE NUMERICAL
C     SOLUTION ALREADY CALCULATED
      NUA=NNPTS+N0
      NEX=NNPTS+1
      DO 59 I=NEX,NUA
      YDPL(I)=ETA(I-NNPTS)*DELOUT
      YDL=YDPL(I)/DELIN
      ETAD=ETA(I-NNPTS)
      WAKE=U(I-NNPTS)-ALOG(ETAD)/XKAP(N)-COUT
      UAPL(I)=USTAR*(UP(YDL,S,TNOTP,CIN,XKAP(N),0.)+WAKE)
      YDPL(I)=(FLOAT(NCYC)*XLC)/ALOG(10.**FLOAT(NCYC))*(ALOG(YDPL(I)/DEL
     1IN))
      UAPL(I)=XL*NL*UAPL(I)/(NL*INCPL*USTAR)
```

```
 59   CONTINUE
      CALL PLOT(YDPL(1),UAPL(1),3)
      DO 60 I=2,NDP
      CALL SYMBOL((FLOAT(NCYC)*XLC)/ALOG(10.**FLOAT(NCYC))*(ALOG(YD(I)/D
     1ELIN)),XL*NL*UD(I)/(NL*INCPL*USTAR),.07,0,0.,-1)
 60   CONTINUE
      CALL PLOT(0.,0.,3)
      XLIM=(FLOAT(NCYC)*XLC)/ALOG(10.**FLOAT(NCYC))*(ALOG(YD(NDP)/DELIN)
     +)
      DO 65 I=1,NUA
      NUAL=I
      IF(YDPL(I).GT.XLIM) GO TO 66
 65   CALL PLOT(YDPL(I),UAPL(I),2)
 66   CONTINUE
      XID=YDPL(NUAL)+2.*HGHT
      YID=UAPL(NUAL)-HGHT/2.
      CALL NUMBER(XID,YID,HGHT,IDEN(N),0.,2HI4)
10    CONTINUE
      EBAR=EBAR/FLOAT(NSTA)
      WRITE(6,118)(ITITLE(I),I=1,5),LSYS(IUP1)
      DO 70 I=1,NSTA
 70   WRITE(6,119)IDEN(I),X(I),UE(I),UTAUE(I),XN(I),BETE(I),DELTA(I),
     +DELSTR(I),THETA(I),TUT(I)
      WRITE(6,120) NPAR
      DO 80 I=1,NSTA
 80   WRITE(6,121)IDEN(I),BT(I),UTAU(I),ES(I),CAPK(I),XKAP(I),EPSI(I),
     +TOPLUS(I),CI(I)
      WRITE(6,122) NSTA,EBAR
100   FORMAT(2I4,5A10)
101   FORMAT(E10.3)
102   FORMAT(I4)
103   FORMAT(1H1,5X,5A10,' - ',I4)
104   FORMAT(7F10.0,F10.2)
105   FORMAT(/,5X,'X = ',F6.3,1X,A2,4X,'UE= ',F7.2,1X,A2,'/SEC')
106   FORMAT(/,14X,'EXPERIMENTAL VALUES',/,14X,'DUED X= ',F7.3,' 1/SEC',/
     1,14X,'UTAU= ',F7.3,1X,A2,'/SEC',/,14X,'DELTA= ',F7.4,1X,A2,/,14X,'
     2DELTA*= ',F7.4,1X,A2,/,14X,'THETA= ',F7.4,1X,A2)
107   FORMAT(8F10.0)
108   FORMAT(/,8X,'EXPERIMENTAL VELOCITY PROFILE',/,/,19X,I2,' POINTS',/,1
     14X,'Y (',A2,')',6X,'U/UE')
109   FORMAT(13X,F7.4,5X,F6.4)
110   FORMAT(//,5X,'AFTER ',I2,' ITERATIONS IN DRSRCH, F(X)= ',E13.6,' W
     CITH A',I2,2X,'PARAMETER FIT')
111   FORMAT(5X,'CAPK =',E13.6,2X,'S =',E13.6,2X,'KAPPA =',E13.6,2X,'UTA
     CU =',E13.6,/)
112   FORMAT(5X,'CIN= ',E13.6,5X,'TOPLUS= ',E13.6)
113   FORMAT(/,8X,'BETAC = ',E13.6)
114   FORMAT(//,5X,'MATCH CONDITION CRITERIA FOR VELOCITY PROFILE')
115   FORMAT(5X,'ETAM =  ',F7.4,4X,'NO =  ',I4,4X,'ETAC =  ',F7.4,)
116   FORMAT (1H1,13X, 66H*  EXPERIMENTAL PROFILE  *  ANALYTICAL PROFILE
     1  *  U+ DEVIATION  *,/,14X,  1H*,24X,  1H*,22X,  1H*,16X,  1H*,/,1
     2X,  2HY+,4X,  1H*,5X,  5HUD/UE,7X,  3HUD+,4X,  1H*,5X,  5HUA/UE,5X
     3,  3HUA+,4X,  1H*,3X,  9HUD+ - UA+,4X,  1H*)
117   FORMAT (5X,F7.2,2X,  1H*,3X,F7.4,4X,F7.2,3X,  1H*,3X,F7.4,2X,F7.2,
     13X,  1H*,3X,F9.6,4X,  1H*)
118   FORMAT(1H1,/////////,23X,5A10,/,41X,'(',A7,' UNITS)',
     +    //,///,39X,'EXPERIMENTAL VALUES',/,11X,'ID',6X,'XSTA',5X,'UE',5X
```

```
     +,≠UTAU≠,8X,≠NU≠,6X,≠BETA≠,6X,≠DELTA≠,4X,≠DELTA*≠,3X,≠THETA≠,5X,
     +≠TU≠)
  119 FORMAT(10X,I4,3X,F6.3,2X,F6.2,3X,F6.4,3X,F8.7,3X,F6.3,4(2X,F7.4))
  120 FORMAT(////,15X,≠UNSTEADY WALL + SIMILARITY MODEL       - FULL PROF
     +ILE≠,I4,2X,≠PARAMETER FIT≠,//,11X,  2HID,5X,  4HBETA,5X,  4HUTAU,
     +6X,  1HS,8X,  1HK,8X,  5HKAPPA,2X,  7HEPSILON,4X,  3HTO+,8X,
     +2HCI)
  121 FORMAT (10X,I4,1X,F8.4,2X,F6.3,2X,F7.3,2X,F8.6,3X,F7.4,2(1X,F8.6),
     13X,F6.3)
  122 FORMAT(/,20X,≠MEAN EPSILON OVER≠,I4,2X,≠STATIONS =≠,F8.6)
  130  FORMAT:F10.0)
  200  FORMAT(//,5X,≠LENGTH SCALES≠)
  201  FORMAT(5X,≠DELIN = ≠,F7.5,4X,≠DELOUT = ≠,F7.5)
       RETURN
       END
```

```
      SUBROUTINE DRSRCH (N,NDIM,F,F4,FS,X,DX,EPSI,MAX,EPSIF,ITER,IPRINT,
     1IER)
      EXTERNAL F
      DIMENSION FS(NDIM), X(NDIM), DX(NDIM), EPSI(NDIM)
C
C     DRSRCH - DIRECT SEARCH ROUTINE
C
C     VARIABLES
C            N - NUMBER OF PARAMETERS
C         NDIM - DIMENSION OF ARRAYS
C            F - FUNCTION NAME
C           F4 - FINAL VALUE OF F
C           FS - VECTOR OF INTERMEDIATE F VALUES
C            X - VECTOR OF INITIAL AND FINAL PARAMETER VALUES
C           DX - VECTOR OF INITIAL STEP SIZES
C         EPSI - VECTOR OF CONVERGENCE CRITERION
C          MAX - MAXIMUM NUMBER OF ITERATIONS
C        EPSIF - FINAL CONVERGENCE CRITERION
C         ITER - NUMBER OF ITERATIONS
C       IPRINT - PRINT CONTROL
C          IER - ERROR FLAG
C
      IER=0
      ITER=IER
      IF (IPRINT.EQ.1) WRITE (6,120)
      F4=F(X)
  101 I=0
  102 I=I+1
      NSTEP=0
      X3=X(I)
      F3=F4
      IF (IPRINT.EQ.1) WRITE (6,121) ITER,F3,(X(J),DX(J),J=1,N)
  103 ITER=ITER+1
      IF (ITER.GT.MAX) GO TO 118
      NSTEP=NSTEP+1
      X2=X3
      F2=F3
      X(I)=X(I)+DX(I)
      X3=X(I)
      F3=F(X)
      IF (IPRINT.EQ.1) WRITE (6,121) ITER,F3,(X(J),DX(J),J=1,N)
      IF (F3-F2) 104,104,105
  104 X1=X2
      F1=F2
      GO TO 103
  105 IF (NSTEP-1) 106,106,107
  106 X1=X3
      F1=F3
      DX(I)=-DX(I)
      X(I)=X(I)+DX(I)
      X3=X2
      F3=F2
      GO TO 103
  107 ITER=ITER+1
      IF (ITER.GT.MAX) GO TO 118
      X22=X2**2
      X32=X3**2
```

```
      F2MF3=F2-F3
      AFAC=F1*(X2-X3)-X1*F2MF3+F2*X3-F3*X2
      IF (AFAC.EQ.0.) GO TO 119
      BFAC=X1*X1*F2MF3-F1*(X22-X32)+X22*F3-X32*F2
      X4=-BFAC/(2.*AFAC)
      X(I)=X4
      F4=F(X)
      IF (IPRINT.EQ.1) WRITE (6,122) ITER,F4,(X(J),DX(J),J=1,N)
      DF=F4-F2
      IF (ABS(2.*DF/(F4+F2)).LT.EPSIF) GO TO 114
      DELX=X4-X2
      IF (ABS(DELX).LT.EPSI(I)) GO TO 114
      IF (DX(I).LT.0.) DELX=-DELX
      IF (DF) 108,108,111
  108 IF (DELX) 109,109,110
  109 X3=X2
      F3=F2
      X2=X4
      F2=F4
      GO TO 107
  110 X1=X2
      F1=F2
      X2=X4
      F2=F4
      GO TO 107
  111 IF (DELX) 112,112,113
  112 X1=X4
      F1=F4
      GO TO 107
  113 X3=X4
      F3=F4
      GO TO 107
  114 IF (N.EQ.1) RETURN
      FS(I)=F4
      IF (I-1) 102,102,115
  115 IF (I-N) 102,116,116
  116 IF (ABS(2.*(FS(I)-FS(I-1))/(FS(I)+FS(I-1))).LT.EPSIF) RETURN
      DO 117 J=1,N
  117 DX(J)=DX(J)/1.1
      GO TO 101
  118 IER=1
      WRITE(6,124) MAX
      RETURN
  119 IER=2
      WRITE (6,123) X1,F1,X2,F2,X3,F3
      RETURN
C
  120 FORMAT (1H1,3X, 5HCYCLE,8X, 1HF,13X, 4HX(I),9X, 5HDX(I))
  121 FORMAT ( 5H  E  ,I3,3X,E13.6,6(2X,E13.6))
  122 FORMAT ( 5H  I  ,I3,3X,E13.6,6(2X,E13.6))
  123 FORMAT (5X, 4HX1= ,E13.6, 6H  F1= ,E13.6, 6H  X2= ,E13.6, 6H
     1F2= ,E13.6, 6H  X3= ,E13.6, 6H  F3= ,E13.6)
  124 FORMAT(5X,*DRSRCH FAILED TO CONVERGE IN   *,I4,*ITERATIONS*)
C
      END
```

```
      FUNCTION F(X)
      DIMENSION X(3)
      COMMON/VAR/IVAR(3),X0(3)
      COMMON/DATA/NPAR,NDP,XNU,UI,DUIDX,YD(90),UD(90),DLSTR,UA(90),
     +YDPL(1000),UAPL(1000),NPPT
      COMMON/UOUT/N0,ETA(400),DETA(400),U(400),ETAM,ETA0,COUT,CIN,
     1S,TNOTP,DELIN,DELOUT,USTAR,BETAC
      DATA EPS/1.E-10/
C     FUNCTION F COMPUTES THE ROOT-MEAN-SQUARE ERROR
C     BETWEEN THE MEASURED EXPERIMENTAL VELOCITY PROFILE DATA
C     AND THE THEORETICAL VELOCITY PROFILE.  THE THEORETICAL
C     PROFILE CONSISTS OF THE UNSTEADY WALL LAYER MODEL
C     FOR THE INNER LAYER AND A SELF-SIMILAR PROFILE MODEL
C     FOR THE OUTER REGION.
C
C     ARRANGE VARIABLES INCOMING FROM DSRCH IN CORRECT ORDER
C
      JC=1
      DO 10 I=1,3
      IF(IVAR(I).EQ.0)GO TO 10
      X0(I)=X(JC)
      JC=JC+1
   10 CONTINUE
C
C     CALL UTAUF TO DETERMINE UTAU
C
      XKAP=X0(3)
      S=X0(2)
      CAPK=X0(1)
      CALL UTAUF(CAPK,XKAP)
C
C     COMPUTE RMS ERROR
C
      JLOC=2
      F=0.
      UA(1)=0.000
      DO 20 I=2,NDP
      YDP=YD(I)/DELIN
      ETAD=YD(I)/DELOUT
C
C     COMPUTE THE DEFECT PROFILE AT THE DATA POINT EITHER
C     FROM THE SERIES SOLUTION FOR ETAD LESS THAN ETAM
C     OR BY INTERPOLATION OF THE NUMERICAL SOLUTION FOR
C     ETA GREATER THAN ETAM
C
      IF(ETAD.GT.ETAM)GO TO 30
      CALL U1SER(XKAP,BETAC,COUT,ETAD,U1,U1D,EPS)
      WAKE=U1
      GO TO 40
   30 DO 50 J=JLOC,N0
      X1=ETA(J)-ETAD
      X2=ETA(J-1)-ETAD
      X3=X1*X2
      IF(X3.LT.0.)GO TO 60
   50 CONTINUE
      WAKE=0.
      GO TO 40
```

```
      60   JLOC=J
           WAKE=U(J)-(U(J)-U(J-1))*X1/DETA(J-1)
      40   WAKE=WAKE-ALOG(ETAD)/XKAP-COUT
           UA(I)=USTAR*(UP(YDP,S,TNOTP,CIN,XKAP,0.)+WAKE)
           FT=UD(I)-USTAR*(UP(YDP,S,TNOTP,CIN,XKAP,0.)+WAKE)
      20   F=F+FT*FT
           F=F/FLOAT(NDP)
      70   CONTINUE
           RETURN
           END
```

```
      FUNCTION EDYVIS(XKAP,CAPK,ETA)
      DATA N,XN/4,0.25/
C
C     FUNCTION EDYVIS EVALUATES THE EDDY VISCOSITY FUNCTION
C     OR ITS DERIVATIVE FOR THE OUTER LAYER OF A TURBULENT
C     BOUNDARY LAYER.  THE FUNCTION APPROACHES KAPPA*ETA
C     FOR SMALL ETA, EXPONENTIALLY QUICKLY.  FOR LARGE ETA
C     THE EDDY VISCOSITY FUNCTION APPROACHES THE OUTER CONSTANT
C     K  ALGEBRAICLY
C
C     INPUT PARAMETERS  XKAP - VON KARMAN #CONSTANT#
C                       CAPK - OUTER REGION #CONSTANT# K
C                       ETA  - SCALED OUTER REGION COORDINATE
C
      I=0
      GO TO 10
      ENTRY EDYVISD
      I=1
 10   C=(CAPK/XKAP )**N
      X1=EXP(-C/ETA**N)
      X2=1.-X1
      IF(I.EQ.0)EDYVIS=CAPK
      IF(I.EQ.1)EDYVIS=0.00
      IF(ETA.GT.10.0) GO TO 20
      IF(I.EQ.0)EDYVIS=XKAP*ETA*X2**XN
      IF(I.EQ.1)EDYVIS=XKAP*X2**XN*(1.-C*X1/(X2*ETA**N))
 20   RETURN
      END
```

```
      SUBROUTINE UOUTER(XKAP,CAPK)
      DIMENSION UC(400,2),CO(2),BA(2),F(400),DEL(400),A(400),B(400),
     1C(400)
      COMMON/UOUT/N0,ETA(400),DETA(400),U(400),ETAM,ETA0,COUT,CIN,
     1S,TNOTP,DELIN,DELOUT,USTAR,BETAC
      DATA EPS0,ALPHA,EPS/1.E-10,1.02,1.E-10/
C
C     SUBROUTINE UOUTER COMPUTES A NUMERICAL SOLUTION FOR THE
C     OUTER REGION VELOCITY DEFECT PROFILE GIVEN THE INPUT
C     VARIABLES    XKAP  - VON KARMAN *CONSTANT*
C                  CAPK  - OUTER REGION EDDY VISCOSITY *CONSTANT*
C                  BETAC - CLAUSER PRESSURE GRADIENT PARAMETER
C                  N0    - NUMBER OF MESH POINTS BETWEEN THE MATCH
C                          WITH THE SERIES SOLUTION (FOR SMALL ETA) AND
C                          THE BOUNDARY LAYER EDGE.
C     ON INPUT
C           ETA(I) - MESH POINTS BETWEEN ETAM AND ETA0
C           DETA(I) - VARIABLE STEP SIZE (INITALLY UNIFORM AND
C                     EQUAL TO H FOR FIRST 6 MESH POINTS, THEN
C                     SUCCESSIVELY INCREASING BY A FACTOR ALPHA)
C           U(I)    - NUMERICAL SOLUTION FOR VELOCITY DEFECT AT ETA(I)
C           ETAM    - MATCH POINT BETWEEN SERIES AND NUMERICAL SOLUTION
C           ETA0    - LARGEST VALUE OF ETA(I)
C           COUT    - OUTER REGION LOG-LAW *CONSTANT*
C
C     FIX THE MATCH POINT
C
      ETAM=0.5*CAPK/XKAP
C
C     FIX THE OUTER VALUE OF ETA
C
      X1=1./2.*BETAC
      X2=X1-1.
      X3=-(2.*BETAC+1.)/(2.*BETAC)
      IF(X1.GT.0.)ETA0=SQRT(-2.*CAPK*ALOG(EPS0)/X1)
      IF(X1.EQ.0.)ETA0=-SQRT(ABS(CAPK/X2))*ALOG(EPS0)
      IF(X1.LT.0.)ETA0=SQRT(ABS(CAPK/X1))*EPS0**(X3)
C
C     DEFINE THE MESH
C
      N1=N0-1
      ETA(1)=ETAM
      H=(ETA0-ETAM)/(4.+(1.-ALPHA**(N0-5))/(1.-ALPHA))
      DO 10 I=1,N1
      IF(I.LT.6)DETA(I)=H
      IF(I.GE.6)DETA(I)=ALPHA*DETA(I-1)
      ETA(I+1)=ETA(I)+DETA(I)
 10   CONTINUE
C
C     CALCULATE THE ELEMENTS OF THE TRIDIAGONAL MATRIX FOR
C     THE NUMERICAL SOLUTION FOR THE DEFECT PROFILE
C
      XP=ETA(1)+0.5*H
      EP=EDYVIS(XKAP,CAPK,XP)
      EPD=EDYVISD(XKAP,CAPK,XP)
      PJP=(EPD+X1*XP)/EP
      QJP=X2/EP
```

```
      DO 20 J=2,N1
      GAM=1.
      IF(J.GE.6)GAM=ALPHA
      X3=0.25*DETA(J)*DETA(J)
      X4=0.5*DETA(J)
      XM=XP
      XP=ETA(J)+X4
      EP=EDYVIS(XKAP,CAPK,XP)
      EPD=EDYVISD(XKAP,CAPK,XP)
      PJM=PJP
      PJP=(EPD+X1*XP)/EP
      QJM=QJP/GAM
      QJP=X2/EP
      A(J)=-1.-GAM-X4*(PJP-PJM)+X3*(QJP+QJM)
      B(J)=1.+X4*PJP+X3*QJP
   20 C(J)=GAM-X4*PJM+X3*QJM
C
C   DEFINE TWO INITIAL GUESSES FOR COUT
C
      CO(1)=1.
      CO(2)=0.75*CO(1)
C
C   CALCULATE TWO NUMERICAL SOLUTIONS FOR U FOR ETA GREATER
C   THAN ETAM FOR GUESSED VALUES OF COUTER
C
      DO 30 K=1,2
      CALL U1SER(XKAP,BETAC,CO(K),ETAM,UC(1,K),UCDS,EPS)
      F(1)=0.
      DEL(1)=UC(1,K)
      DO 40 J=2,N1
      X1=A(J)+C(J)*F(J-1)
      F(J)=-B(J)/X1
   40 DEL(J)=-C(J)*DEL(J-1)/X1
C
C   BACK SUBSTITION
C
      UC(N0,K)=0.
      DO 50 J=2,N1
      J1=N0-J+1
      UC(J1,K)=F(J1)*UC(J1+1,K)+DEL(J1)
   50 CONTINUE
C
C   CALCULATE DERIVATIVE OF NUMERICAL SOLUTION AT
C   ETA=ETAM WITH SLOPING DIFFERENCE FORMULA
C
      UCDN=(-274.*UC(1,K)+600.*UC(2,K)-500.*UC(3,K)
     1+400.*UC(4,K)-150.*UC(5,K)+24.*UC(6,K))/(120.*H)
C   CALCULATE DIFFERENCE BETWEEN NUMERICAL AND SERIES DERIVATIVE
C   SOLUTION AT ETA=ETAM.
C
      BA(K)=UCDS-UCDN
   30 CONTINUE
C
C   COMBINE TWO NUMERICAL SOLUTIONS TO OBTAIN THE TRUE
C   VALUES OF U(I) AND COUT
C
      B1=-BA(2)/(BA(1)-BA(2))
```

```
      B2=1.-B1
      COUT=B1*CO(1)+B2*CO(2)
      DO 60 J=1,NG
      U(J)=B1*UC(J,1)+B2*UC(J,2)
   60 CONTINUE
      RETURN
      END
```

```
      SUBROUTINE U1SER(XKAP,BETAC,COUT,ETA,U1,U1D,EPS)
      DATA NMAX/100/
C
C   SUBROUTINE U1SER EVALUATES THE VELOCITY DEFECT FUNCTION U1
C   AND ITS DERIVATIVE U1D AT THE INPUT VALUE OF ETA, FROM
C   A SERIES SOLUTION (OBTAINED BY THE METHOD OF FROBENIOUS)
C   WHICH IS VALID FOR SMALL ETA AND WHICH SATISFIES THE
C   ORDINARY DIFFERENTIAL EQUATION FOR THE SIMILARITY DEFECT
C   PROFILE U1.
C
C   INPUT PARAMETERS: XKAP  - VON KARMAN #CONSTANT#
C                     BETAC - CLAUSER PRESSURE GRADIENT PARAMETER
C                     COUT  - OUTER REGION LOG-LAW #CONSTANT#
C                     EPS   - CONVERGENCE TOLERANCE
C
      U1=U1D=0.
      X1=ALOG(ETA)
      X2=2.*BETAC
      X3=X2+1.
      FACA=1./XKAP
      FACB=COUT
      ASUM=FACA
      BSUM=FACB
      ASUMD=BSUMD=0.
      DO 10 I=1,NMAX
      X4=FLOAT(I-1)
      X5=X4+1.
      X6=1./(X5*X5*XKAP)
      X7=(X2+X4*X3)*X6
      FACB=(-FACB*X7+(X7-X6)*FACA/X5)*ETA
      FACA=-FACA*ETA*X7
      ASUM=ASUM+FACA
      BSUM=BSUM+FACB
      TESTA=ASUMD
      TESTB=BSUMD
      ASUMD=ASUMD+X5*FACA
      BSUMD=BSUMD+X5*FACB
      IF(I.LE.2)GO TO 10
      IF(ASUMD.EQ.0.0)GO TO 5
      IF(ABS(1.-TESTA/ASUMD).GT.EPS)GO TO 10
    5 IF(ABS(1.-TESTB/BSUMD).LT.EPS)GO TO 20
   10 CONTINUE
      PRINT 30, NMAX,XKAP,BETAC,COUT,ETA,EPS
   30 FORMAT(//,1X,#SERIES CALCULATION IN U1SER HAS NOT CONVERGED AFTER#
     +I4,2X,#TERMS#,//,1X,#XKAP= #,E12.5,3X,#BETAC= #,E12.5,
     +3X,,#COUT= #,E12.5,3X,#TOLERANCE= #,E12.5,//)
      STOP
   20 U1=BSUM+X1*ASUM
      U1D=(BSUMD+X1*ASUMD+ASUM)/ETA
      RETURN
      END
```

```
      SUBROUTINE UTAUF(CAPK,XKAP)
      COMMON/DATA/NPAR,NDP,XNU,UI,DUIDX,VJ(90),UD(90),DLSTR,UA(90),
     +YDPL(1000),UAPL(1000),NPPT
      COMMON/UOUT/NO,ETA(400),DETA(400),J(400),ETAM,ETA0,COUT,CIN,
     1S,TNOTP,DELIN,DELOUT,USTAR,BETAC
      DATA EPS,MAX/1.E-8,20/
C
C   UTAUF COMPUTES THE VALUE OF UTAU ITERATIVELY USING
C   THE MATCH CONDITION AND ALSO THE OUTER REGION DEFECT
C   PROFILE
C
C   EPS - EXIT TOLERANCE FOR TWO SUCCESSIVE ITERARES FOR UTAU
C   MAX - MAXIMUM NUMBER OF ITERATIONS IN UTAUF
C
      CIN=CINF(S,TNOTP,XKAP,0.,1.)
      REX=UI/XNU
      USTRA=USTAR
      DO 10 I=1,MAX
      DELOUT=DLSTR/USTRA
      DELIN=1./(REX*USTRA)
      BETAC=-DUIDX*DELOUT/(UI*USTRA)
      IF(BETAC.LT.-.50) BETAC=-.50
      CALL UOUTER(XKAP,CAPK)
      XA=1./(ALOG(DELOUT/DELIN)/XKAP+CIN-COUT)
      IF(I.NE.1)GO TO 20
      FB=USTRA-XA
      USTRB=USTRA
      USTRA=XA
      GO TO 10
   20 FA=USTRA-XA
      X1=USTRA-FA*(USTRB-USTRA)/(FB-FA)
      TEST=ABS(1.-USTRA/X1)
      IF(TEST.LT.EPS)GO TO 30
      IF(ABS(FB).LT.ABS(FA)) GO TO 15
      USTRB=USTRA
      FB=FA
   15 USTRA=X1
   10 CONTINUE
      WRITE(6,40) MAX,USTRA,X1
   40 FORMAT(/,1X,'ITERATION HAS FAILED TO CONVERGE IN UTAUF,
     1AFTER',I4,' ITERATIONS',/,1X,'LAST TWO ITERATES FOR UTAU ARE',
     22E16.8,/)
   30 USTAR=USTRA
      RETURN
      END
```

```
      FUNCTION CINF(S,TNOTP,XKAP,PPLUS,ROOTPR)
C
C * * * FUNCTION CINF USES THE WALL COMPATIBILITY CONDITIONS TO
C * * * CALCULATE THE INNER REGION CONSTANTS CINER AND TNOTP FOR A
C * * * GIVEN VALUE OF S FOR BOTH THE TEMPERATURE AND THE VELOCITY
C * * * PROFILE IN THE INNER LAYER OF A TURBULENT BOUNDARY LAYER.
C * * * ROOTPR = 1. FOR THE VELOCITY PROFILE CASE.
C * * * PPLUS = 0.  FOR THE TEMPERATURE PROFILE CASE.
C
      DATA GM,ROOTPI,EPSI,ITMX/-0.4045393481091 79,1.772453850905 52,1.E-1
     +0,20/
      JC=0
      X1=0.5*S*ROOTPR*ROOTPI*XKAP
      S2=S*S
      X2=2.*XKAP*S2*PPLUS/3.
      AL=EXP(-1.-X1-X2)
      DO 10 K=1,ITMX
      X3=ALOG(AL)
      X4=AL+1.
      AL2=AL*AL
      X5=SQRT(1.-AL2)
      C=AL
      AL=AL-(X1*X5+X4*X3+1.-AL+X2*(AL2+4.*AL+1.)/X4)/(-AL*X1/X5+
     +    X3+1./AL+X2*(AL2+2.*AL+3.)/(X4*X4))
      IF(ABS(AL/C-1.).LE.EPSI)GO TO 20
   10 CONTINUE
      JC=1
   20 AL2=AL*AL
      X4=1.-AL2
      TNOTP=AL2*S2/X4
      X5=SQRT(X4)
      CINF=X1/X5+GM-0.5*ALOG(S2+TNOTP)+1./(AL+1.)
     +    +(0.25*X2*(1.-9.*AL2)-PPLUS*TNOTP*XKAP*(3.*AL2-4.*AL+1.)/3.)/X4
      CINF=CINF/XKAP
      IF(JC.EQ.0)GO TO 30
      WRITE(6,40)K,TNOTP,CINF,AL,C
      STOP
C
   40 FORMAT(1X, 30HNO CONVERGENCE IN  CINF  AFTER,I4, 11H ITERATIONS,/,
     +1X, 7HTNOTP =,E15.5,10X,6HCINF =,E15.5,10X,4HAL =,E15.5,10X,5HALP
     +=,E15.5,/)
C
   30 RETURN
      END
```

```
      FUNCTION UP(YP,S,TNOTP,CIN,XKAP,PPLUS)
C
C * * * FUNCTION UP CALCULATES THE TIME-MEAN TEMPERATURE OR VELOCITY
C * * * PROFILE IN THE WALL LAYER OF A TURBULENT BOUNDARY LAYER
C * * * FOR SPECIFIED VALUES OF THE PARAMETERS LISTED BELOW.
C * * *        YP - Y+,SCALED WALL LAYER COORDINATE
C * * *        S  - S ,CYCLE TIME PARAMETER
C * * *        TNOTP - T0+,SIMILARITY PARAMETER
C * * *        CIN - INNER REGION LOG-LAW CONSTANT CI OR BI
C * * *        XKAP - KAPPA (VON-KARMAN CONSTANT) OR KAPPA-THETA
C * * *        PPLUS - WALL LAYER PRESSURE GRADIENT PARAMETER. (PPLUS
C * * *                IS ZERO FOR THE TEMPERATURE PROFILE CASE.)
C * * *NOTE:A CALL TO UP SHOULD NORMALLY BE PRECEDED BY A CALL TO
C * * *      CINF WHICH COMPUTES CIN AND TNOTP, GIVEN S.
C
      DATA X1,SRPI/-0.40453934810917 9,1.7724538509055 16/
      P(X)=-2.*PPLUS*(X+TNOTP)/3.
      R(X)=CIN+(0.5*ALOG(X+TNOTP)-X1)/XKAP+0.5*PPLUS*(S2+2.*TNOTP)
      Q(X,Y,ZA)=(2.*X*X+1.)*Y+2.*X*ZA/SRPI
      Z(X,Y,ZA)=4.*((2.*X*X+1.)*XI(X)+X*XIP(X)-0.125*SRPI*(6.*X*X+1.)*Y
     +          -0.75*X*ZA)/(SRPI*XKAP)
      W(X,Y,ZA)=(X**4+3.*X*X+0.75)*Y+X*(X*X+2.5)*ZA/SRPI-3.*X*X
C
C * * * PRECIS IS THE VALUE OF X SUCH THAT EXP(-X*X) MAY BE COMPUTED
C * * * WITHOUT INCURRING AN UNDEFLOW.
C
      PRECIS=25.9361455
C
      S2=S*S
      TPS2=S2+TNOTP
      H=0.5*YP/SQRT(S2+TNOTP)
      H0=0.5*YP/SQRT(TNOTP)
      ERFH=ERF(H)
      ERFH0=ERF(H0)
      EXPH=EXPH0=0.
      IF(H.LT.PRECIS)EXPH=EXP(-H*H)
      IF(H0.LT.PRECIS)EXPH0=EXP(-H0*H0)
      UP=TPS2*(R(S2)*Q(H,ERFH,EXPH)+Z(H,ERFH,EXPH))
     +   -TNOTP*(R(0.)*Q(H0,ERFH0,EXPH0)+Z(H0,ERFH0,EXPH0))
      IF(PPLUS.EQ.0.)GO TO 10
      IF(H.LT.PRECIS)GO TO 20
      UP=UP-0.5*(S2*S2+2.*S2*TNOTP)*PPLUS
      GO TO 10
   20 IF(H0.LT.PRECIS)GO TO 30
      WH=W(H,ERFH,EXPH)
      WH0=H0**4+.75
      GO TO 40
   30 WH=W(H,ERFH,EXPH)
      WH0=W(H0,ERFH0,EXPH0)
   40 UP=UP+TPS2*P(S2)*WH-TNOTP*P(0.)*WH0
   10 UP=UP/S2
      RETURN
      END
```

```
      FUNCTION XI(X)
      DATA SRPI,GAMO,EPSI/1.772453850905516,0.5772156649015328,1.E-10/
C
C * * * FUNCTION XI EVALUATES THE TRIPLE INTEGRAL IN THE UNSTEADY
C * * * WALL LAYER MODEL.THE TOLERANCE EPSI IS THE NUMBER OF
C * * * SIGNIFICANT FIGURES DESIRED FOR XI AND ITS DERIVATIVE
C * * * XIP AND IS MACHINE DEPENDENT.
C
      XI=0$IF=1
      IF(X.LE.0.) RETURN
      GO TO 1
      ENTRY XIP
      XI=0.$IF=2
      IF(X.LE.0.) RETURN
 1    X2=X*X
      FAC=2.*X2
      M=100
      SUM=0.
      SUMT=0.
      TERM=1.
      IF(X.GE.5.30) GO TO 110
      IF(IF.EQ.2) GO TO 100
      TERM=X
      ALPHA=1.
      DO 2 I=1,M
      TERM=TERM*FAC/FLOAT(2*I+1)
      SUM=SUM+TERM*ALPHA
      IF(ABS((SUM-SUMT)/SUM).LT.EPSI) GO TO 3
      ALPHA=ALPHA+1./FLOAT(I+1)
2     SUMT=SUM
3     XI=0.25*EXP(-X2)*SUM
      RETURN
100   DO 4 I=1,M
      TERM=TERM*FAC/FLOAT(2*I-1)
      SUM=SUM+TERM/FLOAT(I)
      IF(ABS((SUM-SUMT)/SUM).LT.EPSI) GO TO 5
4     SUMT=SUM
5     XI=0.25*EXP(-X2)*SUM
      RETURN
110   IF(IF.EQ.2) GO TO 120
      DO 6 I=1,M
      TERM=TERM*FLOAT(2*I-1)/FAC
      TERMA=TERM/FLOAT(I)
      IF(TERMA.LT.EPSI) GO TO 7
6     SUM=SUM+TERMA
7     XI=SRPI*(ALOG(X2)+GAMO-SUM)/8.
      RETURN
120   DO 8 I=1,M
      TERM=TERM*FLOAT(2*I-1)/FAC
      IF(TERM.LT.EPSI) GO TO 9
8     SUM=SUM+TERM
9     XI=SRPI*(1.+SUM)/(4.*X)
      RETURN
      END
```

```
      SUBROUTINE LOGAX(NCYC,XLC,HGHT)
C     SUBROUTINE LOGAX PLOTS THE X-AXIS LOGARITHMICALLY
C
C     INPUT PARAMETERS
C     NCYC =    NUMBER OF CYCLES
C     XLC  =    X LENGTH OF ONE CYCLE
C     HGHT =    HEIGHT OF AXIS LABEL
C          = 0 FOR NO LABEL
      DIMENSION XLOG(8)
      TCK1=HGHT
      IF(HGHT.LE.0.) TCK1=XLC/20.
      TCK2=TCK1/2.
C     SET UP EIGHT TIC  MARKS PER CYCLE
      DO 1 I=1,8
    1 XLOG(I)=ALOG10(FLOAT(I+1))*XLC
      DO 3 N=1,NCYC
      XN=N
      XNM1=XN-1.
      XLCNM1=XLC*XNM1
      IF(N.EQ.1) CALL PLOT(XLCNM1,TCK1,3)
      CALL PLOT(XLCNM1,0.,2)
      DO 2 I=1,8
      X=XLCNM1+XLOG(I)
      CALL PLOT(X,0.,2)
      CALL PLOT(X,TCK2,2)
    2 CALL PLOT(X,0.,2)
      XNLC=XN*XLC
      CALL PLOT(XNLC,0.,2)
    3 CALL PLOT(XNLC,TCK1,2)
      IF(HGHT.LE.0.) GO TO 5
      NUM=10**NCYC
      FAC=3.*HGHT/7.
      TNUM=FLOAT(9-NCYC)*FAC
      NCYCP1=NCYC+1
      DO 4 N=1,NCYCP1
      NNUM=NCYCP1-N
      XNUM=FLOAT(NNUM)*XLC-TNUM
      TNUM=TNUM+FAC
      YNUM=-1.5*HGHT
      CALL NUMBER(XNUM,YNUM,HGHT,NUM,0.,2HI5)
    4 NUM=NUM/10
      XSYM=XLC*FLOAT(NCYC)/2.-2.*FAC
      YSYM=-3.*HGHT
      CALL SYMBOL(XSYM,YSYM,HGHT,2HY+,0.,2)
    5 CALL PLOT(0.,0.,3)
      RETURN
      END
```

```
      SUBROUTINE SHFTYAX(NL,NPLTPP,XL,INCPL,HGHT)
C     SUBROUTINE SHFTYAX PLOTS THE Y-AXIS FOR A MULTIPLE NUMBER
C     OF CURVES ON THE SAME PLOT WITH SHIFTED Y-AXIS ORIGINS
C
C     INPUT PARAMETERS
C     NL     =    NUMBER OF POINTS LABELED NON-ZERO
C     NPLTPP =     NUMBER OF POINTS LABELED ZERO
C                   (EQUAL TO NUMBER OF AXIS SHIFTS)
C     XL     =    LENGTH BETWEEN AXIS TICS (SPACING)
C     INCPL  =    0
C     HGHT   =    HEIGHT OF AXIS LABEL
      TCK=HGHT
      IF(HGHT.LE.0.) TCK=XL/10.
      N=NPLTPP+NL-1
      CALL PLOT(TCK,0.,3)
      CALL PLOT(0.,0.,2)
      Y=0.
      DO 1 I=1,N
      Y=Y+XL
      CALL PLOT(0.,Y,2)
      CALL PLOT(TCK,Y,2)
 1    CALL PLOT(0.,Y,2)
      IF(HGHT.LE.0.) GO TO 4
      NUM=NL*INCPL
      FAC=6.*HGHT/7.
      XNUM=-2.5*FAC
      YNUM=Y-HGHT/2.
      DO 2 I=1,NL
      IF(NUM.LE.99) CALL NUMBER(XNUM,YNUM,HGHT,NUM,0.,2HI2)
      IF(NUM.GT.99) CALL NUMBER(XNUM-FAC,YNUM,HGHT,NUM,0.,2HI3)
      YNUM=YNUM-XL
 2    NUM=NUM-INCPL
      XNUM=-1.5*FAC
      DO 3 I=1,NPLTPP
      CALL NUMBER(XNUM,YNUM,HGHT,NUM,0.,2HI1)
 3    YNUM=YNUM-XL
      XSYM=-3.*HGHT
      YSYM=XL*FLOAT(N)/2.-FAC
      CALL SYMBOL(XSYM,YSYM,HGHT,2HU+,90.,2)
 4    CALL PLOT(0.,0.,3)
      RETURN
      END
```

APPENDIX D

TEST CASE

The turbulent boundary layer prediction code presented in Appendix C is set up to guide the user in understanding the code's operation. Comments are used to explain input variables and to denote where major operations are taking place.

The user supplied code input begins with "PROGRAM MAIN"; an integer value for each of the model parameters K, S, and κ is read in a 3I2 format. This integer value determines if the parameter is to be optimized or not; an integer value of 0 indicates no optimization for the corresponding variable and 1 indicates parameter optimization. The next variables to be read are "ITERM", "IPRINT", "EPS", and "NA" in 2I4, E6.1,I4 format. The "ITERM" variable denotes the maximum number of cycles to be performed in direct search. "IPRINT" is a print control parameter which determines if printing of intermediate optimization results is included in the output. The "EPS" parameter is the exit tolerance for convergence of the optimized parameters and "NA" denotes the number of mesh points for the outer region numerical solution to the similarity equation. A typical value of "NA" is 350 to ensure good accuracy and should be increased in applications where there is an intense velocity variation

in the outer layer. After reading in all of these variables, the program then calls "SUBROUTINE PROFIT" which reads in experimental data pertinent to the run.

"SUBROUTINE PROFIT" begins by reading in a four digit identification number for the data run "ID". The choice of an identifier is up to the user's discretion and will be successively incremented by one for each subsequent data station that is examined in the data set under consideration. The "ID" identifier is followed by "IUINT" which denotes whether the input experimental data is in English (ID=0) or metric units (ID=1). The selection of metric or English units is important to the input since this determines a conversion factor which is used in the code. A user supplied title for the data set is then read which is printed in the output. The number of data stations "NSTA" is read followed by input parameters for plotting. These plot parameters are read as "NCYC, NPLTPP, XLC, XL, NL, INCPL" and are accompanied by self-explanatory comments describing their function in the code. Their purpose is to allow maximum flexibility in obtaining plotted profiles to meet the requirements of the user. The only plotting comment worth mentioning here is that the "NPLTPP" parameter denotes the number of curves to be plotted on one plot using the shifted Y-axis method. If there are more data stations than the NPLTPP parameter (NSTA>NPLTPP), then another plot will be drawn to plot the remaining curves.

The data that follows is read for each data station and the sequence described in this paragraph is repetitive for subsequent data stations. First, the kinematic viscosity "XNU" is read in E10.3 format followed by "X, UE, UTAUE, DELTA, DELSTR, THETA, DUEDX, BETE" in 7F10.0, F10.2 format; these variables represent the x-location on the wall, local mainstream velocity, experimental value of u_τ, experimental value of the boundary layer thickness δ, experimental value of displacement thickness δ^*, experimental value of momentum thickness θ, local value of the velocity gradient dU_e/dx, and the value of the Clauser pressure gradient parameter β_c respectively. An optional read statement follows which reads the value of mainstream turbulence level "TUT" for examination of mainstream turbulence effects. The number of experimental velocity data points "NDP" is read next followed by the starting values of the model parameters K, S, and κ denoted by $x\phi(1)$, $x\phi(2)$, and $x\phi(3)$ respectively. These starting values are used to initiate optimization in the direct search subroutine. The experimental velocity profile data points are then read in F10.0 format starting with the x-coordinate values which signify the distance from the wall "YD". These are followed by the corresponding y-coordinates values which denote the nondimensionalized velocities "UD" represented by the ratio of velocity over the local mainstream

velocity u/U_e. "SUBROUTINE PROFIT" then calls "SUBROUTINE DRSRCH" to initiate the optimization of the profile parameters.

The direct search subroutine calls all other subroutines to evaluate the optimization function F(x). After the optimization has been completed, information pertinent to the model is printed out and a plot of the analytical profile and experimental data points is made. A listing of the output for one data station is presented on the subsequent pages. An output summary similar to that in Table 5.1 for all data stations is printed at the end of the output listings for all data stations.

UT MAINSTREAM TURBULENCE TEST DATA - 1001

X = 40.300 FT UE= 98.76 FT/SEC

EXPERIMENTAL VALUES
DUEDX= 0.000 1/SEC
UTAU= 4.029 FT/SEC
DELTA= .5900 IN
DELTA*= .0824 IN
THETA= .0573 IN

EXPERIMENTAL VELOCITY PROFILE
61 POINTS

Y (IN)	U/UE
0.0000	0.0000
.0053	.3870
.0065	.4110
.0075	.4450
.0085	.4750
.0095	.4900
.0111	.5230
.0123	.5340
.0133	.5460
.0155	.5610
.0176	.5730
.0197	.5830
.0211	.5900
.0223	.5940
.0247	.6010
.0267	.6090
.0287	.6150
.0302	.6200
.0368	.6350
.0438	.6500
.0508	.6650
.0566	.6750
.0633	.6840
.0707	.6950
.0765	.7030
.0838	.7140
.0907	.7230
.0963	.7290
.1034	.7380
.1103	.7450
.1163	.7510
.1237	.7590
.1308	.7660
.1473	.7830
.1651	.8010
.1824	.8160
.2007	.8300
.2178	.8460
.2353	.8600
.2528	.8720
.2709	.8860
.2877	.8980
.3059	.9110
.3405	.9330
.3756	.9520
.4109	.9680
.4455	.9820
.4806	.9910

.5153	.9960
.5505	.9980
.5853	1.0000
.6205	1.0000
.6553	1.0000
.6906	1.0000
.7255	1.0000
.7604	1.0000
.7953	.9990
.8309	1.0000
.8653	1.0000
.9003	.9990
.9355	.9990

```
  CYCLE          F              X(I)           DX(I)
E    0      .128712E-03     .168000E-01     .100000E-02
E    1      .103942E-03     .178000E-01     .100000E-02
     2      .101538E-03     .188000E-01     .100000E-02
     3      .117028E-03     .198000E-01     .100000E-02
I    4      .100118E-03     .184343E-01     .100000E-02
I    5      .100113E-03     .184212E-01     .100000E-02
I    6      .100112E-03     .184110E-01     .100000E-02
I    7      .100112E-03     .184101E-01     .100000E-02

   AFTER  7 ITERATIONS IN ORSRCH, F(X)=   .100056E-01 WITH A 1  PARAMETER FIT
   CAPK =  .184101E-01  S =  .110254E+02  KAPPA =  .447900E+00  UTAU =  .415889E+0

   CIN=   .573116E+01      TOPLUS=   .276188E-02

      BETAC =  0.

   MATCH CONDITION CRITERIA FOR VELOCITY PROFILE
   ETAM =    .0206     N0 =   350     ETA0 =    .9208

   LENGTH SCALES
   DELIN =  .00004     DELOUT =  .16306
```

	EXPERIMENTAL PROFILE		ANALYTICAL PROFILE		U+ DEVIATION
Y+	UD/UE	UD+	UA/UE	UA+	UD+ - UA+
0.00	0.0000	0.00	0.0000	0.00	0.000000
10.98	.3870	9.19	.3458	8.21	.977821
13.47	.4110	9.76	.3926	9.32	.436896
15.54	.4450	10.57	.4249	10.09	.476712
17.61	.4750	11.28	.4521	10.74	.543342
19.68	.4900	11.64	.4750	11.28	.356673
22.99	.5230	12.42	.5043	11.98	.444207
25.48	.5340	12.68	.5217	12.39	.292495
27.55	.5460	12.97	.5339	12.68	.288464
32.11	.5610	13.32	.5552	13.18	.138810
36.46	.5730	13.61	.5707	13.55	.055549
40.81	.5830	13.84	.5832	13.85	-.004265
43.71	.5900	14.01	.5904	14.02	-.009292
46.20	.5940	14.11	.5960	14.15	-.048285
51.17	.6010	14.27	.6062	14.39	-.122776
55.31	.6090	14.46	.6137	14.57	-.111887
59.45	.6150	14.60	.6206	14.74	-.133214
62.56	.6200	14.72	.6254	14.85	-.128945
76.23	.6350	15.08	.6439	15.29	-.210444
98.73	.6500	15.44	.6598	15.67	-.233038
105.24	.6650	15.79	.6732	15.99	-.194993
117.25	.6750	16.03	.6829	16.22	-.187475
131.13	.6840	16.24	.6929	16.45	-.211514
146.46	.6950	16.50	.7029	16.69	-.188439
158.48	.7030	16.69	.7103	16.87	-.172684
173.60	.7140	16.96	.7191	17.08	-.119974
187.89	.7230	17.17	.7270	17.26	-.095266
199.49	.7290	17.31	.7333	17.41	-.101808
214.20	.7380	17.53	.7411	17.60	-.072509
228.49	.7450	17.69	.7484	17.77	-.081438
240.92	.7510	17.83	.7547	17.92	-.088436
256.25	.7590	18.02	.7624	18.10	-.079563
270.96	.7660	18.19	.7695	18.27	-.083912
305.14	.7830	18.59	.7858	18.66	-.065391
342.02	.8010	19.02	.8025	19.06	-.036515
377.85	.8160	19.38	.8181	19.43	-.050706
415.76	.8300	19.71	.8339	19.80	-.091610
451.19	.8460	20.09	.8478	20.13	-.042955
487.44	.8600	20.42	.8613	20.45	-.031608
523.69	.8720	20.71	.8741	20.76	-.049303
561.19	.8860	21.04	.8864	21.05	-.010408
595.99	.8980	21.32	.8972	21.30	.019784
633.69	.9110	21.63	.9080	21.56	.071655
705.37	.9330	22.16	.9263	22.00	.159205
778.08	.9520	22.61	.9420	22.37	.237851
851.21	.9680	22.99	.9551	22.68	.307042
922.89	.9820	23.32	.9655	22.93	.390685
995.60	.9910	23.53	.9741	23.13	.402199
1067.48	.9960	23.65	.9807	23.29	.363097
1140.40	.9980	23.70	.9859	23.41	.286886
1212.49	1.0000	23.75	.9899	23.51	.240924
1285.41	1.0000	23.75	.9928	23.58	.170250
1357.50	1.0000	23.75	.9950	23.63	.118963
1430.63	1.0000	23.75	.9966	23.67	.081484
1502.93	1.0000	23.75	.9977	23.69	.055149
1575.22	1.0000	23.75	.9985	23.71	.036646
1647.52	.9990	23.72	.9990	23.72	.000301
1721.27	1.0000	23.75	.9994	23.73	.015381
1792.53	1.0000	23.75	.9996	23.74	.009816


DATE
FILME
8